Carbonate authigenesis and worm tube mineralization-biogeochemical and geobiological processes at methane seeps on the Congo deep-sea fan

Dissertation

zur Erlangung des Doktorgrades der Naturwissenschaften

am Fachbereich Geowissenschaften der Universität Bremen

vorgelegt von Antonie Haas

Bremen, August 2008

Tag des Kolloquiums:	14. Oktober 2008
Gutachter:	Prof. G. Bohrmann Prof. J. Peckmann
Prüfer:	Prof. R. Rendle-Bühring Prof. G. Mollenhauer

Abstract

This thesis represents an approach to describe biogeochemical and geobiological processes during carbonate authigenesis at the Kouilou methane seeps on the northern Congo Fan off southwest Africa. The work comprises the analyses of methane derived limestones, the formation of carbonates modified by macroorganisms, and the diagenetic mineralization of vestimentiferan worm tubes. In high agreement with other methane seeps, it could be shown that carbonate formation is initially induced by microbial activity of anaerobic methane oxidizing (AOM) consortia. Aragonite and high-Mg-calcite are the carbonate minerals of these carbonate structures. The principle factors in respect of carbonate formation and mineralogy are i.) methane flux intensity ii.) sulfate concentration and iii.) the aggregation of specific AOM consortia. High methane flux is identified to displace carbonate formation towards the seafloor, and favor, due to chemical and kinetic effects, the formation of aragonite. Highly negative carbon isotopic compositions, nearly seawater equivalent oxygen isotopic compositions and the dominance of ANME -2 biomarkers are characteristics of these carbonates. High-Mg-calcite carbonates, in contrast, are characterized by more positive carbon isotopic compositions and the dominance of ANME-1 biomarkers, both a result of moderate methane flux. The positive oxygen isotopic anomalies of the high-Mg-calcites point to reduced seawater access in higher sediment depths, and are very likely a result of a high proximity to decomposing gas hydrates. The shape of the carbonate structures is directly linked to methane migration and related pathway formation, as well as the subsequent aggregation of AOM consortia. Structures formed within the sediments are of nodular, tubular, or irregularly-complex shape, from which the latter varies highly in size. Structures close to the seafloor are of platy shape, and display, in contrast, rough surfaces and a higher porosity.

Modification of carbonate structure formation is observed by benthic bivalves and holothurians. Burrowing activities within the sediments cause seawater infiltration in higher sediment depths and the creation of small-scale niches of highly diverse carbonate chemistry. The assemblage of specific microorganisms and those activities is probably responsible for the local occurrence of protodolomite within some molds.

The colonization of chemosymbiotic vestimentiferan tube worms affects carbonate formation conditions in a comprehensive way. Carbonate precipitates occur close to the posterior worm tube which is used as an important metabolism device within the sediment.

Tube worms change the chemistry by i.) the uptake of sulfide off the sediment, ii.) the release of sulfate into the sediment and iii.) the release of hydrogen ions. The uptake of sulfide maintains AOM induced carbonate formation and prevents carbonate solution by balancing the pH. Whereas sulfate release, enhances carbonate formation by stimulating the turn over of AOM consortia. Additionally, increasing sulfate concentrations are most likely responsible for the predominant formation of aragonite after tube worm colonization. The elimination of hydrogen ions through the posterior tube prevents carbonate formation directly on the tube surface and avoids a reduction of the respiratory area. This is responsible for the co-occurrence of organic tubes (live), partly (dead) and totally lithified posterior tubes (degraded) within some complex tube worm/carbonate aggregates, formed by tube worm colonies. Nodular high-Mg-calcite carbonates, incorporated within the structures are formed prior to tube worm colonization, and are supposably used for tube fixation.

Diagenetic mineralization of posterior vestimentiferan worm tubes finally forms two characteristic mineralization patterns by the carbonate mineral aragonite. The mineralization process starts on the exterior tube and proceeds successively to the interior tube wall. The resulting tube configuration depends on the size and fabric of aragonite crystals. Microcrystalline aragonite crystals do not change the tube wall diameter or its laminar configuration. Whereas tube wall mineralization by inwards growing large-scale aragonite splays results in laminae separation, lateral spreading of the wall and the reduction of the internal tube diameter. Some of the tube walls are rapidly affected by recrystallisation processes. Microcrystalline aragonite crystals get overgrown by radial fibrous aragonite crystals, responsible for the delamination of still unaltered organic laminae and the formation of bulges. Exactly these features were observed in Paleozoic tube fossils, and make it more likely, that these fossil tubes are vestimentiferans.

Zusammenfassung

Im Rahmen dieser Doktorarbeit wurden biogeochemische und geobiologische Prozesse untersucht, die während der authigenen Karbonatbildung an den Kouilou-Methanaustritten auf dem nördlichen Kongofächer vor Südwest-Afrika ablaufen. Die Arbeit umfasst die Analyse von methangenerierten Kalksteinen, die Bildung von Karbonat unter Einfluss von Makroorganismen und die diagenetische Mineralisierung von Vestimentifera-Wurmröhren. In großer Überseinstimmung zu anderen Methanaustritten konnte gezeigt werden, dass die Karbonatbildung durch die mikrobielle Tätigkeit im Zusammenhang mit der anaeroben Methanoxidation (AOM) initiiert wird. Die dominierenden Karbonatphasen sind Aragonit und Hochmagnesiumkalzit. Die Hauptfaktoren, die die Karbonatbildung und die Mineralogie beeinflussen sind i.) die Intensität des Methanflusses ii.) die Sulfatkonzentrationen und iii.) die Ansiedlung von spezifischen AOM-Konsortien. Hoher Methanzufluss verschiebt die Karbonatbildung innerhalb des Sediments in Richtung Meeresboden und fördert durch chemische und kinetische Effekte die Bildung von Aragonit. Die Karbonatphase Aragonit ist durch sehr negative Kohlenstoffisotopenverhältnisse und nahezu meerwasseräquivalente Sauerstoffisotopen-verhältnisse charakterisiert; die anaerobe Methanoxidation wird in diesem Milieu vorrangig durch das ANME-2 Konsortium durchgeführt. Im Gegensatz dazu ist die Hochmagnesiumkalzitphase durch positivere Kohlenstoffisotopenverhältnisse geprägt und die anaerobe Methanoxidation wird durch das ANME-1 Konsortium ausgeführt. Beide Charakteristika werden als ein Ergebnis von moderatem Methanzufluss interpretiert. Die deutlich positiveren Sauerstoffisotopenanomalien der Hochmagnesiumkalzitphase deuten auf einen reduzierten Einfluss von Meerwasser hin und unterstützen eine Bildung in größeren Sedimenttiefen. Die Sauerstoffisotopenverhältnisse sind sehr wahrscheinlich ein Ergebnis von im nahen Umfeld ablaufender Gashydratzersetzung. Die Form der Karbonatstrukturen steht in direktem Zusammenhang mit der Migration von Methan, der in diesem Zusammenhang stehenden Bildung von Wegsamkeiten und der nachfolgenden Ansiedlung von AOM-Konsortien. Karbonatstrukturen die in höheren Sedimenttiefen gebildet wurden sind von knolliger, röhrenförmiger oder ungleichförmig-komplexer Gestalt, welche zusätzlich stark in ihrer Größe variieren. Karbonatstrukturen die nahe dem Meeresboden gebildet wurden, sind von flacher, plattenartiger Form und haben im Gegensatz zu den anderen, neben einer rauen Oberflächen auch eine höhere Porosität.

Die Bildung einiger Karbonatstrukturen ist deutlich durch benthische Muscheln und Holothurien beeinflusst worden. Bioturbation führt zur Meerwasserinfiltration in größere Sedimenttiefen und verursacht die Bildung von Porenräumen mit unterschiedlicher Karbonatchemie. In Abhängigkeit davon verläuft die Ansiedlung von spezifischen Mikroorganismen und deren Aktivität. Hierin wird die Ursache für das lokale Vorkommen von Protodolomit innerhalb einiger dieser verfüllten Grabgängen gesehen.

Umfassende Veränderungen auf die Karbonatbildung werden durch die Gegenwart von chemosymbiotisch lebenden Vestimentifera-Röhrenwürmern verursacht. Karbonate treten an deren in das Sediment reichendes Röhrenende auf, das als wichtiges Stoffwechselorgan genutzt wird. Röhrenwürmer verändern die chemischen Verhältnisse durch i.) die Aufnahme von Sulfid aus dem Sediment, ii.) die Abgabe von Sulfat ins Sediment und iii.) die Abgabe von Wasserstoff-Ionen. Die Aufnahme von Sulfid aus dem Sediment unterstützt die Karbonatbildung und verhindert dessen Lösung durch den Ausgleich des pH-Wertes. Die Abgabe von Sulfat ins Sediment fördert die Karbonatbildung durch die Steigerung der Umsatzraten des AOM-Konsortiums. Zusätzlich sind höhere Sulfatkonzentrationen ein Faktor für die vorrangige Ausfällung von Aragonit, welches die Karbonatstrukturen im Anschluss an die Röhrenwurmbesiedlung im Wesentlichen aufbaut. Die Ausscheidung von Wasserstoff-Ionen über die Röhrenwand verhindert die Karbonatbildung direkt auf der Röhrenoberfläche, wodurch eine Verminderung der Respirationsfläche vermieden werden kann. Es erklärt darüber hinaus, dass gleichzeitige Vorkommen von organischen Röhren (lebend), teilweise (tot) oder komplett lithifizierten (zersetzten) Röhren innerhalb komplexer Röhrenwurmkarbonate, die sich im Bereich von Röhrenwurmkolonien bilden. Knollige Hochmagnesiumkalzite, die im Innern dieser Strukturen vorkommen gehen aus einer Bildungsphase hervor, die vor der Besiedlung durch Röhrenwürmer stattgefunden hat. Diese Karbonate, von den Röhrenwürmern für die Fixierung der Wurmröhre innerhalb des Sediments genutzt, wurden durch nachfolgende Karbonatfällung eingeschlossen.

Die Mineralisierung der Vestimentifera-Wurmröhren während der Diagenese führt zur Ausbildung von zwei charakteristischen Mineralisierungsmustern, beide gebildet durch das Karbonatmineral Aragonit. Der Mineralisierungsprozess beginnt außen an der Röhre und setzt sich sukzessive zum Inneren der Röhre fort. Die letztendliche Röhrenkonfiguration steht in engem Zusammenhang mit der Größe und dem Habitus der Aragonitkristalle. Mikrokristalline Aragonitkristalle rufen keine Veränderungen im Röhrenwanddurchmesser

oder der lamellaren Röhrentextur hervor. Im Gegensatz dazu führt das Wachstum von größeren, fächerförmigen Aragonitkristallen zu einer lateralen Aufspaltung der Röhrenlamellen und minimiert dadurch den Innendurchmesser der Röhre. Einige der untersuchten Röhren zeigen das schnelle Auftreten von Rekristallisationsprozessen. Bereits in einem frühern Stadium werden die mikrokristallinen Aragonitkristalle durch große, fächerförmige Aragonitkristalle überwachsen. Dies führt zur Wulstbildung innerhalb der Röhrenlamellen sowie zur Delamination von noch organischen Lamellen. Genau diese Texturmerkmale wurden auch an paläozoischen Röhrenfossilien entdeckt und deuten darauf hin, dass diese Röhren von Vestimentiferen stammen.

Table of contents

1. Introduction

1.1 Historical view

Petroleum seeps and groundwater discharges in marine environments have been known for thousands of years (Taniguchi, et al., 2002). Detailed knowledge on their origin has not been accumulated until the development of new deep-sea technology in the mid 1960s (e.g. sidescan sonar and towed photographic camera) (Judd and Hovland, 2007). Since then, seeps from many parts of the world's oceans have been discovered, and their occurrence is quite often related to geological phenomena such as tectonically induced high pore-fluid pressure, natural gas seepage, artesian flow or catastrophic erosion and submarine slides (Tunnicliffe et al., 2003). A great deal of attention achieved the discovery of extended chemosynthetic-based fauna at methane seeps at the base of the western Florida Escarpment in 1983 (Paull et al., 1984). Specifically the occurrence of authigenic carbonates in the deep sea, far from well established formation conditions was surprising (e.g. Kulm et al., 1986; Ritger et al., 1987). Moreover, further important aspects differ much to the ambient marine environment. For example the dysaerobic or anaerobic reducing conditions as a result of the presence or discharge of oxygen-depleted fluids, mainly hydrogen sulfide, and methane, and the absence of sufficient supply of photo-synthetically produced food (e.g. MacDonald et al., 1989). However, exactly these life-hostile conditions are responsible for the emergence of overflowing ecosystems. Further exploration of the deep-sea has revealed numerous modern seep sites that sustain luxuriant populations of metazoans and microbes (e.g. Suess et al., 1985; Paul et al., 1992).

1.2 Seepage and global distribution

Cold seeps are commonly associated along continental margins, and have been discovered from the tropics to the poles (Fig. 1; Campbell, 2006), in water depths of down to 6000 m (Sibuet and Olu, 1998).

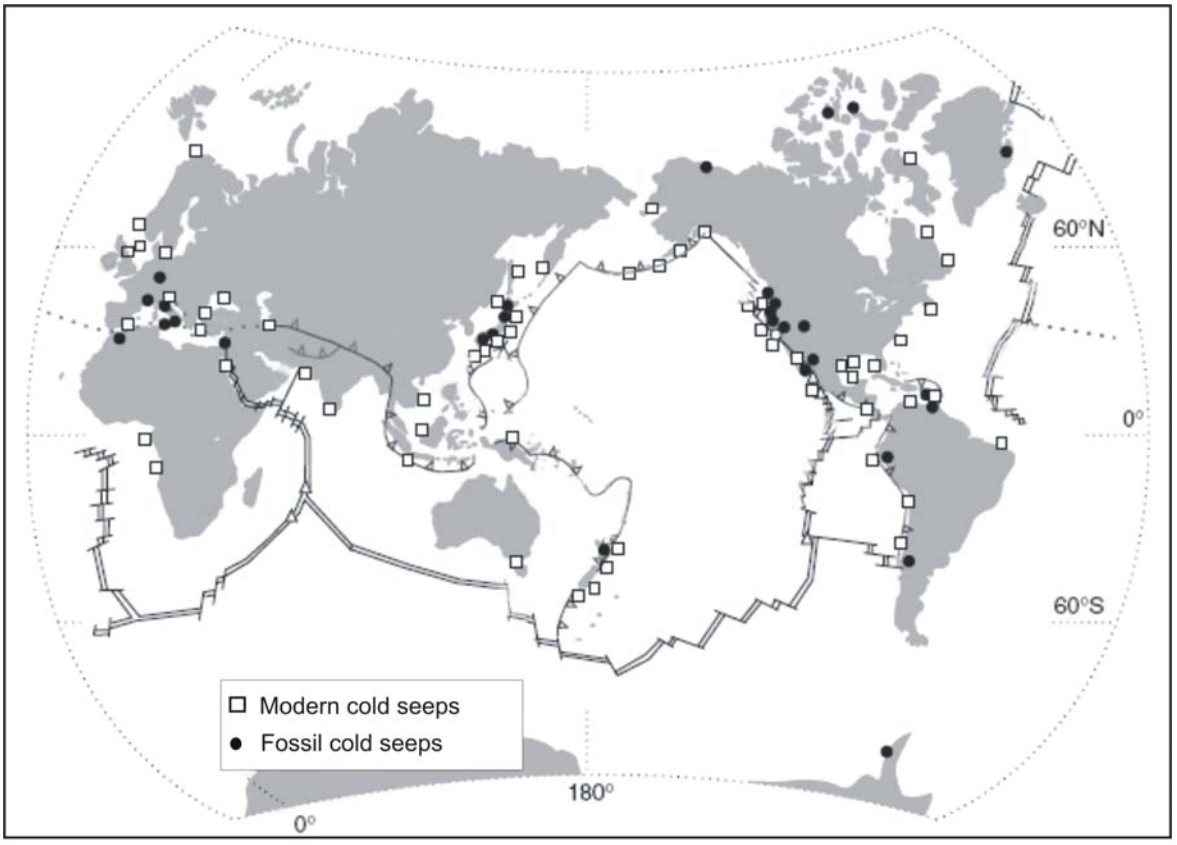

Figure 1. Distribution of modern and fossil cold seeps (Modified from Campbell, 2006)

Many seeps occur at active continental margins, on well-developed accretionary prisms just as well as along erosive margins (e.g. Ritger et al., 1987, Suess et al., 1998; von Rad et al., 1996; Bohrmann et al., 1998; 2002). Especially the accretion of sediment packets scraped from the subducting or the overlying plate against the continental plate causes the mobilisation of overpressurized fluids and gases (Suess et al., 1998). These processes result in fluid and gas-migration along tectonic faults, and the ascending waters are sometimes related to the formation of mud diapirs/ volcanoes on subducting plates (e.g. Aloisi, 2000; Han et al., 2004). On passive margins and in ocean basin structures, high sediment loads or salt tectonics are known mechanisms to cause seepage areas (Fig. 2; e.g. Kennicutt et al., 1988; Borowski et al., 1999; MacDonald et al., 2000; Coleman and Ballard, 2001; Peckmann et al., 2001; Bohrmann, et al. 2003; Gay et al., 2004, 2007; Sahling et al., 2008).

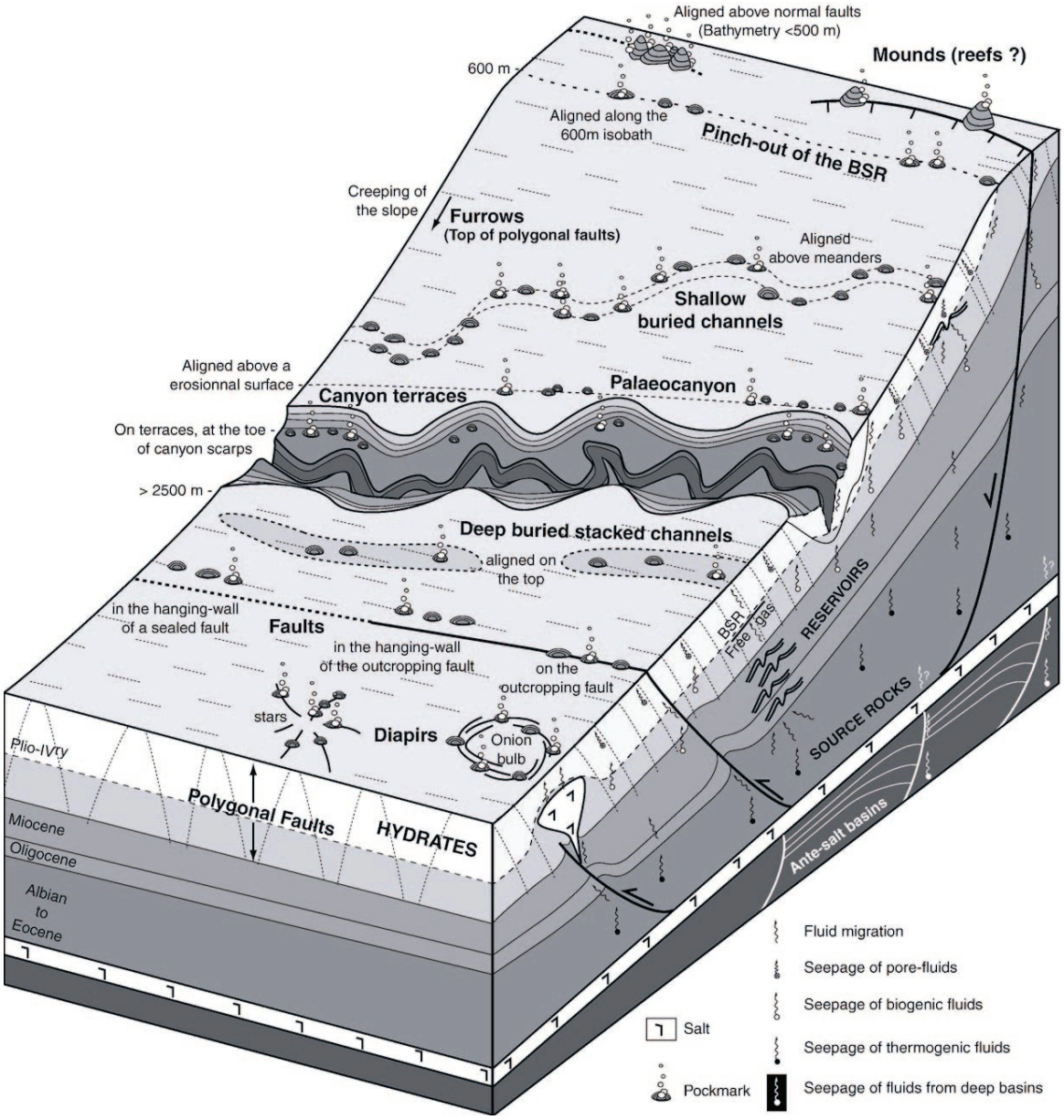

Figure 2. Conceptual 3D block diagram of a passive margin showing the plumbing systems of fluid migration. The organisation of fluid seeps at the seabed is strongly dependent on the nature and shape of the buried reservoirs (i.e. turbiditic channels or salt diapirs) where the fluids originate. Their distribution is also linked to the location of major pathways, such as erosional surfaces and faults (Gay et al., 2007)

Additionally, the mobilisation of seeping agents is sometimes triggered by seismic activities like mass wasting from earthquakes, tsunamis or turbidity currents (e.g. Mayer et al., 1988). Seep origin in shallow sediments is mostly related to the extraordinary high accumulation of organic matter, or submarine springs. Judd and Hovland (2007) suggest that aquifer driven seepage is generally restricted to near-shore areas. Significant hydrocarbon reservoirs, for example, are generally found in areas of high organic carbon burial (Levin, 2005).

1.3 Methane and gas hydrates

Cold-seep fluid's compositions vary in relation to geological settings (see Judd and Hovland (2007) for overview). Although methane is not the agent of all cold seeps, numerous seeps are now known where methane is the driving force. Methane is a common product preferentially generated thermogenically in deeply buried sediments or from microbial processes (e.g. Whiticar, 1986, 1999). It is the lightest and simplest hydrocarbon and it is probably the most abundant and widespread of all gases held within sediments (Hedberg, 1980). Regardless of methane origin, after formation, methane can be present in solution in the pore water, or as a free gas phase. Dissolved or gaseous methane is of lower density compared to the normal pore water, and will initiate migration processes. By an upward migration, methane escapes through the seabed and leads to the formation of seeps (Park et al., 1990). However, migration processes of methane can be interrupted by impermeable sediment-barriers to form natural gas reservoirs, commonly associated with intrasedimentary or seabed doming (Judd and Hovland, 2007), mud diapers and mud vents (Brown, 1990). Moreover, the barrier formation as a result of gas hydrates formation under certain conditions seems to be an important process of gas capture. Natural gas hydrates are ice-like, non-stoichiometric crystalline structures, where gas molecules are physically trapped within a clathrate-like framework of hydrogen-bonded water molecules (Kvenvolden, 1993). The guest molecule is often constituent of natural gas, however, it is mainly methane or another hydrocarbon gas, carbon dioxide and hydrogen sulfide (Fig. 3; Bohrmann and Torres, 2006). At least three polymorphs of gas hydrates are known so far: structures I, II and H (Sloan, 1998). Gas hydrates are stable only in very specific temperature and pressure conditions, which naturally occur in permafrost regions (low temperature regimes) and in the deep oceans (high pressure regimes). The occurrence of gas hydrate within sediments is controlled by their "geothermal gradient" (most commonly ~ 30 °C km^{-1}), and is in respect to the presence of water mostly restricted to the shallow geosphere where the amount of methane exceeds its solubility (Kvenvolden, 2003). Characteristics that simultaneously occur to gas hydrate-barrier formation are the significant dewatering of the surrounding sediments inclusive shrinkage-texture formation (Clennell et al., 1999), a shortage in water in the underlying sediments subsequently leading to an accumulation of free gas. Gas hydrate decomposition causes negative salinity-anomalies by the release of fresh-water. Natural gas

hydrate are sensitive to changes in pressure, temperature or gas undersaturation, and result in the rapidly disintegration of the water-gas combination (Haq, 2003).

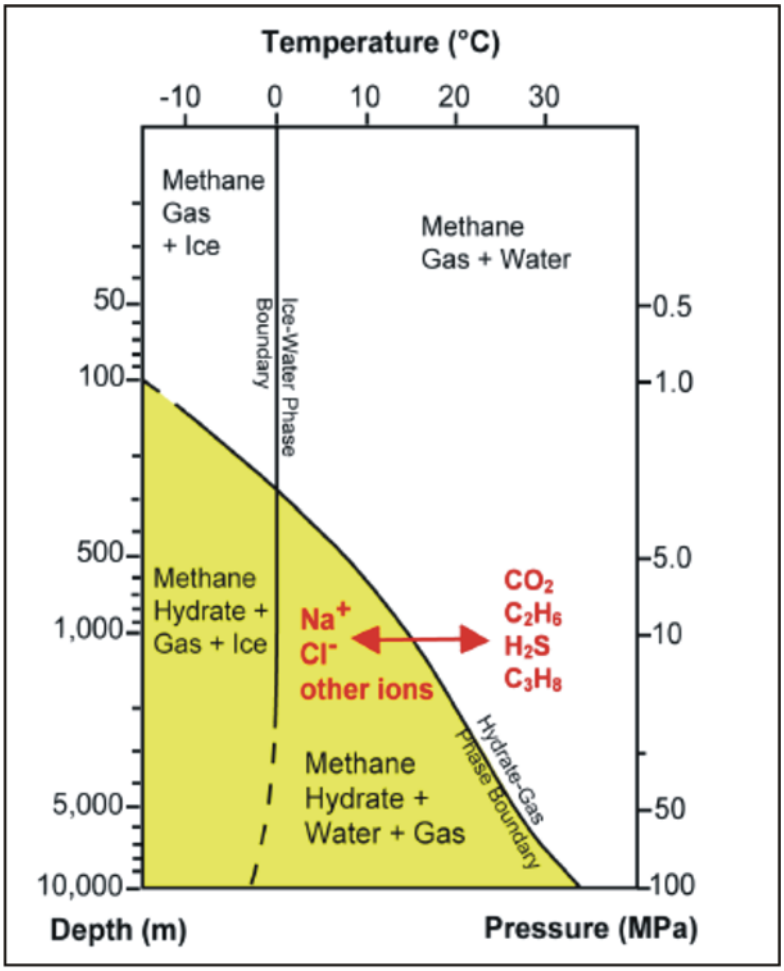

Figure 3. Phase diagram showing the boundary between methane hydrate (yellow) and free methane gas (white) for pure methane/H_2O system. Addition of ions shifts the boundary to the left, decreasing the P/T stability field. The presence of gases like carbon dioxide, hydrogen sulfide or other high-molecular hydrocarbons shifts the curve to the right, thus increasing the P/T field in which methane hydrate is stable (after Kvenvolden (1998), modified by Bohrmann and Torres, 2006).

1.4 Pockmarks

A special feature observed at some methane seeps are pockmark structures. Pockmarks have been reported from several locations all over the world (Whiticar and Werner, 1981; Hovland and Judd, 1988; Judd, 2003; Zühlsdorff and Spiess, 2004, Sahling et al., 2008).

Judd and Hovland (2007) describe pockmarks as follows: "They occur in shallow coastal waters just as well as in deep oceans, and are generally described as shallow seabed depression, typically several tens to hundreds of meters across and deep, preferentially occuring in soft, fine-grained sediments. They are often characterized by erosive formed indentations and lobes, and floors rather undulated than smooth. The eroding process is triggered by agents from the underlying sediments, which are responsible for the removal of the lacking sediments". King and MacLean (1970) assumed that the main agents for pockmark formation are ascending gas or water, initially caused by the upwards migration of overpressured pore water from below (Fig. 4), that increases the sediment porosity by the reduction of the grain-to-grain contact, and therefore the sediments rigidity (Hovland and Curzi, 1989). Gas or fluid accumulation beneath impermeable sediments or gas hydrate barriers are though to be responsible for eruptive outburst of the suppressed gaseous or liquid agents, forming crater-like structures (Judd et al., 1994; Hovland et al. 2005).

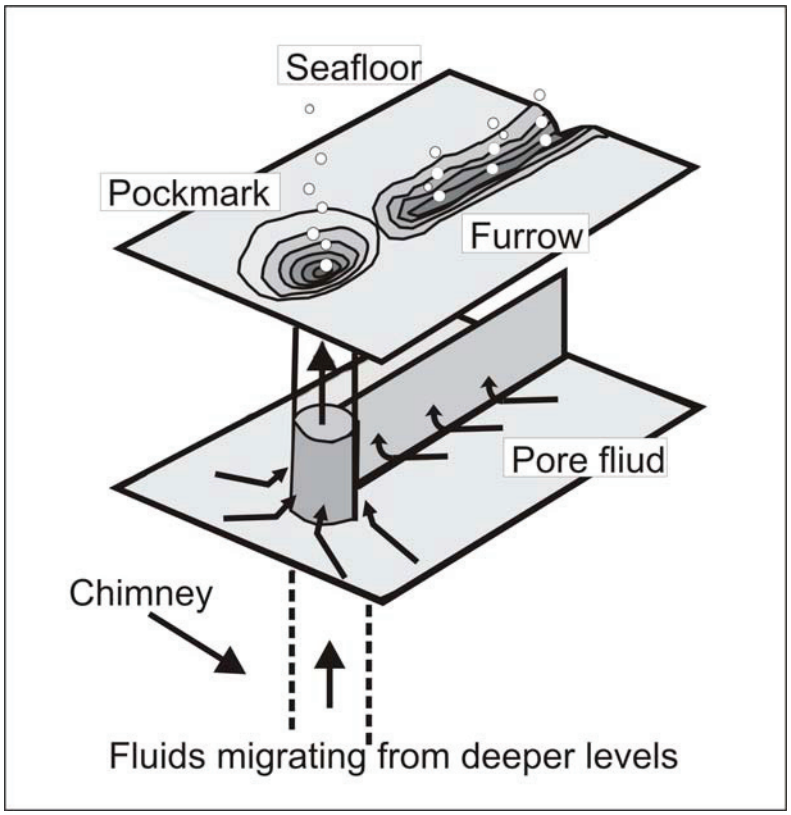

Figure 4. Schematic diagram of fluid migration at seep sites. In dependency of fluid flux intensity and sediment structure, fluids migrate in chimney-like conduits or along faults from deeper levels to the seafloor (Modified from Gay et al., 2004).

1.5 The Anaerobic Oxidation of Methane (AOM)

The anaerobic oxidation of methane (AOM) is the most important methane sink (~90%) in marine environments (Fig. 5; Reeburgh, 1996; Blumenberg et al., 2004). Indications for the occurrence of AOM were firstly found by studies of methane turnover in anoxic marine sediments (Martens and Berner, 1974; Claypool and Kaplan, 1974; Reeburgh, 1976). A relationship of methane presence in respect to the concentrations of sulfate in organic rich sediments had been observed. One theory for this behavior is based on an electron transfer from methane to sulfate, operated by microorganisms (Hoehler and Alperin, 1996).

$$CH_4 + SO_4^{2-}{}_{(aq)} \rightarrow HCO_3^-{}_{(aq)} + HS^- + H_2O_{(l)},\ \Delta G^0 = -33\ kJ\ mol^{-1} \quad (1)$$

(Iversen and Jørgensen, 1985).

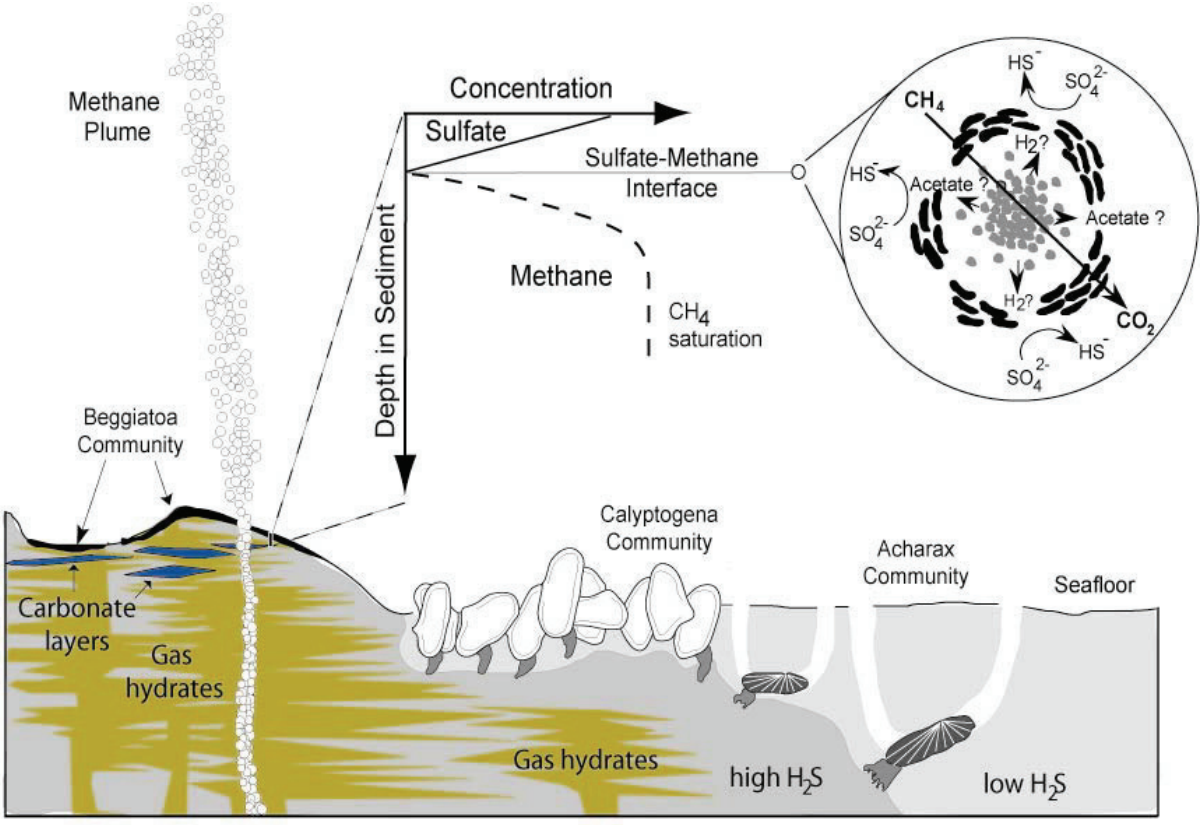

Figure 5. Schematic illustration of seep sediments and the distribution of chemosymbiotic organisms AOM consortium (top) of methanotrophic archaea (light gray dots, middle) surrounded by sulfate reducing bacteria (black rods) operate methane oxidation and sulfate reduction within sediments. The coupled release of sulfide is elementary for the live of thiotrophic organisms (Tréhu et al., 2004).

Recent investigations revealed that distinct communities of anaerobic operating archaea and sulfate reducing bacteria are involved in AOM (Fig. 5).

Up to date, three phylogenetically distinct archaeal lineages have been identified in these communities: ANME-1, 2 and 3 (Hinrichs et al., 1999; Boetius et al., 2000, Niemann, et al. 2006), whereas the examined sulfate reducing bacteria (SRB) stem from the *Desulfosacrina/Desulfococcus* and *Desulfobulbu* groups (Orphan et al., 2002; Knittel et al., 2003; Blumenberg, et al., 2004). The identification of organisms that were involved in AOM is feasible by identifying their chemical fossils (biomarkers), specifically those diagnostic lipid patterns (Pancost et al., 2001). The ratios of the individual lipid components allow their allocation to the different microbial assemblages. Furthermore, carbon isotopic signatures extracted from the distinct components are able to document the methane source, utilized by the former organisms (Elvert et al., 1999).

1.6 Carbonate formation at methane seeps

One important consequence of AOM is an increase in carbonate alkalinity (1).

$$CH_4 + SO_4^{2-} \rightarrow HCO_3^- + HS^- + H_2O \quad (1)$$

The high concentrations of carbon species finally supports the formation of authigenic carbonates in access to calcium rich pore water (equation (2); Fig. 6) (e.g. Ritger et al., 1987; Suess and Whiticar, 1989; Bohrmann et al., 1998; Peckmann et al. 2001; Valentine, 2002).

$$Ca^{2+} + 2HCO_3^- \leftrightarrow CaCO_3\,(s) + CO_2 + H_2O \quad (2)$$

Methane seep carbonates typically comprise one or more of the following carbonate mineralogies: high-magnesium-calcite, aragonite and dolomite (e.g. Kulm et al., 1986; von Rad et al., 1996; Castanier et al., 1999; Judd and Hovland, 2007). The morphologies of the authigenic carbonates are various; chimneys, slabs, crusts, tubes, blocks and nodules are common. The carbonates commonly incorporate background sediments and exhibit a clotted microcrystalline texture (Riding, 2000). Voids and cavities, or brecciation-textures are abundant in the authigenic carbonates. Carbonate mineralogy is assumably a product of distinctive carbonate chemistry caused by methane flux intensity and the turnover-rates of specific AOM consortia (Wallmann et al., 1997; Luff et al., 2003, 2005). Luff et al. (2003) found the preferential crystallization of aragonite in methane super-saturated environments.

Aragonite formation is even enhanced by well-oxygenated formation fluids of lower viscosity (Buczynski and Chafetz, 1991). In contrast, calcite formation is favored over aragonite in the presences of phosphate (Walter, 1986), and low-sulfate conditions are more favorable for calcite formation (Tucker and Wright, 1990; Burton, 1993). Dolomite occurrence has been most commonly interpreted as a replacement of aragonite or calcite over time. Recent investigations have shown that microbial activity is probably responsible for the preferential formation of dolomite under certain conditions (Vasconcelos and McKenzie, 1997; Cavagna et al., 1999; van Lith et al., 2003).

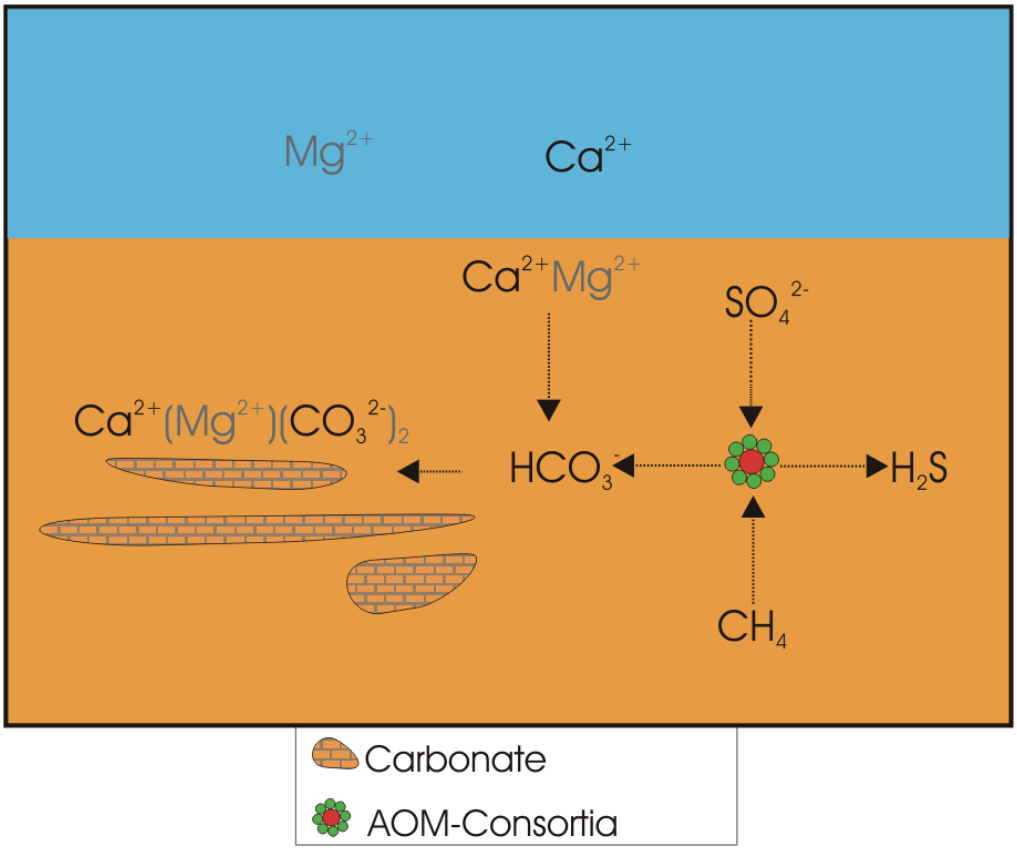

Figure 6. Carbonate formation in methane-seep sediments. AOM released carbonate species reacts with pore water calcium (magnesium) to form calcium (magnesium) carbonate.

The investigation of methane seep carbonates supplies multiple information on those genesis conditions. Beside petrography and variations in mineralogy, stable carbon and oxygen isotopic compositions refer to the environmental conditions like carbon source, precipitation fluid temperature, and its contact to seawater. “Classic” hydrocarbon seep carbonates are depleted in ^{13}C (Campbell, 2006). Moreover, since these carbonate precipitates

simultaneously enclose the present seabed sediments during their formation, they act as important archives for organic and sedimentary remains.

1.7 Chemosymbiotic organisms at methane seeps

At the time of methane seep discovery in the deep-sea, the presence of high masses of fauna was astonishing (Paull, et al., 1984; Kennicutt et al., 1985; Suess et al., 1985). The food supply generated by photosynthesis occurred unlikely in these depths and it remained vague whereon life is based at methane seeps. However, compared to life at hydrothermal vents, and the availability of seeping agents at the discovered seeps, the generation of energy via chemosynthesis seemed most obvious (e.g. Kennicutt, et al., 1985, 1988; Childress et al., 1986).

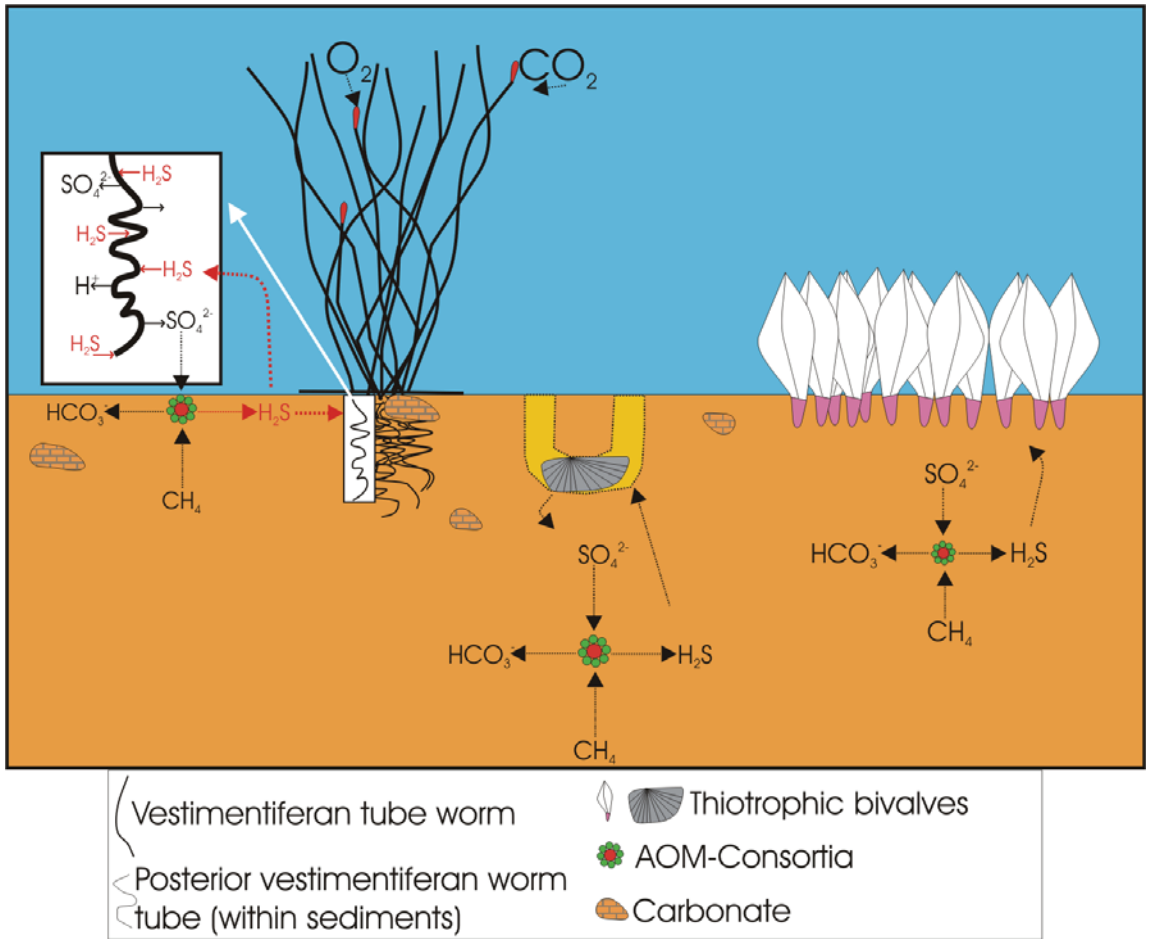

Figure 7. Biochemical processes at methane seeps. Methane migration and concentration are responsible for the accumulation of AOM consortia and the subsequently occurrence and abundance of chemosymbiotic organisms.

Over the past years, it turned out that AOM plays a basic role not only for carbonate formation but also for the settlement of organisms at methane seeps. The AOM coupled release of sulfide, resulting from the sulfate reduction by sulfate reducing bacteria (SRB), is most likely the most important base of life at methane seeps (Fig.7). Methane seep organisms originate their energy by the symbiosis with bacteria, hosted in their tissue. The majority of inhabitants depend on thiotrophic bacteria (e.g. Julian et al., 1999; Freytag et al., 2001), however, few of them contain methanotrophic bacteria (e.g. Childress et al., 1986; Kochevar et al., 1992).

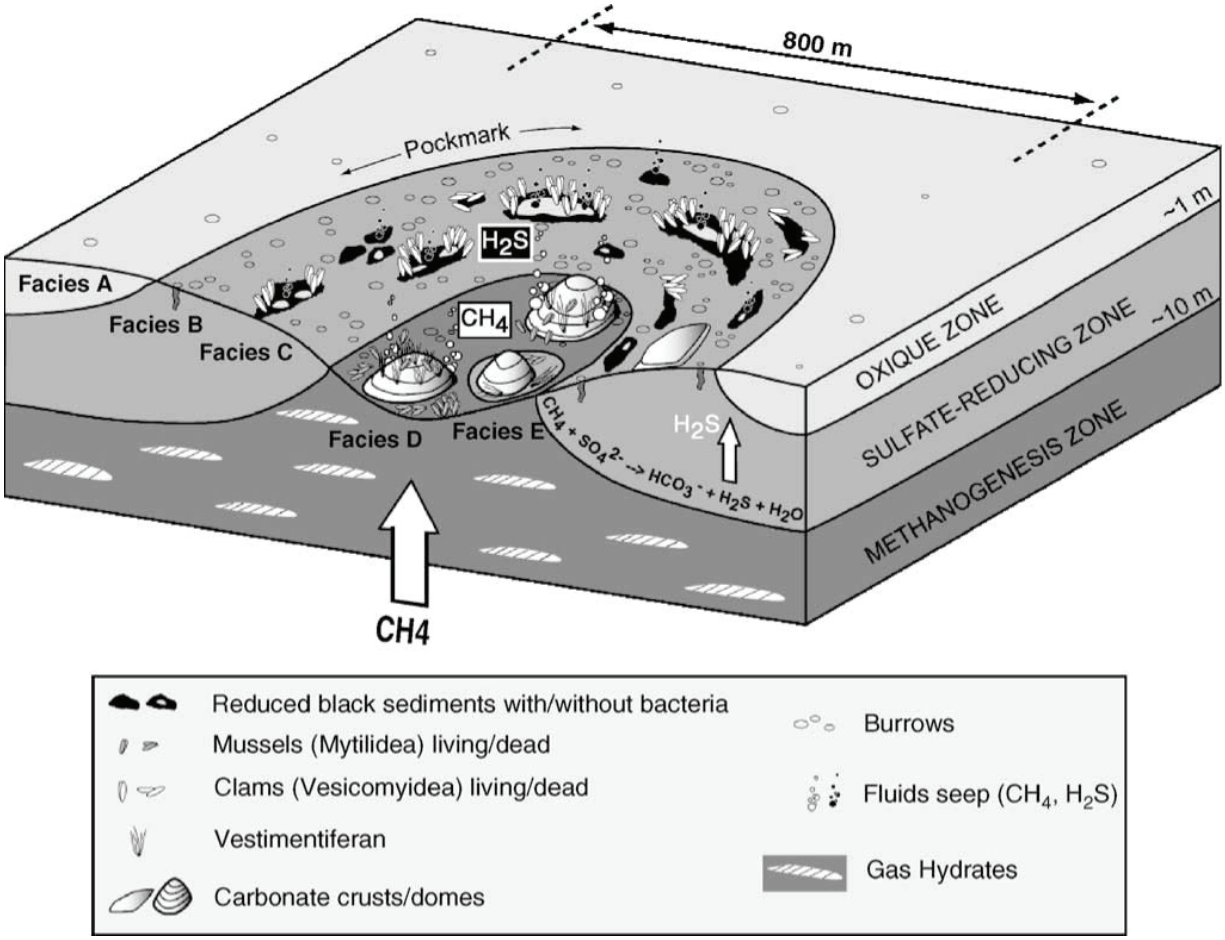

Figure 8. Evolutive model of morphological, chemical and biological features within a pockmark. The centre is dominated by methane-derived authigenic carbonate buildups and endemic bacteria and fauna. The periphery is dominated by sulfide-dependent Vesicomyidia-type fauna living on black reduced sediments and white bacterial mats (Gay et al., 2006)

Endemism of seep species is high and new families, orders and classes have been identified in the last two decades (see Sibuet and Olu, (1998) for overview). The dominant fauna is at high taxonomic levels closely related to the higher taxa of hydrothermal vents in the Pacific (Paull et al., 1984; Kennicutt et al., 1988; Bergquist et al., 2000), but with differences in

species composition, diversity, and abundances (Sibuet and Olu, 1998). Characteristic seep inhabitants are bivalves of the families Vesicomyidae, Mytilidae, Solemyidae, Thyasiridae and Lucinidae. In addition to this, vestimentiferan tube worms (Polychaeta: Siboglinidae) are dominant at many seep sites (MacDonald, 1989; Sibuet and Olu, 1998). However, gastropods, shrimps and symbionts containing sponges are present at some methane seeps (Olu et al., 1997; Levin, 2005). Additionally, as differences exist in use and behavior of the seep organisms in respect to the concentrations of sulfide and/or methane, those distribution within the seepage area is used to get information of actual existing seepage activities and intensities (Fig. 8; e.g. MacDonald, 1989; Sahling et al., 2002, Levin et al. 2003; Paull et al., 2005; Gay et al., 2006). Moreover, seep communities change over time in respect to species diversity and population density. At an initial stage, seepage areas are dominated by less endemic species in high density. Established seepage areas, in contrast, are characterized by higher taxonomic diversity with increasing numbers of non-symbiont containing taxa. Decreasing number of species was determined with increasing depths of methane seep location (Sibuet and Olu, 1998).

1.8 From biosphere to geosphere - Mineralization of modern seep organisms

Taphonomy is the science of the “laws of burial” (from the Greek taphos (grave) + nomos (earth, soil)), and is the study of the transition of organic remains from the biosphere into the lithosphere or the process of “fossilisation” from death to diagenesis (Martin, 1999). Taphonomic investigations were first conducted by Leonardo da Vinci (1452-1519), who used observations on living and dead bivalves to infer transportation processes (Martin, 1999). Today, the examination of taphonomic processes gives access to information of death, decay, and disintegration of organisms. Estimations of environmental circumstances while degradation and the loss of morphological characteristics while mineralization are subject of these examinations. And the establishment of detail knowledge is fundamental for the interpretation of fossils since differing states of fossil preservation (taphofacies) are again and again responsible for fossil misinterpretation (Little and Vrijenhoek, 2003). Moreover, fossil identification is related to information on the way of life and the positive interpretation of fossil records. Thus, taphonomy comprises of manifold information of distinguishable scientific issues and scales as e.g. the first appearance of an organism, its radiation and

world-wide distribution, just as well as the taxonomical classification and the evolutionary development.

Biogenic remains are subject not only to physical degradation, but also chemical alteration that recycles biogeochemically important elements such as carbon sequestered in hardparts (Martin, 1999). The examination of these processes at methane seeps is still almost unexplored by their late discovery. Fossil preservation is generally related to certain conditions like rapid burial, anoxic sediments, bioturbation and authigenic mineral formation (e.g. Seilacher et al., 1985; Plotnick, 1986a; Allsion, 1988a). In these environments, microbial degradation of organic material proceeds via nitrate or sulfate reduction (Castanier et al., 1999). And specifically where nitrate operates as electron acceptor, carbonate crystallisation will be supported (Martin, 1999) (see equation, 1).

$$(CH_2O)_{106}\,(NH_3)_{16}H_3PO_4 + 84.8HNO_3 \rightarrow 106CO_2 + 42.4N_2 + 148.4H_2O + 16NH_3 + H_3PO_4 \quad (1)$$

(Canfield and Raiswell, 1991)

The decay of proteinous organisms does not only release carbonic and other acids but also releases off substances such as ammonia and amines (Berner, 1968). That results in a rise of pH and enables the formation of calcium carbonate:

$$NH_3 + Ca^{2+} + HCO_3^- \rightarrow CaCO_3 + NH_4^+ \quad (2)$$

(Berner, 1968)

Most sulfate reducers, in contrast, do preferentially degrade small organic substances like simple monomers and fermentation products than polymers (Megonigal et al., 2005). Sulfate reducing bacteria will rather enhance carbonate dissolution, if the released sulfide accumulates and subsequently leads to a decrease of the pH.

$$(CH_2O)_{106}(NH_3)_{16}H_3PO_4 + SO_4^{2-} \rightarrow 106HCO_3^- + 53H_2S + 16NH_3 + H_3PO_4 \quad (3)$$

(Canfield and Raiswell, 1991)

Sulfide can be removed e.g. by pyrite formation or consumption by thiotrophic organisms (Jørgensen, 1982). Subsequently increasing concentration of bicarbonates while sulfate reduction arise carbonate alkalinity causes carbonate supersaturation (Berner, 1970).

2. Motivation and objectives of the study

The detailed investigation of the Kouilou pockmark area on the Congo deep-sea fan, within R/V METEOR Cruise 56/2 in 2002, was based on results acquired within R/V METEOR cruise M47/3 in 2000. Then, the existence of numerous pockmark structures, the presence of near surface gas hydrates, huge amounts of authigenic carbonates and chemosymbiotic fauna was evidenced by geophysical, geochemical and geological work. In contrast to that previous cruise, M56/2 was accomplished to achieve information on the regional distinctions and similarities within individual pockmarks. This includes information on descending fluids like methane or other gases, those origins, the distribution of gas hydrate and its composition, as well as the specifications of carbonates and the configuration of chemosymbiotic seep-fauna. Especially the deployment of video systems like e.g. a TV-sled offered the opportunity to visualize the crater-like structures within the hemipelagic sediments, which were characterized by widespread carbonate structures, extensive vestimentiferan tube worm colonies, mytilid mussels, thyasirid and vesicomyid clams, as well as holothurians. Additionally, the use of a TV-guided grab enabled the controlled sampling of extraordinary high amounts of carbonate structures, and the extraction of intact bush-like vestimentiferan tube worm colonies off the sediments.

Just in respect to the huge amounts of highly diverse morphologies of the carbonate structures, it became clear, that their formation has to be related to variations of environmental conditions. Main forms were nodules, tubes, or structures of irregular-complex shape, whereas other samples were platy or organically formed. Beside this, the samples comprised of some other extraordinary features. The retrieved bush-like vestimentiferan colonies revealed pronounced carbonate aggregates attached at those posterior ends within the sediments. These highly complex structures are of various sizes and occurred sometimes like lithified “root-balls”. Furthermore, worm tubes of different states of preservation were discovered within these tube worm/ carbonate aggregates.

Major questions are related to three main parts: i) the basic principles of carbonate formation ii) the presence of carbonate aggregates at vestimentiferan tube worms, and iii) their taphonomic processes.

i)

- What are the fundamental processes of carbonate formation? Are there significant variations in mineralogy or in stable carbon and oxygen isotope chemistry? And if so, how are they related to seep-related processes?
- What mechanisms and environmental conditions are responsible for the formation of the different carbonate structures and textures?

ii)

- Which processes are responsible for the formation of pronounced tube worm/ carbonate structures?
- What role has the worm itself on carbonate formation and which consequences arise for its life?
- When exactly did carbonate formation happen in this area? Is it prior to the worm colonization, during life-time or post-mortem?
- What is the impact of carbonate formation on tube worm colonies?

iii)

- What morphological details got lost while tube transformation from biosphere to geosphere?
- Is it possible to reconstruct the mineralization sequence(s)? What mineral(s) are involved?
- What kind of mineralization pattern is finally formed? Does recrystallisation processes take place?
- What similarities or variations exist between modern fossilized tubes and ancient tube fossils?

In summary, the first aim of this thesis is giving an overview of the basic processes of carbonate authigenesis, related to the access to general information of the biogeochemical characteristics of the Congo methane seeps. Furthermore, the detailed examinations of the carbonate structures are accomplished to display co-occurring variations in carbonate chemistry and the identification of the regulating factors within the pockmark sediments.

The first manuscript "***Carbonate authigenesis at the Kouilou-pockmark structures on the Congo deep-sea fan"*** provides the first systematic description of authigenic carbonate structures retrieved from three lately discovered pockmarks structures on the Congo deep-sea fan. Data of x-ray powder diffraction (XRD), stable carbon and oxygen isotope

measurements, biomarker analyses, and field emission-scanning electron microscopy (FE-SEM) are interpreted for estimations on formation conditions.

Authors: Antonie Haas, Jörn Peckmann, Marcus Elvert, Heiko Sahling and Gerhard Bohrmann

Status: submitted to Marine Geology

The second aim of this thesis deals with new insights into geobiological interactions of vestimentiferan tube worms and carbonate formation, specifically the environmental changes within the sediment after tube worm colonization.

The second manuscript "***Vestimentiferan tube worms modify carbonate precipitation - examples form methane seeps on the Congo deep-sea fan***" examines the formation and presence of carbonate aggregates at the posterior of vestimentiferan worm tubes. Main objectives are metabolism processes operated through the posterior tube, their impact on carbonate chemistry, and the consequences arising of pronounced carbonates.

Authors: Antonie Haas, Jörn Peckmann, Heiko Sahling and Gerhard Bohrmann

Status: prepared for submission to Geology

The third aim is related to the examination of taphonomic processes that are responsible for the mineralization of vestimentiferan worm tubes. The reconstruction of mineralization sequences and the identification of characteristic mineralization pattern were the main purpose of this work.

The third manuscript "***Mineralization of vestimentiferan tubes at methane seeps on the Congo Deep-Sea Fan"*** has its focus on the mineralization of vestimentiferan worm tubes while fossilisation. Tube bearing carbonates allowed the reconstruction and documentation of characteristic mineralization pattern occuring on modern vestimentiferan worm tubes, and gives fundamental information for the interpretation of fossil tubes.

Authors: Antonie Haas, Crispin Little, Heiko Sahling, Gerhard Bohrmann, Tobias Himmler and Jörn Peckmann

Status: Deep Sea Research 1, in review

3. Carbonate authigenesis at the Kouilou pockmarks on the Congo deep-sea fan

Antonie Haas[1], Jörn Peckmann [1], Marcus Elvert [1], Heiko Sahling [1], Gerhard Bohrmann[1]

[1]MARUM, University of Bremen, Leobener Str., 28359 Bremen, Germany

submitted to Marine Geology

Abstract

Different types of limestones recovered from three pockmarks (named "Kouilou pockmarks") in approximately 3100 m water depth on the Congo deep-sea fan consist of methane-derived carbonate phases including high-Mg-calcite, aragonite, and protodolomite. The carbonate aggregates are in the shape of nodules, tubes, crusts, slabs, and molds; the latter are interpreted to represent casts of former burrows of bivalves and holothurians. Pyritiferous nodules consisting of high-Mg-calcite acted as nuclei for composite aggregates. They formed relatively deep within the sediments and appear to have been primarily surrounded by microbial mats. The microbial consortium that induced nodule formation by anaerobic oxidation of methane was dominated by archaea of the phylogenetic ANME-1 group. Aragonitic crusts, on the other hand, resulted from the activity of archaea of the ANME-2 cluster closer to the seafloor. Methane is the predominant carbon source of carbonates ($\delta^{13}C$ values as low as −58.9‰ V-PDB) as well as archaeal biomarkers ($\delta^{13}C$ values as low as −140‰ V-PDB). Oxygen isotope values ranging from +3.6 to +5.3‰ V-PDB are too high for precipitation in equilibrium with seawater, probably reflecting the destabilization of gas hydrates, which are particular abundant at the Kouilou pockmarks.

Keywords: Methane seep, carbonate, pockmark, gas hydrate, biomarker, archaea, sulfate-reducing bacteria

3.1 Introduction

Hydrocarbon seepage in marine sediments is a frequently observed phenomenon in several marine settings (Suess et al., 1985; von Rad et al., 1996; Bohrmann et al., 1998; Bohrmann et al., 2002). The anaerobic oxidation of methane (AOM), conjointly operated by consortia of methane-oxidizing archaea and sulfate-reducing bacteria, is the most important biogeochemical process at methane seeps (e.g., Boetius et al., 2000). This process leads to an increase of (1) carbonate alkalinity, inducing the precipitation of carbonate minerals and (2) concentration of sulfide, which is the substrate for sulfide-oxidizing microorganisms at seeps. Authigenic seep carbonates have been intensively studied, as they provide an excellent archive of past seepage-associated processes and environmental parameters (Ritger et al., 1987; Bohrmann et al., 1998; Aloisi et al., 2000; Peckmann et al., 2001). Stable carbon isotopic compositions of carbonate phases indicate that methane is commonly the most important carbon source. Furthermore, biomarker data confirm that microorganisms are crucial for the precipitation of authigenic carbonates (Elvert et al., 1999; Peckmann et al., 1999; Thiel et al., 1999; Pancost et al., 2001; Pape et al., 2005). The composition of AOM communities varies in response to changing environmental conditions (Blumenberg et al., 2004; Nauhaus et al., 2005), which is reflected in different mineralogies of carbonate precipitates (Reitner et al., 2005a). AOM has been found to be promoted above gas hydrate-bearing sediments due to the dynamic release of methane from deeper gas reservoirs and ascending fluids (Elvert et al., 1999; Suess et al., 1999). The simultaneous release of hydrate water leads to an increase in the ^{18}O content of porewater, which has been used as an explanation for positive oxygen isotope anomalies in seep carbonates (e.g., Aloisi et al., 2000).

Here we report the results of a comprehensive study on authigenic carbonates from the Congo deep-sea fan, including petrography, mineralogy, as well as stable isotope and biomarker analyses. The carbonates recovered from near-surface sediments exhibit highly variable shapes such as nodules and slabs, tubes generated by the cementation of fluid pathways, and carbonate-casted burrows produced by benthic organisms. Carbonate mineralogy is apparently closely related to the intensity of seepage reflected by specific groups of archaea involved in AOM.

3.2 Geological setting

Seafloor spreading initiated the creation of the passive continental margin of southwest Africa in the Early Cretaceous. In the Early Aptian up to 1000 m thick salt-deposits accumulated, which were subsequently buried by black shale and bituminous sandstones during anoxic conditions in the Late Aptian (Unzelmann-Neben, 1998). The formation of an aggradational carbonate/siliciclastic ramp started in the Late Cretaceous and lasted until the Early Oligocene, followed by the deposition of primarily land-derived sediments (Séranne, 1999). Almost the entire Equatorial Africa has been drained by the Congo River system since the Miocene. Today, riverine influx of terrigenous sediment induces suspension clouds that support the high productivity zone of the Congo River estuary (Schneider at al., 1997). In prolongation of the Congo River mouth, deep incisions and strong erosion favor the transport of riverine terrigenous material directly into the deep-sea. This process resulted in the formation of a 2000 to 3000 m thick sediment fan, that reaches down to the lower Congo basin (Gay et al., 2006).

An area with several pockmarks was identified by detailed seismic and echo-sounding profiling in approximate 3100 m water depth on the deep-sea fan during cruises M47/3 and M56 with RV Meteor (Sahling et al., 2008; Fig.1). The so-called “Kouilou pockmarks” range from several tens to hundreds of meters in diameter and a few to tens of meters in depths. They include three large individual pockmarks, namely “Worm Hole”, “Hydrate Hole”, and “Black Hole”. These pockmarks are characterized by columnar zones of seismic blanking generated by focused fluid migration and strong subsurface reflectors, which represent gas hydrate and carbonate deposits (Spiess et al., 2006; Sahling et al., 2008).

The seepage of methane-bearing fluids is probably due to the remobilization of hydrocarbons from the Late Aptian black shale sediments migrating through salt-diapirs (Emery et al., 1975). However, there is also evidence for an alternative origin of fluids from buried channel-levee systems of ancient turbidity currents (Gay et al., 2006).

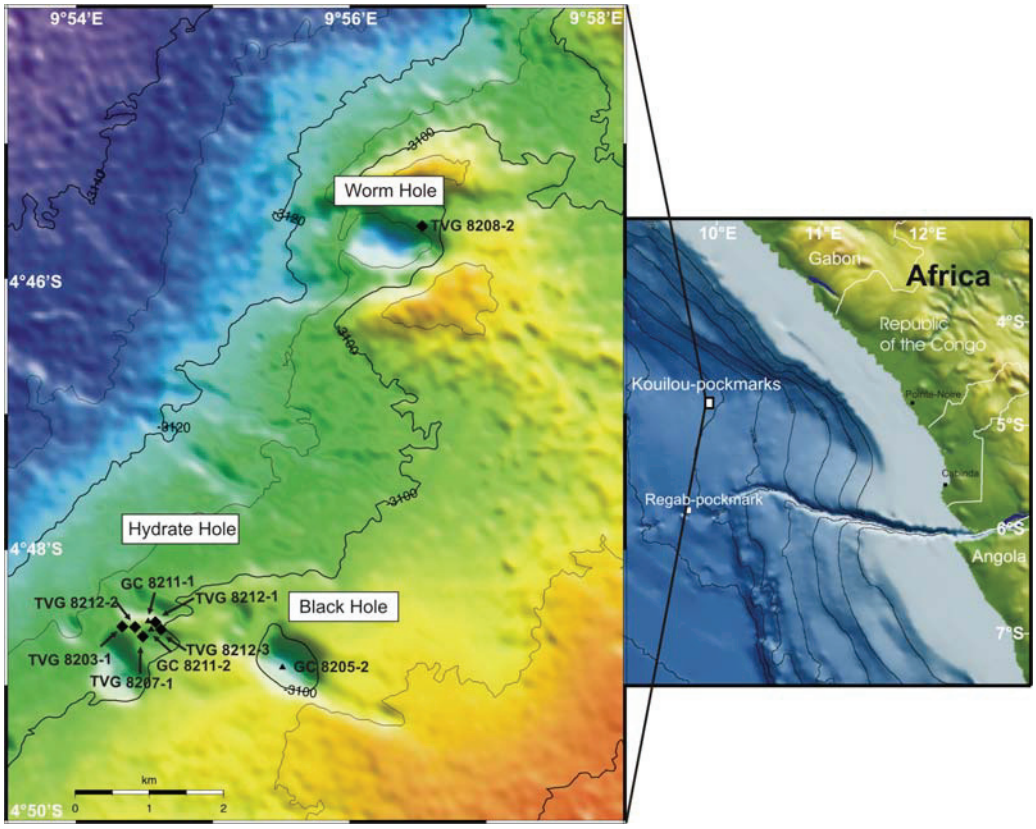

Figure 1. Right: Overview-map of the south-west African continental margin, the Congo River estuary, and the Congo Canyon; modified after Sahling et al. (2008). Left: Map showing the position of the Kouilou pockmarks named "Worm Hole", "Black Hole" and "Hydrate Hole". Symbols indicate sampling positions during RV METEOR Cruise M56 (triangles = gravity cores, diamonds = TV-guided grabs).

3.3 Methods

A total of 34 carbonate samples (Tab. 1) from 3 gravity cores (GC) and 6 TV-guided grabs (TVG) were selected for detailed analyses after visual examination. Samples were preferentially taken from TV-grab stations (GeoB 8203-1, 8207-1, 8212-1, 8212-2, 8212-3 (Hydrate Hole), and 8208-2 (Worm Hole); see Fig. 1 for locations). Four samples were taken from gravity cores GeoB 8211-1, 8211-2 (Hydrate Hole) and 8205-2 (Black Hole). The samples were examined and categorized according to their shape and macroscopic features. Afterwards, the samples were cut into sections for sub-sampling, thin section preparation, x-ray powder diffraction (XRD), field emission-scanning electron microscopy (FE-SEM), stable carbon and oxygen isotope measurements, and biomarker analyses.

Location	Water depth	Sample	$\delta^{13}C$	$\delta^{18}O$
Hydrate Hole				
TVG 8203-1	3110 m	8203-1-11/1	−45.1±0.01	4.2±0.06
Latitude	**Longitude**	8203-1-11/2	−55.6±0.07	5.0±0.04
04°48.57' S	009°54.50'E	8203-1-11/3	−43.8±0.05	4.1±0.03
		8203-1-12/1	−54.5±0.04	4.2±0.04
TVG 8207-1	3109 m	8207-1-40/1	−57.4±0.07	3.9±0.01
Latitude	**Longitude**	8207-1-40/2	−57.7±0.05	4.2±0.01
04°48.59' S	009°56.46' E	8207-1-41/1	−58.0±0.05	3.9±0.03
		8207-1-41/2	−56.4±0.04	3.7±0.04
		8207-1b/1	−54.8±0,05	4.2±0,07
		8207-1b/2	−51.8±0,05	5.1±0,07
		8207-1b/3	−55.7±0,05	4.9±0,07
		8207-1c/1	−54.9±0,05	4.5±0,07
		8207-1c/2	−50.5±0,05	4.3±0,07
GC 8211-1	3109 m	8211-1-1/1	−44.2±0.05	3.9±0.01
Latitude	**Longitude**	8211-1-1/2	−45.6±0.03	3.9±0.02
04°48.55' S	009°54.55' E	8211-1-2/1	−54.1±0.05	4.0±0.03
GC 8211-2	3111 m	8211-2-1/2	−52.4±0.05	5.1±0.03
Latitude	**Longitude**			
04°48.56' S	009°54.53' E			
TVG 8212-1	3110 m	8212-1-3/1	−51.1±0.02	4.4±0.01
Latitude	**Longitude**	8212-1-3/2	−49.3±0.04	4.8±0.01
04°48.56' S	009°54.56' E	8212-1-3/3	−50.7±0.04	3.9±0.03
		8212-1-3/4	−49.0±0.04	4.0±0.02
		8212-1-20a/1	−47.0±0.06	4.1±0.04
		8212-1-20a/2	−50.9±0.04	5.3±0.02
		8212-1-7/1	−49.5±0.05	4.4±0.01
		8212-1-7/2	−55.9±0.04	3.8±0.04
TVG 8212-2	3113 m	8212-2a	−57.9±0.04	4.1±0.01
Latitude	Longitude	8212-2c/1	−53.3±0.05	4.0±0.01
04°48.56' S	009°54.50' E	8212-2-17a	−56.4±0.04	4.5±0.02
		8212-2-17c/1	−53.5±0.05	4.2±0.03
		8212-2-17c/2	−49.9±0.03	3.6±0.01

TVG 8212-3	3109 m	8212-3-29a/1	–49.9±0.03	5.1±0.02
Latitude	**Longitude**	8212-3-29a/2	–30.6±0.04	4.0±0.04
04°48.57' S	009°54.57' E	8212-3-29a/3	–32.4±0.03	4.3±0.02
		8212-3-29a/4	–46.2±0.03	4.7±0.04
		8212-3-13a/3	–30.5±0.02	4.1±0.02
		8212-3-13a/1	–48.3±0.06	4.3±0.03
Worm Hole				
TVG 8208-2	3120 m	8208-2-1	–47.7±0.06	4.0±0.03
Latitude	**Longitude**	8208-2-2	–45.7±0.05	4.0±0.04
04°45.61' S	009°56.53'E	8208-2-1K	–49.6±0.02	5.0±0.02
		8208-2-2K	–48.1±0.02	4.9±0.02
		8208-2-3K	–43.5±0.02	5.0±0.02
		8208-2-4K	–45.4±0.01	5.1±0.03
		8208-2-5K	–48.6±0.02	4.8±0.01
		8208-2-2F	–46.6±0.02	4.7±0.02
Black Hole				
GC 8205-2	3118m	8205-2 a/1	–54.8±0.05	4.6±0.07
Latitude	**Longitude**	8205-2 a/2	–50.4±0.05	4.7±0.07
04°48.80' S	009°55.45' E			

Table 1. List of carbonate precipitates examined including location, water depth, and stable C and O isotope data.

Qualitative and semi-quantitative mineralogical composition of the samples was analyzed by XRD measurements using a Philips PW 1820 instrument (CoKα) at the Alfred-Wegener-Institute in Bremerhaven. The samples were ground with an agate mortar and pestle, mixed with an internal standard (α-Al_2O_3), homogenized with ethanol and prepared as random oriented powder slides. Scans were run between 20° to 60° at a scanning speed of 0.01° 2θ steps. Semi-quantitative abundances of different carbonate minerals were determined using standard calibration curves of different mineral mixtures (precision ± 3 wt %). The shift in the d (104) calcite peak was used to determine the $MgCO_3$ content of Mg-calcite according to Lumdsen (1979). Thin sections were stained with a mixture of potassium ferricyanide and alizarin red dissolved in 0.1% HCl or Feigl's solution and examined with a petrographic microscope under transmitted light. A LEO 1530 Gemini field emission-scanning electron microscope (FE-SEM) with an energy-dispersive X-ray spectrographic analyzer (EDX) was used for microfabric analysis and phase identification (Earth Science Department, University

of Göttingen). Samples for stable carbon and oxygen isotope analyses were obtained by using a hand-held micro drill. The sample powders were treated with 100% phosphoric acid at 75°C in an online carbonate preparation line (Carbo-Kiel-single sample acid bath) connected to a Finnigan Mat 251 mass spectrometer at the Center for Marine Environmental Research (MARUM) at the University of Bremen. All isotope values are expressed using the δ-notation relative to the Vienna Peedee Belemnite Standard (V-PDB) and are reported in per mil (‰) with a standard deviation of ≤ 0.07‰. Calculations of $\delta^{18}O_{aragonite+calcite}$ were performed assuming a bottom water temperature of 2.5°C and 0.2 ‰ SMOW (cf., Pierre and Fouquet, 2007) after Hudson and Anderson (1989) and Kim and O'Neil (1997), respectively. Total carbon contents were obtained with a Vario EL III analyzer at the MARUM.

Two carbonate samples (GeoB 8212-2a and 8207-1b) were chosen for biomarker analysis at the MARUM. The samples were crushed (about 5 to 6 g), spiked with internal standards of known concentration, and ultrasonically extracted three times with 50 ml dichloromethane/methanol (2:1, v:v). Separation of the lipid extracts into three compound fractions (hydrocarbons, ketones, and alcohols) was performed by column chromatography using silica gel SPE glass cartridges (Niemann et al., 2005). Elemental sulfur was removed from the hydrocarbon fractions by adding activated copper and stirring for 2 h. Alcohols were analyzed as trimethylsilyl ethers (TMS-derivatives) formed by reaction with bis-(trimethylsilyl)triflouroacetamid in pyridine (70°C, 1 h). Hydrocarbons and alcohol TMS-derivatives were identified using a Thermo Finnigan DSQ equipped with a 30-m DB-5MS fused silica capillary column (0.32 mm ID, 0.25 μm film thickness). The gas chromatograph (GC) temperature program used was: injection at 60°C, 2 min. isothermal; from 60°C to 150°C at 10°C $min.^{-1}$; from 150°C to 310°C at 4°C min^{-1}; 45 min. isothermal. Using identical GC conditions, biomarker concentrations were determined with a Thermo Finnigan Trace GC and flame ionization detection. Likewise, compound-specific carbon isotope analyses were carried out with a Thermo Electron Trace GC coupled via a Thermo Electron GC-combustion-III-interface to a Thermo Electron $Delta^{plus}$ XP mass spectrometer. Carbon isotope ratios of alcohols have been corrected for the addition of carbon atoms during TMS-formation. Reported biomarker $\delta^{13}C$ values have a standard deviation of ≤ 0.6‰.

3.4 Results

3.4.1 Seafloor observations and sediments at the pockmark sites

Seafloor investigations revealed very similar surface features at the three investigated pockmarks. Numerous carbonate precipitates are distributed on the seafloor within the pockmarks (Fig. 2A-C) and the sediments.

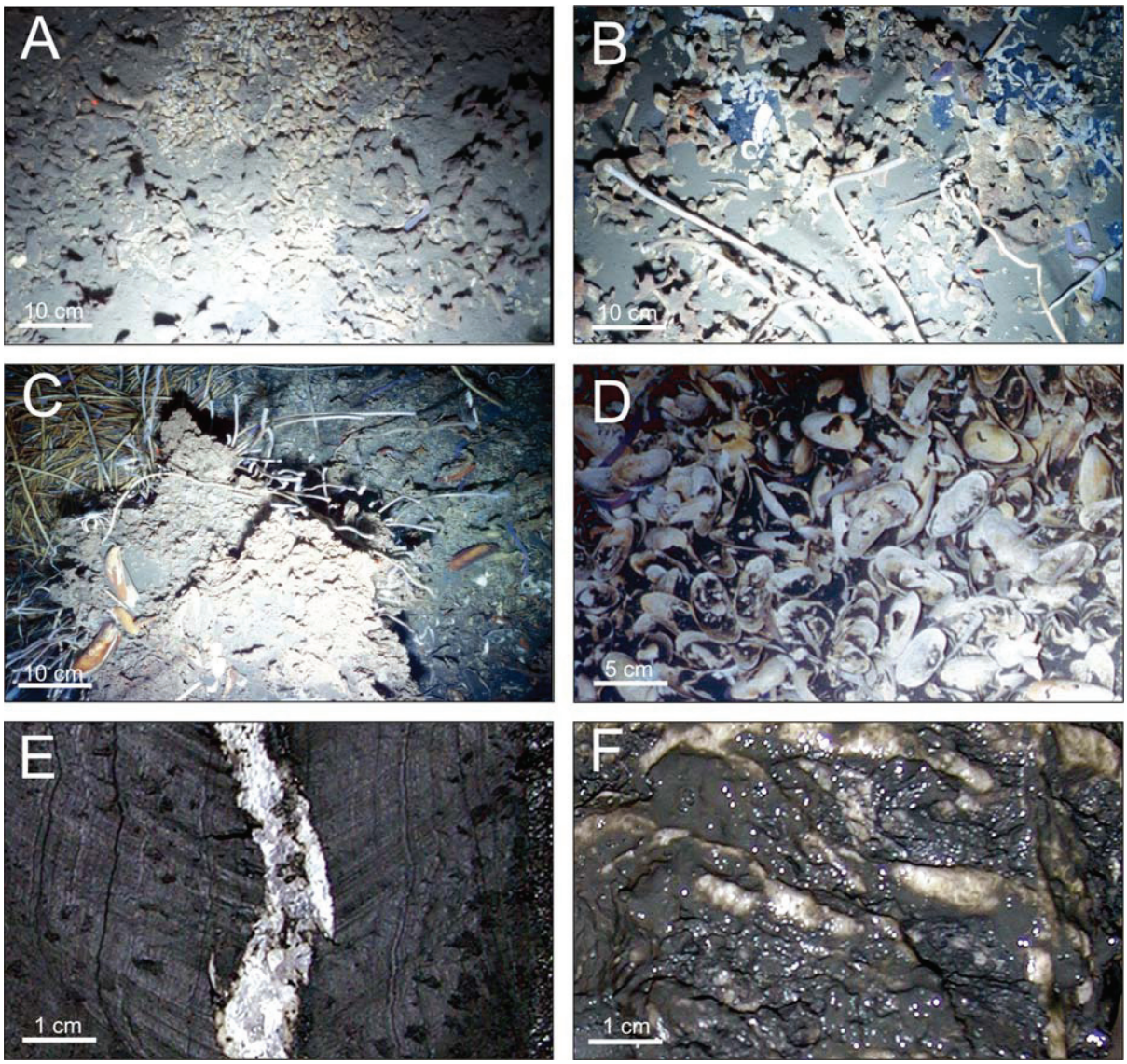

Figure 2. Photographs of seafloor features at the Kouilou-pockmarks taken by a towed camera sled. (A) Carbonate crusts covered by sediment at Worm Hole pockmark. (B) Irregular carbonate crusts and tubes of vestimentiferan tube worms at Black Hole pockmark. (C) Exposed carbonate densely populated by vestimentiferan tube worms and mytilid bivalves at Worm Hole pockmark. (D) Area of seepage characterized by dark-gray sulfide-rich sediments, clusters of clams, and holothurians at the Hydrate Hole pockmark. (E) A vertically orientated gas hydrate vein penetrating the hemipelagic mud of GC 8211-2, taken at Hydrate Hole pockmark. (F) Horizontally layered gas hydrate aggregation in sediments of core GeoB 8205-2 from Black Hole pockmark.

The pockmarks are also characterized by vestimentiferan tube worm colonies, ranging in size from several meters to tens of meters in diameter, abundant holothurians, and solemyid and vesicomyid clams, as well as mytilid mussels (Fig. 2C, D). Carbonate mineralization directly associated with vestimentiferan tubes is described elsewhere (Haas et al., submitted). Gas-expansion cracks and gas hydrates were found in almost all gravity cores at different depths in the hemipelagic sediments represented by olive-green mud that contains diatoms, foraminifera, minor amounts of pyrite, and feldspars. Gas hydrates occurred as vertical vein-like conduits (Fig. 2E) or as irregular layers of variable width (Fig. 2F).

3.4.2 Authigenic carbonates

3.4.2.1. Nodular carbonates

Precipitates of nodular shape and up to 2 cm in diameter represent the smallest carbonate samples obtained (Fig. 3A). The nodules consist of high-Mg-calcite (<40 wt. %) that is cementing background sediment. They are homogenous and medium to dark gray in color (Fig. 3A, B). $MgCO_3$ contents range from 10 to 13 mol% (mean: 11.5 mol %), and are the lowest of all high-Mg-calcites analyzed. Dispersed pyrite is abundant in the matrix of the nodules, and a few nodules are surrounded by pyrite seams. FE-SEM and combined EDX-analyses indicate that some nodules are coated by organic substances, possibly representing remains of microbial mats (Fig. 3B).

Nodules either occur (1) scattered in the sediment or (2) incorporated in composite authigenic carbonate aggregates (Fig. 3C). Nodules within composite carbonates are clearly recognizable and are often overgrown by acicular aragonite (Fig. 3D). In some composite carbonate aggregations, nodules are volumetrically dominant (Fig. 3C-E). Nodules are particularly abundant in carbonate aggregations surrounding the posterior ends of tube worm colonies (Fig. 3F). Many composite carbonate precipitates even exhibit a bulbous outer shape due to enclosed nodules (Fig. 3E, F).

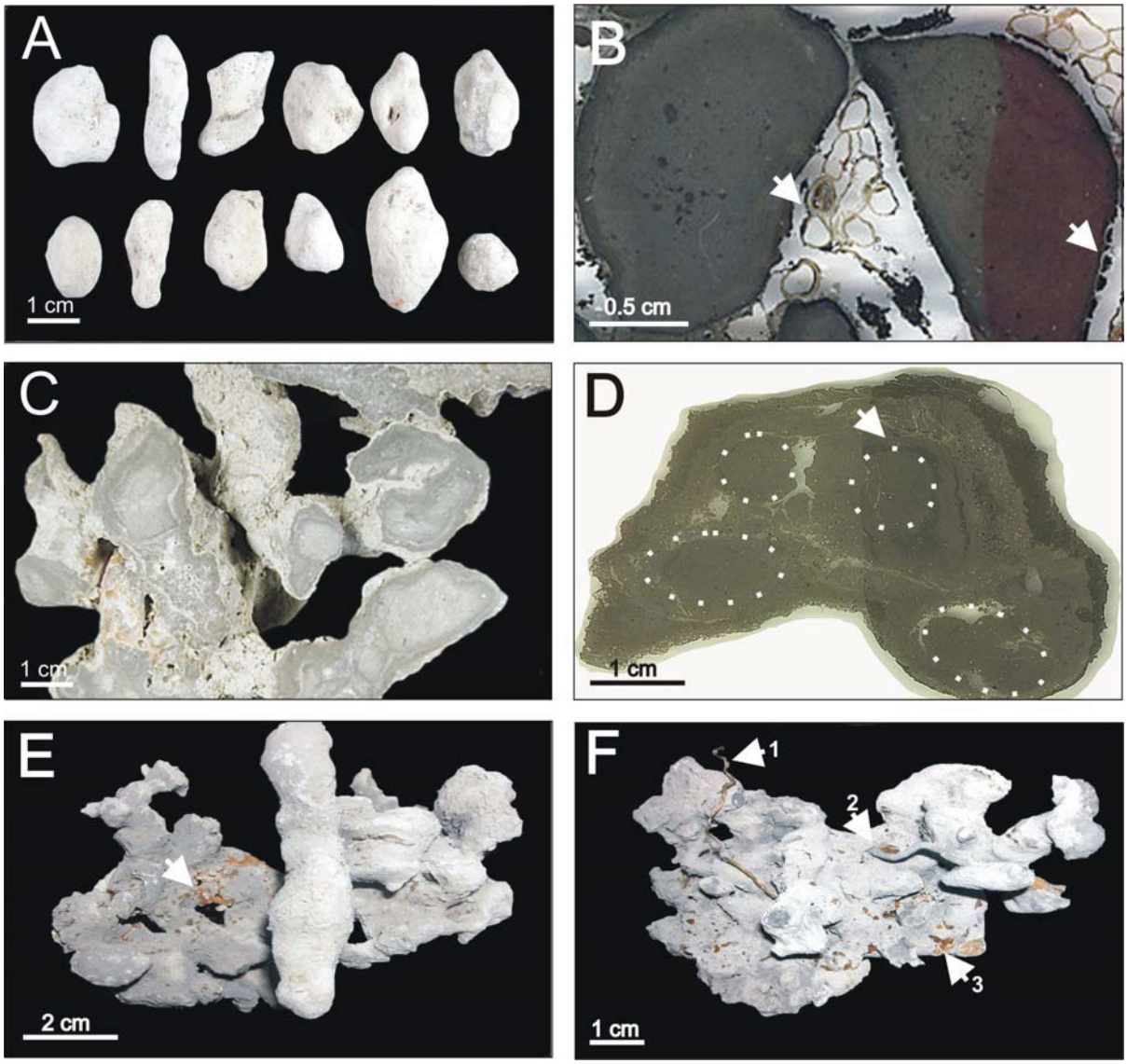

Figure 3. Nodular carbonates and composite carbonate aggregations containing nodules. (A) Nodular carbonates are the smallest precipitates found at the Kouilou pockmarks (GeoB 8208-2 Worm Hole; GeoB 8203-1 Hydrate Hole). (B) Nodules covered by organic matter (right arrow; residual microbial mat?). Posterior part of vestimentiferan worm tubes (left arrow; GeoB 8203-2-1 Hydrate Hole). (C) Nodules cemented by later authigenic carbonate (GeoB 8212-2 Hydrate Hole). (D) Composite aggregate containing nodules. The arrow points to aragonite layers surrounding a nodule (Feigl's solution stained thin section, right part; GeoB 8212-2d). White dotted lines indicate nodule margins. (E) Highly irregular composite aggregate with nodules. The arrow indicates botryoidal aragonite. (F) Composite aggregate from the posterior part of a vestimentiferan tube worm settlement. Organic worm tubes (arrow 1) occur beside completely lithified tubes (arrow 2). Botryoidal aragonite is forming the surface of the aggregate in places (arrow 3).

3.4.2.2. Carbonate-filled molds

Carbonate precipitates related to bioturbation show rather irregular shapes, representing casts of burrows. The elongated aggregates with smooth surfaces are up to 3 cm in diameter and up to 15 cm in length (Fig. 4A). A relation of this type of aggregate to the burrowing activity of bivalves is supported by the presence of shell fragments of thyasirid clams enclosed in two samples. Micritic high-Mg-calcite forms the matrix of these carbonates and is accompanied by minor acicular aragonite. Other elongated carbonate aggregates show small-scale layering of aragonite and high-Mg-calcite, which may has been caused by burrowing organisms (Fig. 4B-D). The diameter of these aggregates is identical to that of holes generated by holothurians. A few samples of this type of carbonate contain protodolomite, represented by $MgCO_3$ contents of 37.5 mol%. Individual dolomite crystals, showing no indication of recrystallisation, were also detected by FE-SEM.

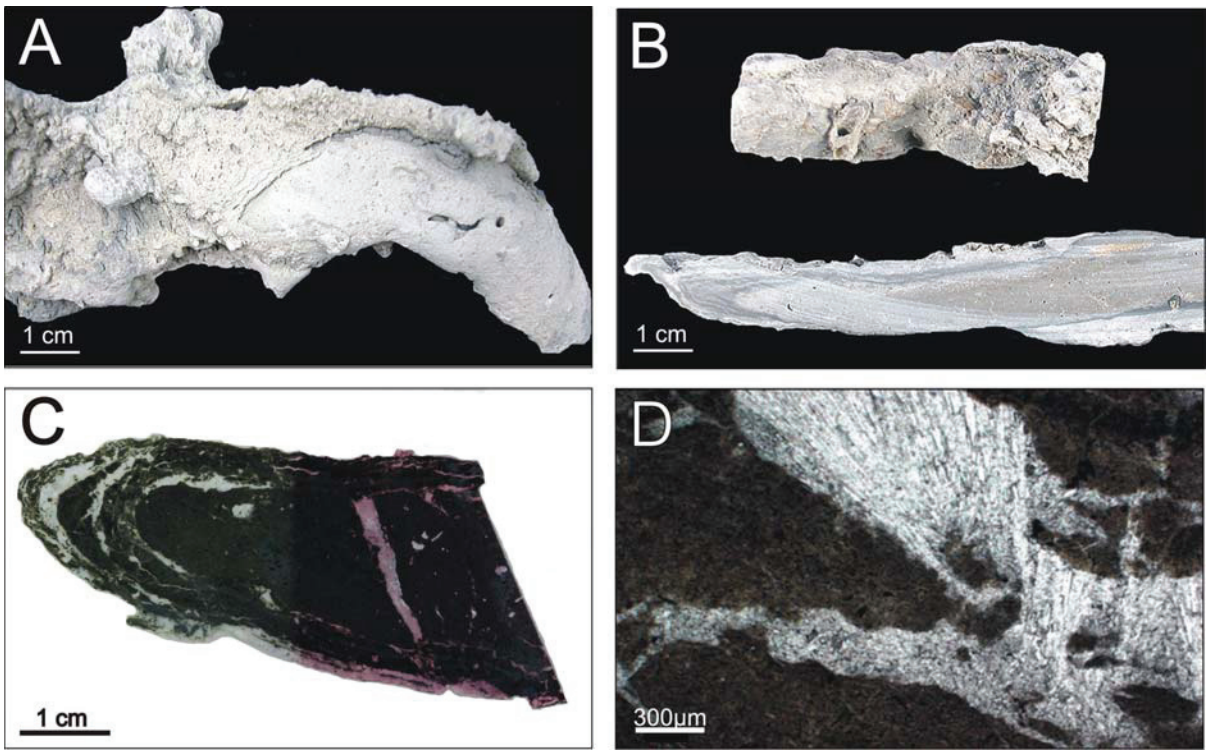

Figure 4. Bioturbation-related carbonate precipitates. (A) Elongated carbonate aggregate that precipitated in a burrow supposedly produced by a bivalve. (B) Elongated carbonate aggregate that probably formed in a holothurian burrow. (C) Thin section of an elongated carbonate (GeoB 8212-2g) displaying small-scale interbedded layers of aragonite cement within microcrystalline high-Mg-calcite. (D) Detail of (C) revealing acicular aragonite in the micritic matrix.

3.4.2.3. Carbonate crusts and slabs

Carbonate crusts and more irregular slabs are characterized by rough surfaces (Fig. 5A). Thickness of the platy carbonates ranges from a few mm to a few cm; lengths and widths are up to 10 cm (Fig. 5B). Almost all thin crusts contain pure aragonite. The total carbonate content is up to ~60 wt. %. Some crusts consist of several layers representing successive generations of carbonate formation. Beneath an uppermost layer, younger layers with mineralized fluid conduits underneath are found, indicating downward-directed aggregation (cf., Greinert et al., 2002; Peckmann et al., 2002). Sample GeoB 8212-1-3, a crust formed of three layers, varies in its mineralogical composition. Whereas the two upper layers consist of pure aragonite, the lower layer is made of a mixture of aragonite (87% of the total carbonate content) and high-Mg-calcite. Moreover, the total carbonate content in the lower layer is very low (approximately 38 wt. %). Both upper layers contain about 51 wt. % carbonate. Barite and organic material (putative remains of microbial mats) are found to cover some crusts and slabs (Fig. 5C, D).

3.4.2.4. Carbonate tubes

Tubular carbonate aggregates (Fig. 5E, F) up to 20 cm in length probably represent preserved conduits of fluid-seepage. They are characterized by partial or complete lack of sediment infill. The internal openings vary between 1 and 3 cm in diameter. The massive, often more than 1 cm thick tube walls consists of microcrystalline high-Mg-calcite (15 mol% $MgCO_3$). Patches of microcrystalline and acicular aragonite are sometimes present close to or on exterior and interior surfaces. The total carbonate content is around 40 wt. %.

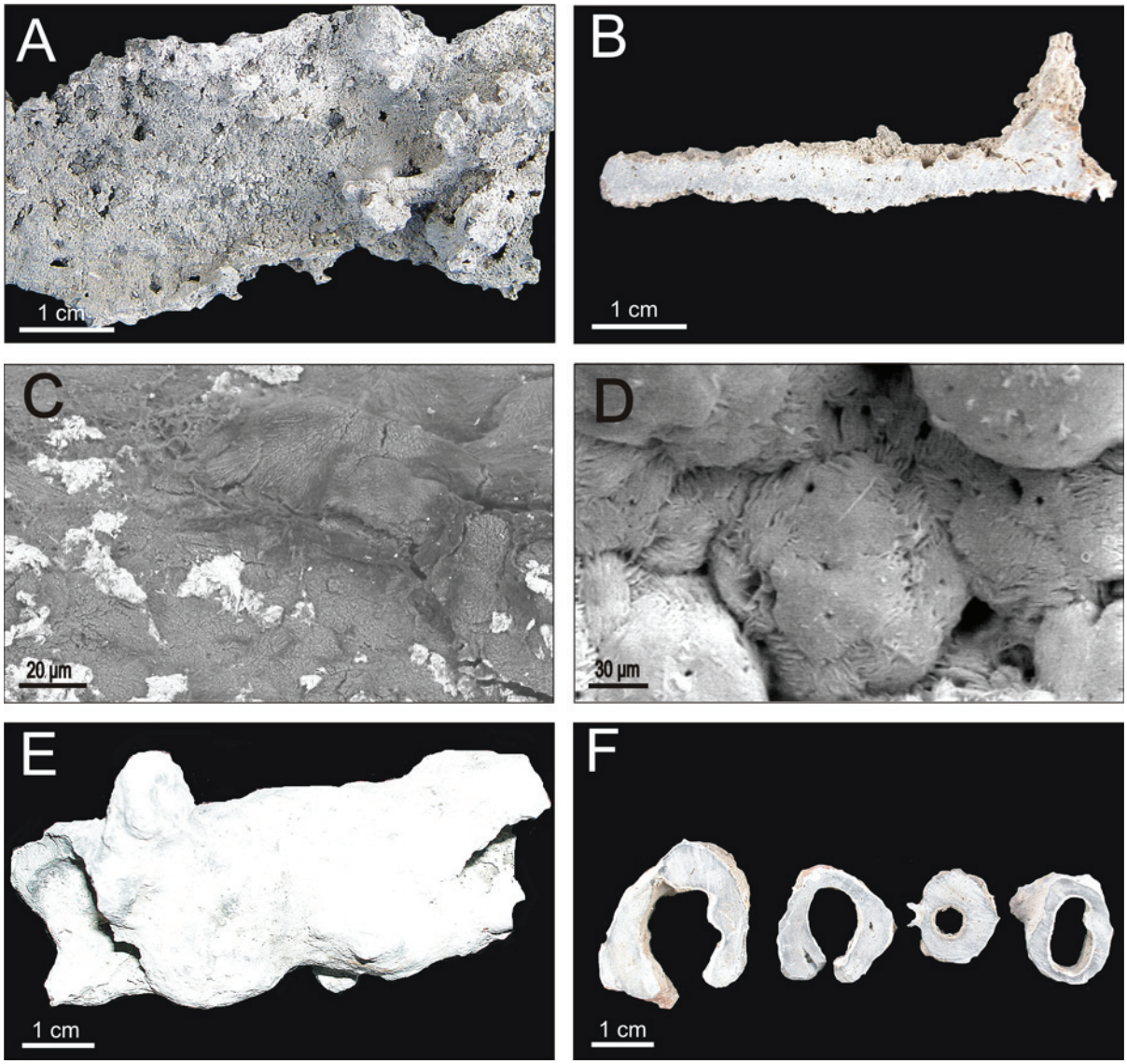

Figure 5. (A) Carbonate crusts are characterized by very rough surfaces (GeoB 8207-2 Hydrate Hole). (B) Cross section of a carbonate crust. (C) FE-SEM photomicrograph of slab surface, back scatter image. Scattered whitish barite precipitates and putative organic matter (blackish) on aragonite (dark-gray). (D) Individual barite crystals in larger aggregates reveal a platy habit. (E) Carbonate tube with a massive wall resembling gas hydrate conduits (GeoB 8212-1, Hydrate Hole). (F) Cross sections of some tubes (GeoB 8212-1, GeoB 8212-2, GeoB 8212-3, all Hydrate Hole; GeoB 8208-2 Worm Hole).

3.4.3 Stable carbon and oxygen isotopic composition

$\delta^{13}C$ values of carbonate bulk samples (mixture of at least two mineralogies) show a wide range from −58.9 to −30.5‰ (mean: −49.7 ± 6.8‰; n = 46, Fig. 6).

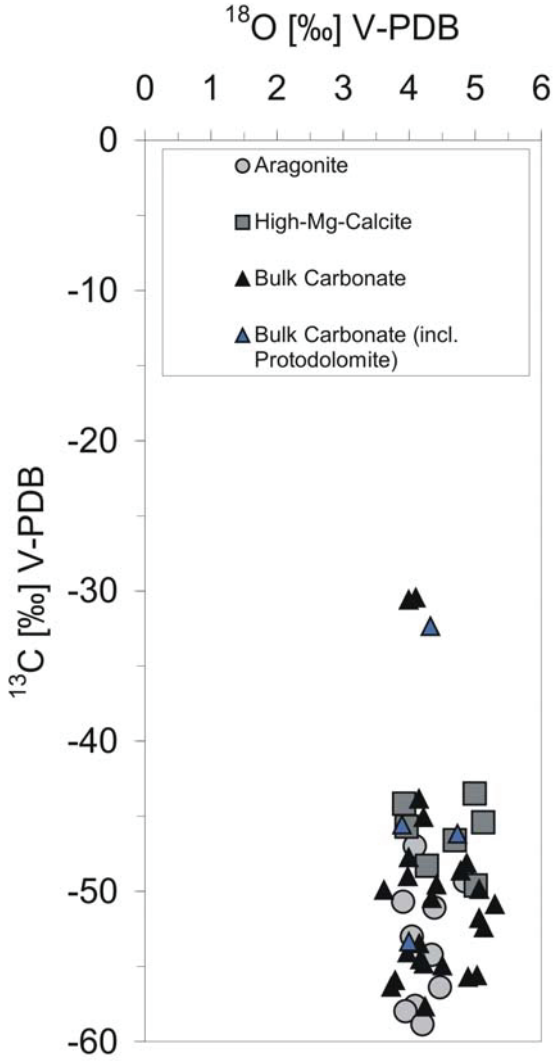

Figure 6. Stable carbon and oxygen isotopic compositions of the Kouilou pockmark carbonates.

Several isotope values were obtained for pure aragonite and high-Mg-calcite samples. The values of pure aragonite vary from −58.9 to −50.0‰ (mean: −53.6 ± 4.1‰; n = 10), whereas high-Mg-calcite revealed slightly less negative values ranging from −49.6 to −43.5‰ (mean: −46.2 ± 2.2‰; n = 7; Fig. 7, left). Carbon isotope compositions show little variations

between the different pockmarks. Although samples from Black Hole yielded the least negative $\delta^{13}C$ values (mean: –46.9‰), this difference is rather a function of mineralogy than of location. Black Hole samples consist of nearly pure high-Mg-calcite. Carbon isotope compositions of protodolomite-containing bulk carbonates are in the range of high-Mg-calcites. Stable oxygen isotope compositions of all samples vary between +3.6 and +5.3 ‰ (mean: 4.4 ± 0.5‰; n = 34; Fig. 6). $\delta^{18}O$ values for pure aragonite range from +3.9 to +4.8 ‰ (mean: +4.2 ± 0.3‰; n = 10). High-Mg-calcite varies from +3.9 to +5.1‰ (mean: +4.6 ±0.5‰; n = 7). $\delta^{18}O$ values of aragonite are on average less positive than those of high-Mg-calcite (Fig. 7, right). There is no apparent difference in $\delta^{18}O$ values between the three sites. Likewise, $\delta^{18}O$ values of carbonates containing protodolomite show little variability (+3.9 to +4.3‰), although the samples were obtained from different sites within the Hydrate Hole pockmark.

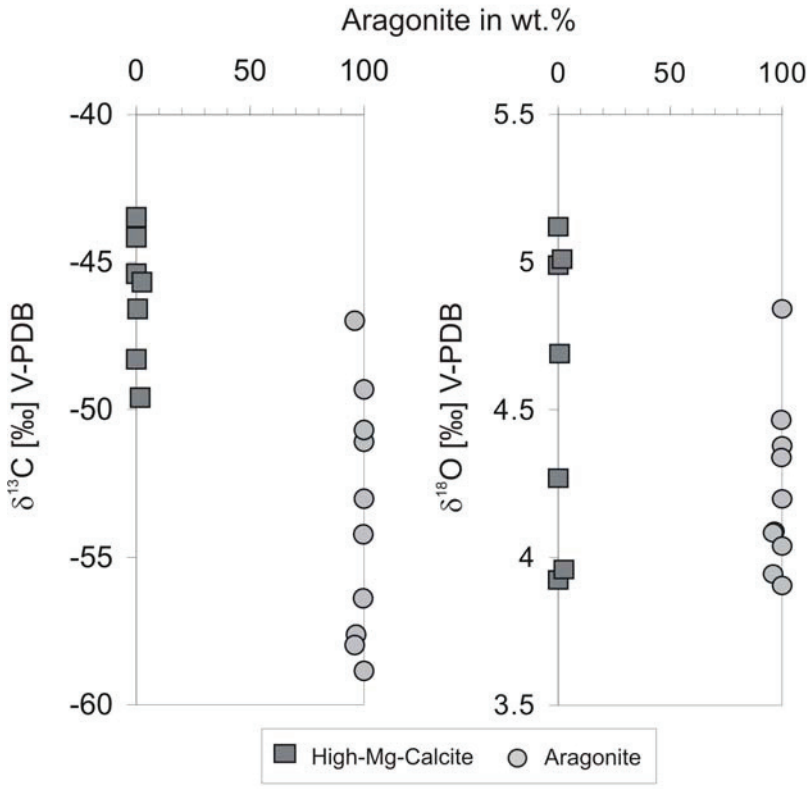

Figure 7. Stable carbon (left) and oxygen (right) isotope ratios related to aragonite and calcite contents (0 wt.% aragonite correspond to 100 wt.% high-Mg-calcite).

3.4.4. Biomarker analyses

Results of biomarker analyses of two carbonate precipitates (high-Mg-calcite sample GeoB 8212-2a and aragonite sample GeoB 8207-1b) from Hydrate Hole are shown in Table 2.

	ANME-1 dominated	**ANME-2 dominated**
	8212-2/a (surface)	**8207-1b/1 (surface)**
	Contents (in µg g^{-1} carbonate dry weight)	
Crocetane	0.14	1.55
PMI	0.23	0.58
PMI:2	0.23	0.07
DAGE C31:1b	0.51	0.80
DAGE C32:2a	0.06	3.32
DAGE C32:2b	0.58	1.27
DAGE C33:2	1.39	1.41
Archaeol	0.65	11.72
***sn*-2-hydroxyarchaeol**	0.33	25.19
	Stable carbon isotope compositions ($\delta^{13}C$ in ‰ versus V-PDB)	
Crocetane	–87	–140
PMI	–129	–101
PMI:2	–136	nd
DAGE C31:1b	–121	–112
DAGE C32:2a	nd	–118
DAGE C32:2b	–114	–117
DAGE C33:2	–119	–116
Archaeol	–135	–132
***sn*-2-hydroxyarchaeol**	–137	–134

Table 2. Contents and stable carbon isotope compositions of biomarkers indicative for ANME-communities in two carbonate samples from Hydrate Hole pockmark (ndet: not detected, nd: not determined). The abbreviation scheme used for the DAGEs is based on Elvert et al. (2005).

Both samples contain significant amounts of specific biomarkers attributed to methanotrophic archaea (cf., Elvert et al., 1999; Hinrichs et al., 1999; Thiel et al., 1999) involved in AOM (crocetane, crocetene (Cr:1), pentamethylicosane (PMI), its diunsaturated

homologue (PMI:2), archaeol, and *sn*-2-hydroxyarchaeol). Moreover, a series of non-isoprenoidal dialkyl glycerol diethers (DAGEs), ranging from $C_{30:0}$ to $C_{34:2}$, all of which have been reported earlier (Hinrichs et al., 2000; Pancost et al., 2001, Elvert et al., 2005), is detected with highest amounts found for the DAGEs $C_{31:1b}$, $C_{32:2a}$, $C_{32:2b}$, and $C_{33:2}$. Stable carbon isotope analyses show that all biomarkers are highly depleted in ^{13}C. $\delta^{13}C$ values of biomarkers of known archaeal origin range from –140 and –129‰, with exceptions detected for crocetane in sample GeoB 8212-2a (–87‰) and PMI in sample GeoB 8207-1b (–101‰). DAGEs are usually less ^{13}C-depleted than the archaeal biomarkers, showing $\delta^{13}C$ values in the range from –121 to –112‰.

3.5 Discussion

3.5.1. Implications on geochemical patterns

3.5.1.1 Stable carbon isotope compositions

The strongly negative carbon isotope compositions of carbonates (as low as –58.9‰; Fig. 6) from the three Kouilou pockmarks reveal ^{13}C-depleted methane as the main carbon source. Parent methane is usually significantly more depleted in ^{13}C than the resulting carbonate precipitates (Peckmann and Thiel, 2004). Since gas hydrate-bound methane at the close-by REGAB pockmark shows a $\delta^{13}C$ value of –69.3‰ (Charlou et al., 2004), a microbial origin of methane is likely. Only three bulk carbonate samples from the central part of Hydrate Hole display significantly less negative $\delta^{13}C$ values of around –30‰ (Fig. 6). These values either reflect relative enrichment in ^{13}C as a function of increasing maturity (cf., Whiticar, 1999) and ongoing consumption of methane, or a higher contribution of carbonate from other sources (e.g., marine carbonate). However, the first scenario seems unlikely, as other samples recovered from the same site (GeoB 8212-3, GC GeoB 8211-1) show much lower values.

Nodules at Kouilou pockmarks formed during an initial stage of carbonate precipitation. As they cement background sediment, their least negative carbon isotope values probably reflect significant admixture of shell carbonate (e.g., foraminifera). Almost all bulk samples follow a trend of high-Mg-calcite contents corresponding to relatively high $\delta^{13}C$ values (Fig. 6). This trend may be partly explained by more admixtures of detrital

carbonates in calcite rather than in aragonite phases. Systematic variations of carbon isotope composition related to mineralogy were previously observed for stable oxygen isotope signals of carbonates from the Cascadian subduction zone (Bohrmann et al., 1998). In this respect it is interesting to note that carbonate mineralogy is probably a function of methane flux intensity and related to microbial consumption efficiency and kinetic isotopic fractionation. Luff and Wallmann (2003) suggested that the occurrence of aragonite reflects high methane flux rates and efficient methane oxidation. Assuming that stronger ^{13}C depletion correlates with higher methane fluxes, this scenario can explain the offset between $\delta^{13}C$ values of calcite and aragonite of the Kouilou carbonates.

3.5.1.2 Stable oxygen isotope compositions

The stable oxygen isotopic composition of authigenic carbonates provides further information about environmental conditions such as the fluid source and temperature during precipitation (e.g., Han et al., 2004). Carbonate precipitation is accompanied by a temperature-depended oxygen isotope fractionation relative to the solution from which the carbonates precipitate. This fractionation would lead to $\delta^{18}O$ values of +3.9‰ for the Kouilou aragonites and +3.5‰ for the Kouilou calcites at the present bottom water temperature, respectively (cf., Kim and O'Neil, 1997; Hudson and Anderson, 1989). These calculations differ slightly from the measured average $\delta^{18}O$ value of +4.2±0.3 for aragonite, and differ significantly for high-Mg-calcite (+4.6±0.5). Tarutani et al. (1969) first recognized a discrepancy of the oxygen isotope fractionation in the presence of Mg^{2+} in the calcite lattice, and concluded that the incorporation of one mol% Mg^{2+} causes an increase in $\delta^{18}O$ of +0.06‰ at a temperature of 25°C. Consideration of this factor minders the resulting discrepancy in the Kouilou samples to approximately +0.7‰ with respect to the calculated value of +3.5‰ for high-Mg-calcites. Even wider offsets between measured and calculated values for calcite compared to aragonite have previously been reported from other locations as well (Bohrmann et al., 1998; Pierre and Fouquet, 2007).

Another parameter that influences oxygen isotope ratios is pH; the reduction of one pH-unit results in an increase in the $\delta^{18}O$ value of +1.42‰ in calcium carbonate (Zeebe, 1999). The pH values in sediment cores from the different Congo pockmarks varied between 7.5 and 7.8, and hydrate bearing sediments (Geo 8212-5) showed small-scale variations from 7.6 to 8.5, possibly as a result of gas hydrate water admixture (S. Kasten, pers. comm.).

However, it is unknown, if these values reflect the conditions during mineral precipitation. Kim and O'Neil (1997) calculated ^{18}O contents for carbonate precipitation initiated at pH 7.8. For example, a difference of 0.7 units to a pH value of 8.5 would already lead to an offset of around −1‰. Applying this to the Kouilou carbonates, aragonites might precipitate at higher pH values.

Water derived from clay mineral dehydration (e.g., smectite-illite transformation) in greater depths could be another factor that may cause higher ^{18}O contents in carbonates (Dählmann and DeLange, 2003). An apparently more obvious explanation for Kouilou carbonates is gas hydrate destabilization. Gas hydrate bearing sediments have been found in depths greater than 0.5 m at all Kouilou pockmarks (Sahling et al., 2008). During gas hydrate formation, water enriched in ^{18}O is preferentially incorporated into the hydrate, whereas the surrounding fluids become depleted in ^{18}O. The opposite effect occurs during gas hydrate destabilization when ^{18}O-enriched water is released. $\delta^{18}O$ measurements of such waters at other locations revealed values of up to +3.0‰ SMOW (Davidson et al., 1983). Unusually high $\delta^{18}O$ values of carbonates from gas hydrate-bearing seep sites from the Cascadia subduction zone (Bohrmann et al., 1998), the eastern Mediterranean Sea (Aloisi et al., 2000), and the REGAB pockmark field in the vicinity of the Kouilou pockmarks (Pierre and Fouquet, 2007) have been explained by this effect. It seems likely that gas hydrate dissociation is to the most part responsible for the unusually high $\delta^{18}O$ values of the Kouilou carbonates.

3.5.1.3 Biomarkers

Biomarker analysis of modern and ancient authigenic carbonates is a useful tool for the identification of methanotrophic communities mediating carbonate precipitation (Elvert et al., 1999; Thiel et al., 1999; Peckmann and Thiel, 2004; Stadnitskaia et al., 2005; Birgel et al., 2008). Methane-oxidizing archaea and sulfate-reducing bacteria can be identified by specific lipid biomarker patterns preserved in the carbonate matrix. Furthermore, stable carbon isotopic measurements of these biomarkers provide evidence if methane was used as a carbon substrate by the microorganisms (Elvert et al., 1999; Hinrichs et al., 1999; Thiel et al., 1999; Pancost et al., 2000). The biomarker distributions of two major phylogenetical groups of methanotrophic consortia are well-characterized, the ANME-1 and ANME-2 groups

(Blumenberg et al., 2004). A third group of methanotrophic archaea, the ANME-3, was only recently identified (Niemann et al., 2006; Lösekann et al., 2007).

Based on the presence and the relative abundances of biomarkers, the respective ANME group can be identified (Niemann and Elvert, in press). Characteristic for ANME-1 is a dominance of archaeol over *sn*-2-hydroxyarchaeol (OH-Ar/Ar-ratio < 0.8), whereas high contents of hydroxyarchaeol and crocetane typify ANME-2 (Blumenberg et al., 2004). Moreover, DAGEs, suggested to be derived from sulfate-reducing bacteria, seem to be relatively more abundant when ANME-1 groups are the major methane oxidizers (Stadnitskaia et al., 2005). In the selected carbonates from Hydrate Hole, two different methanotrophic archaeal groups were identified to dominate in the carbonate-forming process: (1) ANME-1 (high-Mg-Calcite sample GeoB 8212-2a; OH-Ar/Ar-ratio: 0.51) and (2) ANME-2 (aragonite sample GeoB 8207-1b; OH-Ar/Ar-ratio: 2.15). ANME-1 dominance is also characterized by a higher proportion of DAGEs ($C_{33:2}$ dominant) in comparison to archaeol and *sn*-2-hydroxyarchaeol (Table 2). ANME-2 dominance, by contrast, is typified by higher amounts of isoprenoidal glycerol diethers (up to 25.19 μg g^{-1} carbonate dry weight) whereas DAGEs ($C_{32:2a}$ dominant) are relatively reduced. Moreover, the high-Mg-calcite sample is associated with a relatively high content of crocetane and Cr:1, while the ANME-1 dominated aragonitic sample GeoB 8212-2a shows higher contents of PMI:2.

Previous studies showed that the occurrence and abundance of different ANME groups seem to be linked to specific habitats and environmental conditions. For example, ANME-1 groups preferable occur at sites of lower methane concentrations (Nauhaus et al., 2005) and greater depths within the sediment than ANME-2, which are often reported to be dominant near the sediment-water interface at high flux sites (Elvert et al., 2005; Knittel et al., 2005; Niemann et al., 2005). In authigenic carbonate samples, biomarkers seem to be effectively preserved to reconstruct such differences (Leefmann et al., 2008; Stadnitskaia et al., 2008). Accordingly, the formation of nodular carbonates such as GeoB 8212-2a was taking place deeper within the sediment and at moderate methane fluxes based on the predominance of diagnostic biomarkers of ANME-1 archaea. By contrast, biomarkers of ANME-2 groups were dominant in carbonate slab GeoB 8207-1b, indicating higher methane fluxes and a precipitation closer to the seafloor.

3.5.2 Implications on different types of carbonate precipitates at the Kouilou pockmarks

3.5.2.1 Nodular carbonates

Different theories exist with respect to the formation of carbonate concretions, assuming either concentric or pervasive growth (see Mozley, 1996; Raiswell and Fisher, 2000 and references therein). Based on stable carbon isotopes, a microbial origin of concretions is usually inferred (Mozley and Burns, 1993). The Kouilou nodules are smaller than most carbonate concretions and lack septarian cracks. They resemble carbonate concretions from methane seeps of the northern Black Sea, which have been found to be surrounded by microbial mats (Reitner et al., 2005b). It is likely that the organic matter covering the Kouilou nodular carbonates represents degraded microbial mats. As for the Black Sea concretions, biomarker analyses confirm the former presence of an ANME-1-dominated AOM community agreeing with an analogous mode of formation.

Highly positive $\delta^{18}O$ values of the nodules (+4.8 ± 1.9‰; n=10) show the highest disequilibrium to the ambient seawater of all carbonates, possibly reflecting formation deeper within the sediment (Fig. 8A). Similarly, the dominance of biomarkers of ANME-1 archaea indicates that nodular carbonates formed somewhat deeper below the seafloor than other types of carbonate aggregates (Tab. 2). This greater depth is reflected by relatively low carbonate contents of around 37 to 39 wt. %, caused by lower primary sediment porosities due to higher sediment load. Less pore water may also results in higher viscosities of the carbonate precipitating medium. Under these conditions, calcite precipitation is known to be favored over aragonite formation (Buczynski and Chafetz, 1991), agreeing with the dominance of high-Mg-calcite in the nodular carbonates. Additionally, carbonate mineralogy is controlled by the growth rate, with aragonite being favored by high concentrations of carbonate ions (Given and Wilkinson, 1984). The concentric layers of aragonite present near the margin of some nodules may be indicative of an episodically increase of carbonate concentrations, possibly caused by higher methane flux (cf., Luff and Wallmann, 2003).

Dispersely distributed framboidal pyrite within nodules and pyrite seams coating some nodules, probably representing corrosion events (cf., Campbell et al., 2002), are interpreted as products of bacterial sulfate reduction. Pyritiferous carbonate nodules enclosed in Jurassic seep limestones (Peckmann et al., 1999) closely resembles the nodules from the Kouilou pockmarks, probably representing ancient analogues. Many of the recovered

Kouilou composite carbonates contain nodules. Some aggregates enclose only few scattered nodules, whereas others predominantly consist of nodules, resulting in a nodular fabric. Nodules served as nuclei for larger and more complex aggregates. In the process of aggregation, interspaces between nodules became successively filled by later carbonate phases, finally resulting in bone-shaped and tuberose aggregates. These composite aggregates can reach several tens of cm in length and height (see Fig. 3E).

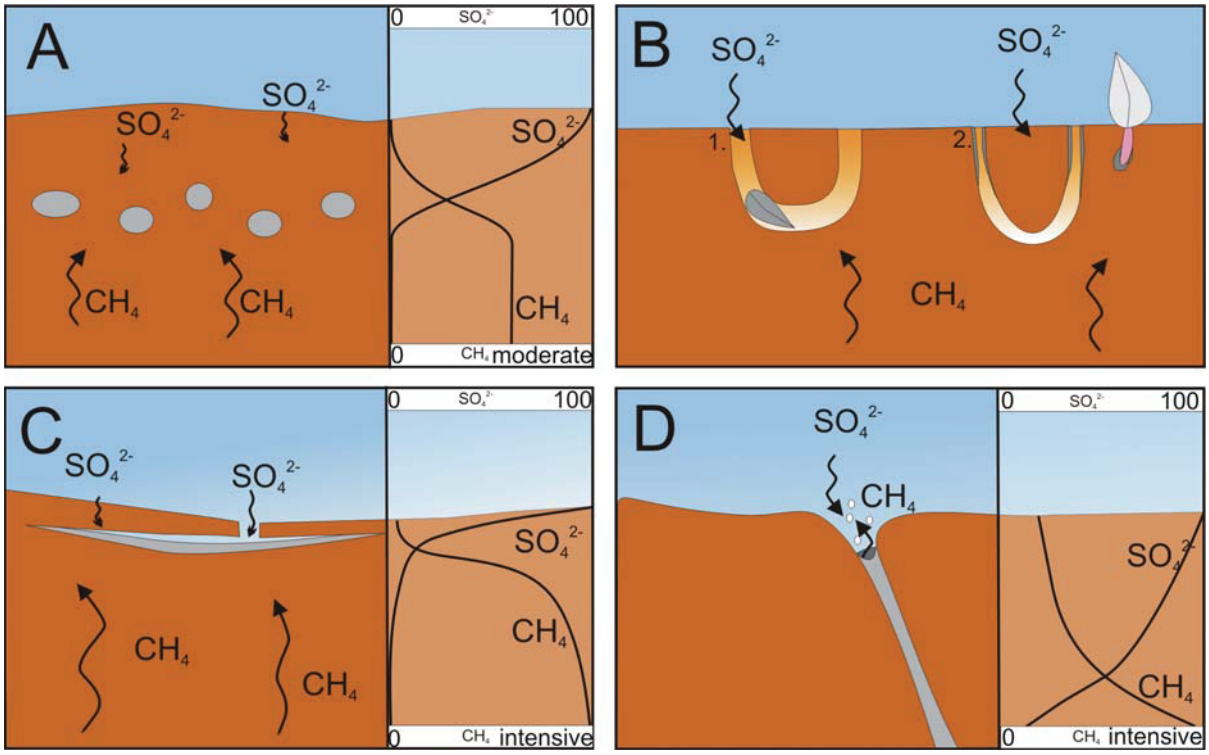

Figure 8. Precipitation model proposed for Kouilou-pockmark carbonates. (A) Nodular carbonates supposedly formed as a result of aggregation (bluish dots) of AOM consortia in the sediment. Moderate methane flux is assumed for this type of precipitate. See postulated methane/sulfate concentration profiles. (B) Bioventilation of burrowing organisms like bivalves and holothurians lead to discontinuous seawater infiltration and variations in pore water chemistry. Carbonate precipitation is probably linked to hotspots of AOM activity, resulting from burrowing activity. (C) Larger carbonate slabs and crusts formed in the sediment close to the seafloor. (D) Carbonate tubes within conduits of gas and fluids formed at variable, mostly greater depths.

3.5.2.2 Carbonate filled molds

An abundant variety of carbonate precipitates at the Kouilou seeps are aggregates that apparently filled burrows. Depending on the burrowing organism, different molds result. Massive aggregates supposedly formed in burrows of bivalves (Fig. 4A). Apart from size and

shape of the molds, the occurrence of bivalve shells within the aggregates supports this interpretation. Carbonate precipitation probably proceeded under relatively stable conditions, as the carbonate matrix is homogeneous lacking obvious zoning (Fig. 8B). Similar carbonate aggregates have been found at the REGAB pockmark (Pierre and Fouquet, 2007).

More filigree tubular carbonates predominantly consisting of high-Mg-calcite are probably related to burrowing holothurians, which are particular abundant as revealed by video-tracks (Fig. 2 A-D). Small-scale layering of aragonite and high-Mg-calcite dominated portions in the tubular aggregates indicates successive backfilling. The different mineralogies reveal that environmental conditions probably varied during the formation of the carbonate infill (Fig. 8B). It is well-established, that burrowing organisms can significantly affect growth of anaerobically operating consortia of methane oxidizers and sulfate reducers (Cordes et al., 2005), which, in turn, modify carbonate formation.

A remarkable feature of this type of mold is the occurrence of protodolomite. Dolomite can be the product of recrystallisation, since high-Mg-calcite and aragonite are thermodynamically metastable phases, which convert to stable low-Mg-calcite or dolomite over time (Burton, 1993). However, direct dolomite precipitation is also known to take place when supersaturation overcomes low-temperature kinetic barriers (e.g., Baker and Kastner, 1981; Aloisi et al., 2000). Dolomite precipitation is favored when sulfate is removed from the pore water by intense sulfate reducing microbial activity (Kelts and McKenzie, 1982). Sulfate occurs in seawater as a magnesium/sulfate ion pair (Wartmann et al., 2000). The uptake of sulfate by sulfate-reducing bacteria leads to the dissociation of this pair and to adsorption of Mg^{2+} ions on the cell surfaces of sulfate-reducing bacteria (van Lith et al., 2003). A specific binding of $Mg^{2+}$and Ca^{2+} ions on bacterial surfaces favors dolomite formation, due to the higher Mg^{2+} concentrations in the seawater (van Lith et al., 2003). Thus, at seeps dolomite may precipitate as a result of extensive sulfate-dependent AOM, leading to an increase in alkalinity, accumulation of Mg^{2+} ions, and depletion of sulfate.

3.5.2.3 Carbonate crusts and slabs

The formation of crusts and slabs proceeded in more porous sediments. Total carbonate contents of up to 57 wt. % reflect the highest primary sediment porosity during initial precipitation. High porosities and the dominance of biomarkers of ANME-2 archaea indicate that carbonate precipitation occurred close to the seafloor (Fig. 8C). The almost purely aragonitic mineralogy is in good agreement with the preferred precipitation of

aragonite from sulfate-laden (sulfate inhibits high-Mg-calcite formation) fluids of lower viscosity due to higher seawater infiltration into unconsolidated sediment close to the seafloor (cf., Buczynski and Chafetz, 1991). The very negative $\delta^{13}C$ values (as low as −58.9‰) are probably related to higher methane fluxes agreeing with preferred aragonite precipitation over calcite due to higher supersaturation (Given and Wilkinson, 1984; Luff and Wallmann, 2003). $\delta^{18}O$ values of +3.7 to +4.8‰ are rather close to calculated equilibrium values and, thus, a composition of pore water close to that of seawater is likely.

The formation of layered carbonate crusts provides insight into temporal changes in pore water compositions. In sample GeoB 8212-1-3, the upper, older two layers exclusively consist of aragonite. However, the younger layer below contains 13 wt.% of high-Mg-calcite. This pattern is consistent with reduction of seawater infiltration into the sediment with time, possibly partly due to a sealing effect by the crust. As a consequence, aragonite precipitation diminished and a shift toward precipitation of high-Mg-calcite occurred (cf., Luff et al., 2004).

Interestingly, two carbonate slabs (GeoB 8207-1b and 1c) reveal barite precipitates on their surfaces. Barite precipitation at seeps is governed by sulfate-dependent AOM. The depletion of pore water sulfate by AOM causes barite dissolution, and increases barium concentrations in pore waters (Torres et al., 1996). Upon transport of these barium-enriched fluids, barite precipitates in contact with sulfate-rich fluids (cf., Castellini et al., 2006). Secondary barite has also been recognized in carbonate aggregates from the REGAB pockmark. There, no barium was detected in the surrounding sediments and the occurrence of barium was therefore attributed to diagenetic fluids (Pierre and Fouquet, 2007).

3.5.2.4 Carbonate tubes

The tubular carbonates (Fig. 5E-F) probably represent cemented fluid or gas conduits. This interpretation is supported by their similarity to gas hydrate-lined conduits and veins in the sediments recovered by gravity cores. Pierre and Fouquet (2007) also interpreted similar aggregates from the REGAB pockmark as former fluid conduits. Positive $\delta^{18}O$ values (as high as +5.0‰) indicate the proximity of a ^{18}O-enriched water source other than seawater suggesting gas hydrate destabilization as a likely mechanism. Total carbonate contents and mineralogy (mostly high-Mg-calcite) are similar to those of nodules (< 40 wt. %), agreeing with carbonate precipitation deeper within the sediment (Fig. 8D).

3.6 Conclusions

Limestones from the Kouilou seeps in the northern Congo Fan off western Africa result from the oxidation of biogenic methane in 3100 m water depth. They consist of a variety of ^{13}C-depleted carbonate phases ($\delta^{13}C$ values as low as −58.9‰) including high-Mg-calcite, aragonite, and protodolomite. Carbonate mineralogy appears to be closely related to the intensity of seepage and the dominant group of AOM consortia. Biomarkers of ANME-1 archaea were preferentially detected in high-Mg-calcite dominated aggregates, supporting their precipitation in more restricted environments at lower methane concentrations. Aragonite preferentially formed closer to the seafloor at higher methane concentrations in the presence of microorganisms of the ANME-2 group. Four different categories of carbonates have been recognized. (1) Pyritiferous carbonate nodules consisting of high-Mg-calcite formed relatively deeper within the sediments as indicated by unusually positive $\delta^{18}O$ values, relatively low carbonate contents, and the dominance of ANME-1 archaea. $\delta^{18}O$ values of these and other carbonate phases are more positive than expected compared to precipitation in equilibrium with seawater. The enrichment in ^{18}O is probably related to destabilization of gas hydrates in the underlying sediments. Carbonate nodules acted as nuclei for composite carbonate aggregates. (2) Carbonate filled molds resulted from the burrowing activity of bivalves and holothurians and subsequent precipitation of carbonate minerals in the burrows. (3) Crusts and slabs formed close to the seafloor as revealed by relatively high carbonate contents and the dominance of biomarkers indicative of ANME-2 archaea. Their mostly aragonitic mineralogy agrees with precipitation from sulfate-rich pore waters. (4) Finally, carbonate tubes are interpreted as the diagenetic infill of former fluid or gas conduits.

Acknowledgements

We thank Sebastian Flotow (MARUM, Bremen) for preparation of thin sections, Rita Fröhlking (Alfred-Wegener-Institut, Bremerhaven) for help with XRD measurements, Dr. Till Heinrichs (Earth Science Department, Göttingen) for FE-SEM investigations and EDX analyses, and Valentina Blinova for help with biomarker analyses. Financial support was provided by the “Deutsche Forschungsgemeinschaft” through the DFG-Excellence Cluster MARUM, Bremen (contribution no. MARUMXXXX).

4. Vestimentiferan tube worms modify carbonate precipitation - examples form methane-seeps on the Congo deep-sea fan

Antonie Haas[1], Heiko Sahling[1], Jörn Peckmann[1], Gerhard Bohrmann[1]

[1]MARUM- Center for Marine Environmental Research at the University of Bremen,

Leobener Str., 28359 Bremen, Germany

to be submitted to Geology

Abstract

Dense populations of vestimentiferan tube worms have been documented at crater-like pockmarks on the Congo deep-sea fan. The bush-like worm colonies are extensively encrusted by carbonate at their posterior ends. Vestimentiferan tube worms host thiotrophic bacteria and, thus, have a chemosynthesis-based metabolism. At seeps, sulfide is generated by the anaerobic oxidation of methane (AOM), which is also the important process for authigenic carbonate precipitation. In this context it is essential to estimate the actual effects of tube worms' on their environment. Sulfide consumption by the tube worms themselves maintains the system of AOM and induces carbonate precipitation. On the other side, simultaneous sulfate release by the tube worms stimulates the activity of AOM, and thus again the sulfide production. Beyond that, the elimination of hydrogen ions prevents the carbonate precipitation directly on the tube surface of living worms. The complex carbonate structures comprise of substructures like nodules, hollow and filled tubes integrated by recurring carbonate precipitation events. Detailed examinations allowed estimations on the chronological sequence of complex carbonate formation: carbonate mineralogy prior to the colonization of vestimentiferan tube worms is dominated by high-Mg-calcite, subsequent to the colonization, carbonate mineralogy changes towards aragonite.

Keywords: Vestimentiferan tube worms; Authigenic carbonate; Chemosymbiosis; Congo

4.1 Introduction

The anaerobic oxidation of methane (AOM) is a fundamental process at methane seeps, comprising of the contemporaneous methane oxidation and sulfate reduction. This process is driven by microbial consortia of methane oxidizing archaea and sulfate reducing bacteria (Boetius et al., 2000). AOM-products, hydrocarbon, and sulfide have significant effects on the environmental chemistry. Increasing concentrations of hydrocarbon heighten carbonate alkalinity and initiate the precipitation of ^{13}C-depleted authigenic carbonates (Ritger et al., 1987; Bohrmann et al., 1998; Peckmann et al., 2001). The simultaneous increase of sulfide enables thiotrophic life and the development of chemosynthetic-based ecosystems at cold seep sites. Prominent endemic inhabitants of seeps are e.g. vesicomyid clams, mytilid mussels, and vestimentiferan tube worms. These organisms host symbiotic bacteria, performing chemosynthesis and pass organic matter they produce on to the host. Nearly all of these organisms operate the sulfide-uptake through body extensions, stretched into the sediment. Contrary to bivalves, this can locate their foot temporarily within the sediment, vestimentiferan tube worms' extent their posterior tube and fix it permanently within the sediment. The specialized wall texture of this tube-part enables the uptake of sulfide (Julian et al., 1999), and the elimination of metabolism waste products (Dattagupta et al., 2006).

Vestimentiferan tube worm colonies recovered from the Kouilou-pockmarks on the Congo deep-sea fan, exhibit pronounced aggregations of carbonate precipitate at their posterior tubes. Since this worm tube-end is an important metabolism-device of the mouth and gutless organisms, the question raises of accruing consequences on the tube worm's behavior and life, and, whether the worms themselves possibly even promote carbonate precipitation by metabolism-waste elimination. Therefore, this paper is focused on the relationship between tube worm's metabolism and carbonate formation. Special attention was paid to comprehensive petrologic, petrographic, and stable isotopic analyses in order to characterize the tube worm-related carbonates and to elucidate potential tube worm/carbonate interactions. Carbon isotopic compositions ($\delta^{13}C$) range from -57.6 to -45‰ PDB, indicating that all carbonates are methane derived. Oxygen isotopic compositions ($\delta^{18}O$) between +3.4 and +5.2‰ PDB indicate for nearly all samples an enrichment in ^{18}O, probably originated from hydrate waters released during gas-hydrate decomposition.

4.2 Material and Methods

The studied carbonate structures were collected by TV-guided grab and gravity core from the Hydrate Hole, Black Hole, and Worm Hole pockmarks during RV METEOR Cruise M56 (Sahling et al., 2008). These pockmarks, named Kouilou pockmark, are at 3100 m water depth on the Congo deep-sea fan on the passive south-western continental margin of Africa (Fig. 1). The pockmarks are characterized by well developed seep communities with vesicomyid and bathymodiolin bivalves and bush-like colonies of the vestimentiferan *Escarpia southwardae* (Andersen., pers. comm.), which occur as aggregations of several tens to hundreds worm individuals. The Kouilou pockmarks are located close to the REGAB pockmark (Charlou et al., 2004; Gay et al., 2006).

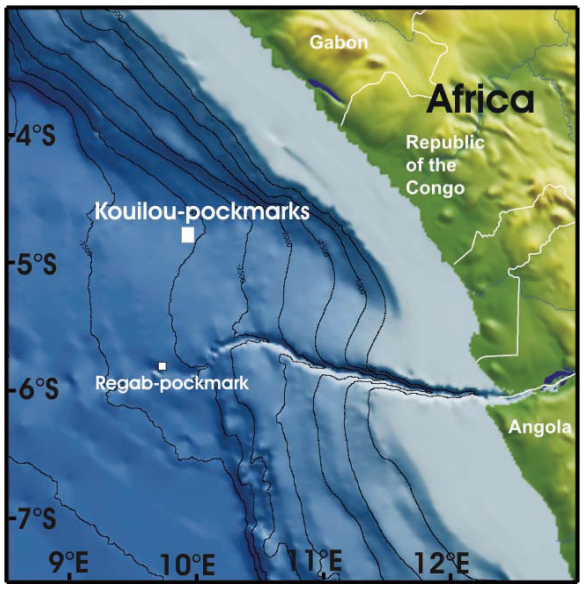

Figure 1. Bathymetric map showing south-western African continental margin, the Congo River estuary, the Congo Canyon, and pockmark areas (modified after Sahling et al., 2008).

Samples of TVG Geo 8203-1, 8212-2 and GC GeoB 8211-2 were categorized based on their morphology and macroscopic features, cut for sub-sampling, thin section preparation, and stable carbon and oxygen isotope measurements. Qualitative and semi-quantitative mineralogical composition of the samples was analyzed by XRD measurements using a Philips PW 1820 instrument (CoKα) at the Alfred-Wegener-Institute in Bremerhaven. The samples were mixed with an internal standard (α-Al_2O_3). Scans were run between 20° to 60° at a scanning speed of 0.01° 2θ. Semi-quantitative abundances of different carbonate mineral

were determined by using standard calibration curves of different mineral mixtures (precision ± 3 wt %). The shift in the d (104) calcite peak was used to determine the $MgCO_3$ content of Mg-calcite according to Lumsden (1979). A split of the carbonate powder was used for stable isotope analyses. The samples were reacted with 100% phosphoric acid at 75°C in an online carbonate preparation line (Carbo-Kiel-single sample acid bath) connected to a Finnigan Mat 252 mass spectrometer at the Center for Marine Environmental Research (MARUM) at the University of Bremen. All values are expressed using the δ-notation relative to the Vienna Peedee Belemnite Standard (V-PDB) and are reported in per mil (‰) with a standard deviation of ≤ 0.07‰ (Tab. 1). High resolution details were examined with a LEO 1530 Gemini field emission-scanning electron microscope (FE-SEM).

Nodules (High-Mg-Calcite-Endmember)	**Ara (wt %)**	**High-Mg-calcite (wt %)**	**$\delta^{13}C$ (‰)**	**$\delta^{18}O$ (‰)**	**Filled Tubes (Aragonite-Endmember)**	**Ara. (wt %)**	**High-Mg-calcite (wt %)**	**$\delta^{13}C$ (‰)**	**$\delta^{18}O$ (‰)**
8203-1-1a	3.8	96.2	-45.0(±0.01)	4.7(±0.01)	8212-2f	98.5	1.5	-51.2(±0.03)	4.6(±0.03)
8203-1-1b	4.4	95.6	-46.9(±0.02)	4.8(±0.02)	8212-2g/1	100.0	0.0	-53.5(±0.02)	4.2(±0.02)
8203-1-1c	19.1	80.9	-48.7(±0.02)	4.5(±0.01)	8212-2g/2	95.9	4.1	-54.0(±0.03)	4.2(±0.02)
8203-1-1d	13.5	86.5	-53.2(±0.03)	4.6(±0.02)	8212-2g/3	99.8	0.2	-55.0(±0.04)	4.1(±0.01)
					8212-2g/4	100.0	0.0	-53.3(±0.01)	4.1(±0.01)
Average/ Standard deviation	**10.2 ±7.4**	**89.9 ±7.4**	**-48.5 ±3.5**	**4.6 ±0.1**	**Average/ Standard deviation**	**98.8 ±1.7**	**1.2 ±1.7**	**-53.4 ±1.4**	**4.2 ±0.2**
Complex Crusts (Bulk samples)					**Hollow Tubes (Bulk samples)**				
8212-2c/2	9.1	90.9	-53.1(±0.05)	3.7(±0.03)					
8212-2c/3	18.6	81.4	-55.3(±0.04)	4.1(±0.02)					
8212-2-35/1	92.0	8.0	-57.6(±0.04)	5.2(±0.02)					
8212-2-35/2	76.7	23.3	-53.4(±0.05)	5.1(±0.03)	8212-2-6d/1	80.5	19.5	-50.6(±0.07)	3.4(±0.04)
8212-2-35/3	21.7	78.3	-51.0(±0.03)	4.2(±0.03)	8212-2-6d/2	81.4	18.6	-47.6(±0.04)	4.1(±0.03)
8212-2-35/4	16.8	83.2	-45.0±0.04)	4.0(±0.02)	8211-2-2/1	74.7	25.3	-52.2(±0.06)	5.1(±0.04)
8212-2-17d	71.9	28.1	-48.9(±0.06)	4.0(±0.01)	8211-2-2/2	78.7	21.3	-46.3(±0.04)	4.3(±0.01)
8211-1-2/2	76.5	23.5	-57.0(±0.03)	4.4(±0.03)	8211-2-1/1	72.6	27.4	-52.4(±0.05)	5.1(±0.01)
Average/ Standard deviation	**47.9 ±34.2**	**52.1 ±34.2**	**-52.1 ±4.3**	**4.4 ±0.5**	**Average/ Standard deviation**	**77.6 ±3.8**	**22.4 ±3.8**	**-49.8 ±2.7**	**4.4 ±0.7**

Table 1. List of the examined carbonate structures: carbonate mineralogy and stable isotope data (measurement error in brackets). All sample numbers without GeoB prefix.

4.3 Results

4.3.1 Macroscopic description and petrography

The complex vestimentiferan tube worm carbonates are aggregations of several distinguishable carbonate substructures like 1.) nodules, 2.) hollow and 3.) filled tubes. These substructures are linked and masked by recurring carbonate precipitation. The final result are structures comprising of massive and filigree elements as complex as lithified root balls or tubers (Fig. 2). Aragonite and high-Mg-calcite are the carbonate minerals; however, they are either related to subtypes or participate to variable portions on their formation. The structures are up to 40 cm in length and several tens of centimeters in width and height.

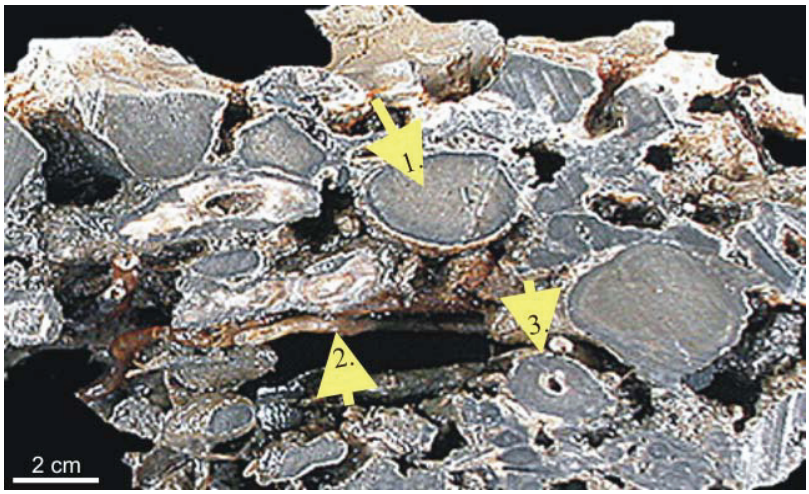

Figure 2. Detail photomicrography of complex crust showing: 1. Nodular carbonate, 2. Organic posterior tube, 3. Lithified posterior tube.

Carbonate nodules (substructure 1) are to remarkable amounts integrated in complex tube worm carbonates (Fig. 2). These nodules are only few centimeters in diameter (Fig. 2, arrow 1). They are composed of light to dark grey micritic calcite containing 10 to 13 mol% $MgCO_3$ (mean: 11.5 mol %). Some of them contain interbedded layers of microcrystalline aragonite towards their exterior. The concentric arrangement of these layers supports a nodular growth. Hollow carbonate tubes (substructure 2) are filigree tubes of approximately 0.5 cm in diameter, which are of variable length (Fig. 3A and B). Hollow tubes predominantly consist of microcrystalline aragonite, and minor amounts of high-Mg-calcite. Botryoidal aragonite aggregates are sometimes present on the surface, and at the interior of

already lithified tube walls. The successive carbonate precipitation on the surface of organic tubes (Fig. 3A) seems to be the initial step for their formation.

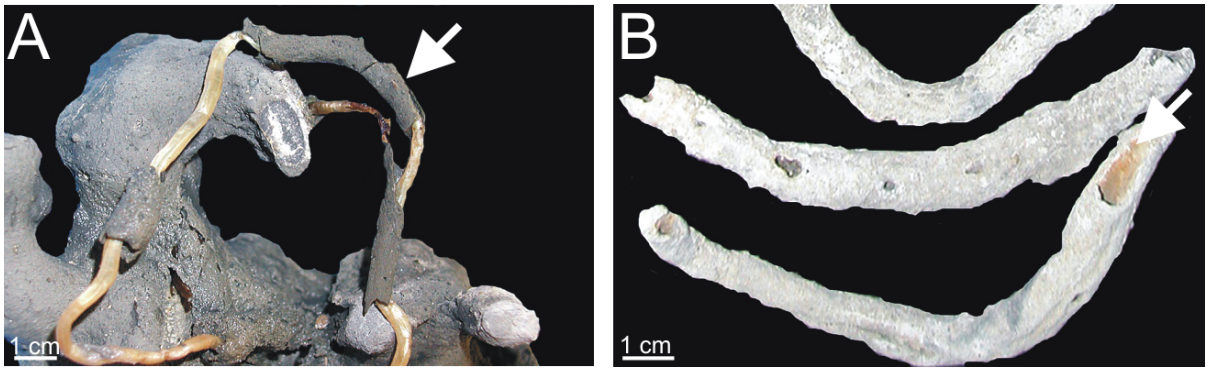

Figure 3. Initial carbonate coatings on organic posterior tubes (A) form finally delicate hollow carbonate tubes (B).

Filled tubes (substructure 3) are represented by more massive tubular structures, typically a few cm in diameter and lengths. They are characterized by yellowish to light-brown isopachous layers of acicular aragonite. Radial fibrous or botryoidal aragonite aggregates are common on the exterior. Their formation is possibly initiated by the calcification of posterior tube-bundles (Fig. 4A and B).

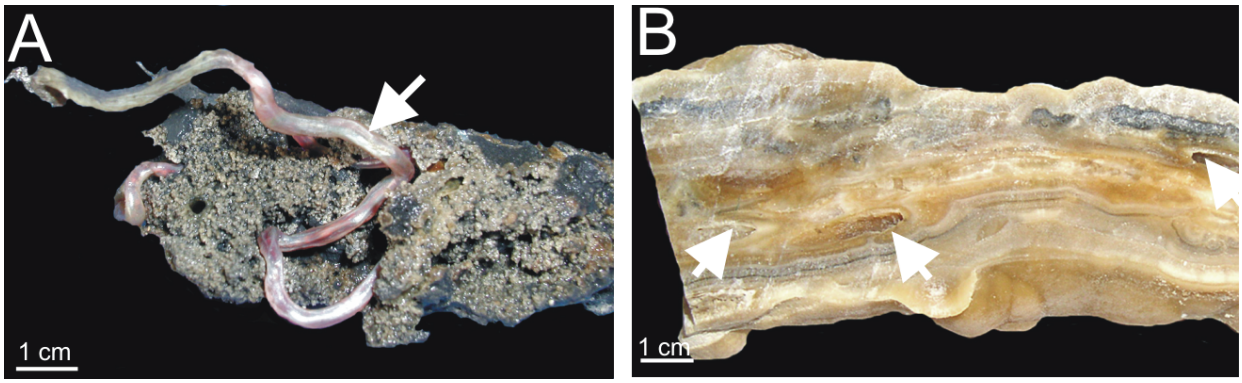

Figure 4. A. Organic worm tubes (white arrow) encased by micritic carbonate. B. Layers of acicular aragonite successively enclose the tubes. Their former presence remains free of precipitates (white arrows).

4.3.2 Stable carbon and oxygen isotopic composition

Stable isotope analyses were conducted on 13 samples (n=22) grouped as nodular carbonates, hollow tubes, filled tubes and samples from the subsequently cementation of

these structures (Tab. 1). In general the stable carbon isotopic compositions ($\delta^{13}C$) range from −57.6 to −45.0 ‰ (mean: −51 ± 3.7 ‰). Only few samples are of pure mineralogy: high-Mg-calcite and aragonite respectively. These carbonate end-members are represented by nodular carbonates (high-Mg-calcite endmember) and filled tubes (aragonite end-member). For aragonites the $\delta^{13}C$ composition is in average −54.1 ±2.1 (n=6) and therefore more negative than for high-Mg-calcites which are in average −46.9 ±0.1 ‰ (n=3). The results of the hollow tubes and the carbonates cementing the complex structures are problematic for interpretation due to the impossibility of isotopic composition allocation to the individual carbonate mineralogy. Oxygen isotopic compositions ($\delta^{18}O$) range between +3.4 and +5.2 ‰ (mean: +4.4 ± 0.5 ‰; n=22). Isotopic compositions of aragonites are in mean +4.4 ± 0.4 ‰; high-Mg-calcite samples are more positive by an average of +4.7 ± 0.6 ‰.

Some trends of isotopic behaviour are recognizable, if the isotope signals are split up in relation to the distinctive carbonate structures. Especially filled tubes reveal a positive correlation of decreasing carbon isotopic compositions and decreasing oxygen isotopic compositions (R^2=0.9). This trend is also observable in nodular carbonates (R^2=0.4). Furthermore, filled tubes and nodular carbonates display that higher contents of aragonite correspond to decreasing carbon isotopic compositions. And additionally reveal both substructures increasing contents of aragonite coinciding with decreasing oxygen isotopic compositions (R^2=0.8, for nodular carbonate).

4.4 Discussion

Although vestimentiferan tube worms were first discovered at hydrothermal vents, these organisms are now known as characteristic inhabitants of cold seeps in the Pacific (Sibuet and Olu, 1998). In the Atlantic, in contrast, vestimentiferans are not known from hydrothermal areas, however, several findings at cold seeps are described along the North American continental margin (e.g. Paull et al., 1984). Recent expeditions discovered vestimentiferan tube worms (*Escarpia southwardae* sp. nov.) also along the continental margin of southwest Africa (e.g. Andersen et al., 2004). These tube worms are associated with pronounced carbonates at their posterior ends (e.g. Sibuet et al., 2002; Sahling et al. 2008). Carbonates in some ways related to tube worms have been described by some authors (e.g. Han et al., 2004; Luff et al., 2004). Initially carbonate precipitation occurred most probably before tube worm colonization, because vestimentiferan tube worm larvae need a

hard substrate to anchor. Those early carbonate precipitates have most likely been used by the nektonic larval stage of the tube worm to settle in the environment (Julian et al., 1999). However, the morphology of at least some of those carbonates point to a relationship, other than only tube-fixation. As the knowledge on tube worms' mode of life has increased, it is conceivable that these unique carbonates are even modified by metabolic activities, processed by the worm via the posterior tube wall.

4.4.1 Impact of tube worm metabolism on carbonate formation

In contrast to the other carbonate subtypes are nodular carbonates most likely present in the sediment prior to the colonisation by vestimentiferan tube worms. This is reasonable to assume since carbonate nodules are the only substructures, which do not contain relicts of tube worms in their matrix. Nevertheless, nodules form in many cases considerable portions of the complex tube worm/carbonate aggregation. This is interpreted as a result of hard substrate usage for tube fixation, and the casual integration of already existing nodules in a net of downward growing posterior tubes.

In contrast to that show hollow and filled-tubes a large influence of the tube worms. Particularly the development of the hollow-tubes (substructure 2), identified as the lithified posterior tubes, initially appeared confusing. Especially the co-occurrence of totally lithified, partly lithified or still unaltered organic posterior tubes, side by side at some of the complex carbonate structures (Fig. 2) raises the questions, on mechanisms controlling carbonate precipitation at the posterior of worm tubes. The different states of calcification within small ranges points on the possibility of active carbonate precipitation prevention. Observations onboard the research cruise directly after the recovery of the tube worm carbonates are important to mention here. Living tube worms, identified by well supplies of blood in the posterior tubes (Fig. 4A), were absolutely free of any carbonate precipitates. And even detailed FE-SEM investigations confirm that these tubes were still unaltered and lack of mineral precipitates. On the other hand, posterior tubes of dead worms were partially or entirely covered by carbonate (Fig. 3A and B). Both observations led to the assumption that living tube worms are able to prevent carbonate precipitation on their tube surface, in order to allow further metabolic exchange with the sediment environment, which would be impeded in the case of carbonate precipitation. Cordes et al. (2005) gave the same interpretation on vestimentiferan tube worms in the Gulf of Mexico. They assumed that tube worms prevent

carbonate precipitation to avoid a reduction of their respiratory surface. Dattagupta et. al. (2006) examined the removal of metabolic waste products of vestimentiferan tube worms in the Gulf of Mexico. The authors concluded that tube worms expel hydrogen ions, produced by their internal sulfide oxidizing symbionts through their posterior tube walls. Because authigenic carbonate precipitation is highly depending on the pH of the pore water solution, a release of hydrogen ions would decrease the pH of the pore fluid, which would prevent precipitation. In contrast, tubes of dead worms are not able to prevent the carbonate-coverage, which subsequently supports the formation of hollow tubes. In fact, degrading tubes may even enhance carbonate precipitation, since nitrogen compounds from the proteinous wall matrix can increase alkalinity and induce carbonate precipitation (Castanier et al., 1999). This would explain why unaltered (living), partly lithified (during degradation) and completely lithified (after degradation) posterior tubes can co-occur at the same carbonate structure.

Similar mechanisms may also affect the formation of filled-tubes (substructure 3); carbonate structures enclosing bundles of worm tubes (Fig. 4A and B). The structure formation is supposedly a result of using already carbonate-cemented (gas/fluid) cracks within the sediment as "growing"-pathways by the tube worm themselves. Their subsequent carbonate filling is assumably modified by the metabolic waste disposal of tube worms. In addition to the expulsion of hydrogen ions it has been shown that vestimentiferans expel sulfate through their posterior tubes (Cordes et al., 2005; Dattagupta et al., 2006; 2008). Doing so, the worm will indirectly support carbonate precipitation, since the additional supply of sulfate maintains or most likely arise AOM turnover rates in the surrounding sediments. This will also heighten carbonate alkalinity and subsequently carbonate precipitation.

4.4.2 Changes in carbonate mineralogy during tube worm colonisation

All examined carbonates are methane derived as shown by their carbon isotopic compositions ranging between -57.6 to -45‰. Carbonate mineralogy is affected by several factors; however, methane turnover by AOM consortia controlled by methane flux intensity seems crucial at methane seeps. Moreover, within sediments of vestimentiferan tube worms carbonate chemistry is additionally modified by the tube worms' metabolism (Fig. 5). Carbonate precipitation prior to tube worm colonization is dominated by high-Mg-calcite, represented by the nodular carbonates. High-Mg-calcite precipitation might be related to

moderate methane flux intensity since aragonite is favoured by the high supply of carbon species due to its rapid crystallisation. Kinetic effects might even explain the distinction in carbon isotopic composition of the high-Mg-calcite or aragonitic endmember.

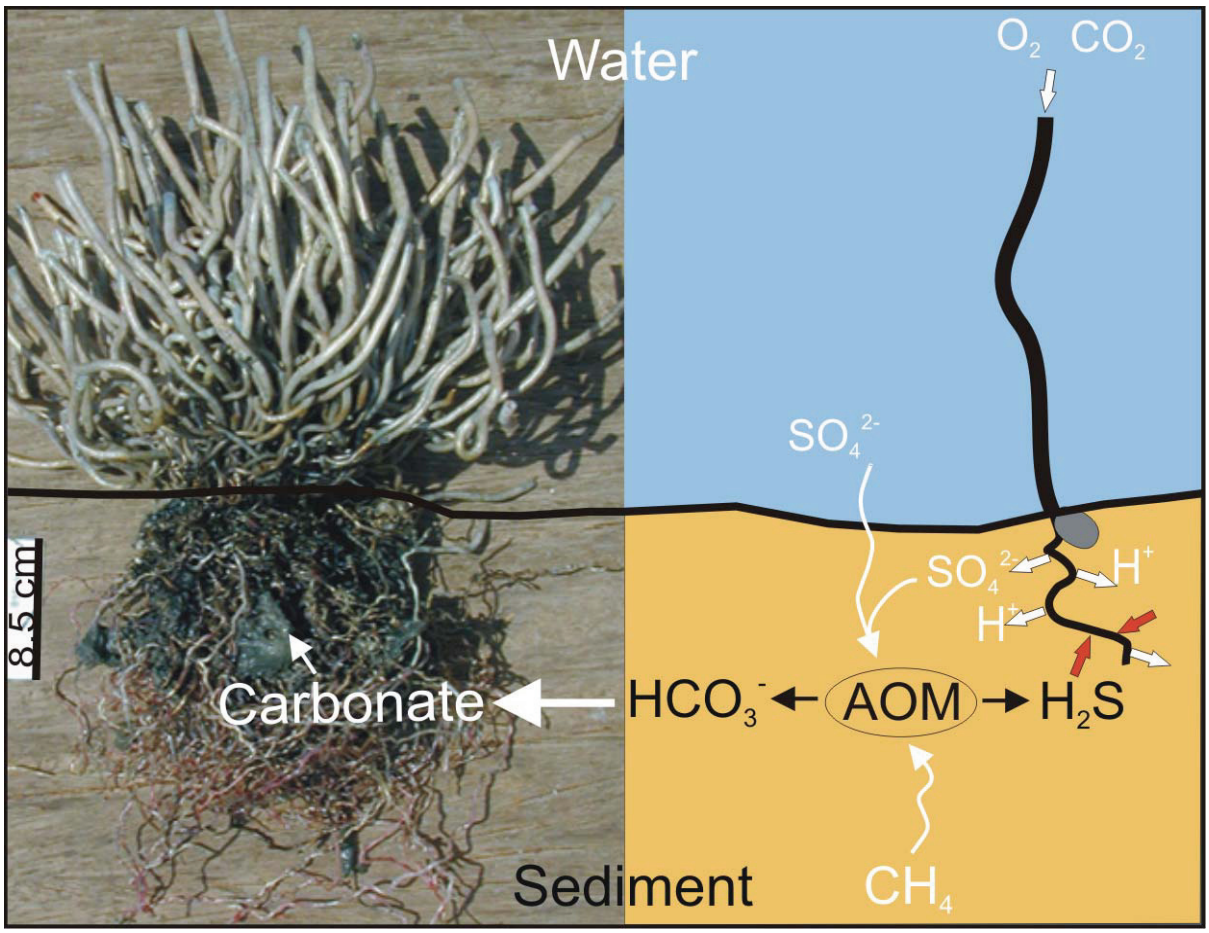

Figure 5. Bush-like vestimentiferan tube worm colony of the species Escarpia southwardae sp.. The posterior ends are heavily encrusted by carbonate (Left). Modification of sediment geochemistry by the uptake of sulfide and the release of sulfate and hydrogen ions through their posterior ends (Right).

Subsequent to their colonization, tube worms' uptake of sulfide maintains carbonate precipitation. High concentrations of sulfide, in contrast, will rather cause carbonate dissolution than precipitation (Han et al., 2004). The concurrently increasing concentrations of sulfate, released as metabolism product of tube worms, should again stimulate the turnover of AOM consortia. This should result in predominance of aragonite, since aragonite is favored over calcite in the presence of sulfate (Walter, 1986). The formation of filled-tubes, which are characterized by well crystallized aragonite, is therefore very likely a consequence of high sulfate concentrations induced by spatially compact living worms. Hollow-tubes, in

contrast, consist beside aragonite to some amount of high-Mg-calcite. This is in high similarity to some carbonate subsamples taken from the matrix of complex tube worm carbonates. Changes in carbonate mineralogy are here probably related to spatial variations in chemistry, probably based on methane availability. Furthermore, small-scale environmental interactions like gas hydrate decomposition will even modify carbonate precipitation as displayed in $\delta^{18}O$ ranging between +3.4 and +5.2.

4.4.3 Influence of carbonate precipitation on the behaviour of tube worms

Carbonate precipitation promotes in either case the formation of barriers within the sediment, which probably minder or disturb the tube worm/sulfide connection. Luff et al. (2004) assumed that those extensive carbonate precipitates lead to the end of tube worms' life. Olu-Le Roy et al. (2007) interpreted lower methane levels of old vestimentiferan tube worm colonies at the Regab-pockmark, as a result of pronounced carbonate precipitates within the sediments. There, higher methane levels were measured within the sediments of young colonies. This is in good accordance to the observations of Freytag et al., (2001), who reported of decreasing sulfide concentrations at old vestimentiferan colonies in the Gulf of Mexico. If sulfide production is only related to AOM, decreasing methane concentration should result in decreasing sulfide concentrations. However, Cordes et al., (2005) suggest that tube worms dissolve existing carbonates in the sediments beneath the posterior ends by the increased release of hydrogen ions to overcome a disconnection to sulfide and to continue tube-growth for respiratory-area enlargement. Furthermore, vestimentiferans are very likely able to maintain their sulfide requirement by the release of sulfate into the sediment. Dattagupta et al. (2008) calculated that vestimentiferan colonies in the Gulf of Mexico release 70% to 90% of their sulfide-turnover as sulfate back into the sediment. It is questionable whether microbial sulfate reduction can supply sufficient sulfide if the process is decoupled from the methane oxidation in order to guarantee the supply of the worms. Therefore, the lifespan of tube worms seems more effected by the presence of sulfide and methane respectively, than by carbonate precipitates.

4.5 Conclusions

Carbonate precipitation at Kouilou-pockmarks on the Congo deep-sea fan is initially initiated by AOM. Carbon isotope compositions reveal their origination from microbial methane. Complex tube worm carbonate structures are aggregations of multiple precipitation events. Their development starts by the colonisation of vestimentiferan tube worms on nodular carbonates, which were probably already within the sediments. The formation of hollow and filled-tubes is directly linked to tube worm's metabolic processes, operated through the posterior end. Especially the elimination of hydrogen and sulfate ions just as well as the uptake of sulfide prevents, modifies or maintains carbonate precipitation. High-Mg-calcite is the dominant carbonate mineralogy prior to the appearance of vestimentiferan tube worms, whereas aragonite is predominantly precipitated after their colonization. The distinctive enrichment of oxygen isotopic compositions of the carbonates in ^{18}O seems to be related to the decomposition of gas hydrates in the underlying sediments. Variations in carbon isotopic compositions in respect to carbonates mineralogy are very probably related to kinetic effects caused by changes in methane flux intensities. The complex carbonate/ tube worm aggregation includes several carbonate components from sequential occurring precipitation.

Acknowledgements

We thank Sebastian Flotow for the preparation of thin sections, and Dr. M. Segl for stable carbon and oxygen isotope measurements (MARUM Bremen). Rita Fröhlking (AWI-Bremerhaven) for x-ray diffraction measurements.. Dr. Till Heinrichs (University of Göttingen) for FE-SEM investigations and EDX-analyses. This study was supported by the Deutsche Forschungsgemeinschaft through the DFG-Research Center 'The Ocean in the Earth System' (contribution no. xxxx).

5. Mineralization of vestimentiferan tube worms at methane seeps on the Congo deep-sea fan

Antonie Haas[1], Crispin T.S. Little[2] Heiko Sahling[1] Gerhard Bohrmann[1] Tobias Himmler[1] Jörn Peckmann[1]

[1]MARUM- Centre for Marine Environmental Research at the University of Bremen,

Leobener Str., 28359 Bremen, Germany

[2]School of Earth Sciences, University of Leeds, Leeds, UK LS2 9JT

submitted to Deep Sea Research 1

Abstract

Vestimentiferan tube worms are prominent members of modern methane seep communities and are totally reliant as adults on symbiotic sulphide-oxidizing bacteria for their nutrition. The sulphide is produced in the sediment by a biochemical reaction called the anaerobic oxidation of methane (AOM). A well-studied species from the Gulf of Mexico shows that seep vestimentiferans 'mine' sulphide from the sediment using root-like, thin walled, permeable posterior tube extensions, which can also be used to pump sulphate and possibly hydrogen ions from the soft tissue back into the sediment to increase the local rate of AOM. The 'root-balls' of exhumed seep vestimentiferans are intimately associated with carbonate nodules, which are a result of AOM. We have studied vestimentiferan specimens and associated carbonates from seeps at the Kouilou pockmark field on the Congo deep sea fan and find that some of the posterior 'root' tubes of living specimens are enclosed with carbonate indurated sediment and other, empty examples are partially or completely replaced by the carbonate mineral aragonite. This replacement occurs from the outside of the tube wall inwards and leaves fine-scale relict textures of the original organic tube wall. The process of mineralization is unknown, but is likely a result of post-mortem microbial decay of the tube wall proteins by microorganisms and/or the precipitation from locally high flux of AOM derived carbonate ions. The aragonite replaced tubes from the Kouilou pockmarks show similar features to carbonate tubes in ancient seep deposits and make it more likely that many of these fossil tubes are those of vestimentiferans. These observations have implications for the supposed origination of this group, based on molecular divergence estimates.

5.1 Introduction

Vestimentiferan tube worms (Polychaeta, Siboglinidae) are prominent tube-forming inhabitants of methane seeps and at these sites comprise a small number of species belonging to the genera *Lamellibrachia*, *Seepiophila*, *Escarpia* and *Paraescarpia* (Andersen et al., 2004; Bergquist et al., 2003; Cordes et al., 2005; Paull et al., 2005; Sahling et al., 2008; Sibuet and Olu-Le Roy, 2002; Sibuet and Olu, 1998). At seeps, vestimentiferans can occur singly, or in colonies that can comprise hundreds to thousands of individual tubes forming bush-like structures. This is the habit of the well studied species *Lamellibrachia luymesi* from the Gulf of Mexico seeps (Bergquist et al., 2003; Cordes et al., 2005). In these 'bushes' the portion of the tubes that are seen above the sediment-water interface have a gently tapering morphology towards the anterior end. The anterior tube walls are thick, tough, laminated structures formed of a complex of proteins with interwoven beta chitin crystallites (Gaill et al., 1992a; Shillito et al., 1995). When *L. luymesi* 'bushes' are extracted from the sediment they often have long (up to 1 m) non-tapering posterior tubes with complex morphologies, bearing resemblance to plant roots. These 'roots' appear to grow downwards into the sediment at the same time as the anterior tubes grow upwards into the water column (Bergquist et al., 2003; Cordes et al., 2005; Dattagupta et al., 2006, 2008). The tube walls of the posterior tube 'roots' are thin, do not contain chitin and are permeable to sulphide (Julian et al., 1999).

Carbonate nodules with a variety of shapes and sizes are often found entangled in the 'roots' of exhumed seep vestimentiferans, including *Lamellibrachia luymesi* from the Gulf of Mexico and *Escarpia southwardae* from the West African coast (Andersen et al., 2004). These carbonates are a by-product of the anaerobic oxidation of methane (AOM), a process by which consortia of archaea and sulphate-reducing bacteria oxidise methane and reduce seawater sulphate in the sediment redox zone, producing hydrogen sulphide and bicarbonate ions (Boetius et al., 2000). AOM is also responsible for a rise of pore-water alkalinity, facilitating rapid carbonate precipitation (Ritger et al., 1987).

Adult vestimentiferans do not have an alimentary canal and are trophically reliant on a symbiotic relationship with thiotrophic bacteria, which they harbour in an organ called the trophosome (Cavanaugh et al., 1981; Childress et al., 1984). The sulphide and oxygen required by the bacteria are delivered to this organ via the blood, with the oxygen coming from seawater through a vascular organ called the plume. In hydrothermal vent

vestimentiferans this is also where hydrogen sulphide from vent fluid enters the vascular system. However, there are negligible concentrations of hydrogen sulphide above the sediment-water interface at seeps (Freytag et al., 2001), and therefore seep vestimentiferans must gain their hydrogen sulphide in another way. It has been established that *Lamellibrachia luymesi* uses its 'roots' both to take up hydrogen sulphide from, and pump sulphate back into, the surrounding sediment (Julian et al. 1999; Freytag et al., 2001; Cordes et al., 2003, 2005; Dattagupta et al., 2006, 2008). This latter process likely increases the local rate of AOM and enables *L. luymesi* to 'mine' sulphide from deep within the sediment for considerable time periods. Indeed, in-situ tube staining experiments indicate that some *L. luymesi* individuals may live for 200 or more years (Bergquist et al., 2000). It is also possible that *L. luymesi* may be able to pump hydrogen ions from its 'roots' into the sediment, which would prevent, or at least retard, carbonate growth on tubes and possibly enable young individuals to bore through existing seep carbonates to gain access to underlying sulphide-rich sediments (Dattagupta et al., 2006, 2008).

Fossil tubes have been found in a large number of ancient seep carbonate deposits, ranging in age from the Devonian to the Miocene (Himmler et al., 2008). Although a few of these tubes are undoubtedly of serpulid origin, the majority were formed by other organisms and have distinctive concentrically laminated tube walls, often showing 'delamination' structures (Peckmann et al., 2005). Various authors have attributed these fossil tubes to vestimentiferans (Campbell et al., 1993; Goedert and Campbell, 1995; Naganuma et al., 1995; Goedert et al., 2000; Himmler et al., 2008), although the Palaeozoic examples are considerably older than the supposed origin of the vestimentiferan tube worms at 126 million years based on molecular divergence estimates (Black et al., 1997; Halanych et al., 1998; Chevaldonné et al., 2002). This has led some workers to question whether the fossil tubes in ancient seep deposits are in fact vestimentiferans (see Peckmann et al., 2005 for discussion).

Here we report on modern vestimentiferan tube worms and associated carbonates from a methane-related pockmark area on the Congo deep sea fan that give us important new insights into taphonomic processes occurring in the seep environment. These processes cause rapid post-mortem replacement of the organic vestimentiferan tube walls by aragonite, preserving fine details of the original tube. This lends weight to the argument that many fossil tubes in ancient seep deposits, including Palaeozoic examples, indeed have a vestimentiferan origin.

5.2 Material and methods

The studied material consists of vestimentiferan 'bushes' and associated carbonates collected by TV-guided grab and gravity core from the Hydrate Hole and Black Hole pockmarks during RV METEOR Cruise M56 (Sahling et al., 2008). Together with Worm Hole, Hydrate Hole and Black Hole are within the Kouilou pockmark field at 3100 m water depth on the Congo deep sea fan on the passive south-western continental margin of Africa (Fig. 1).

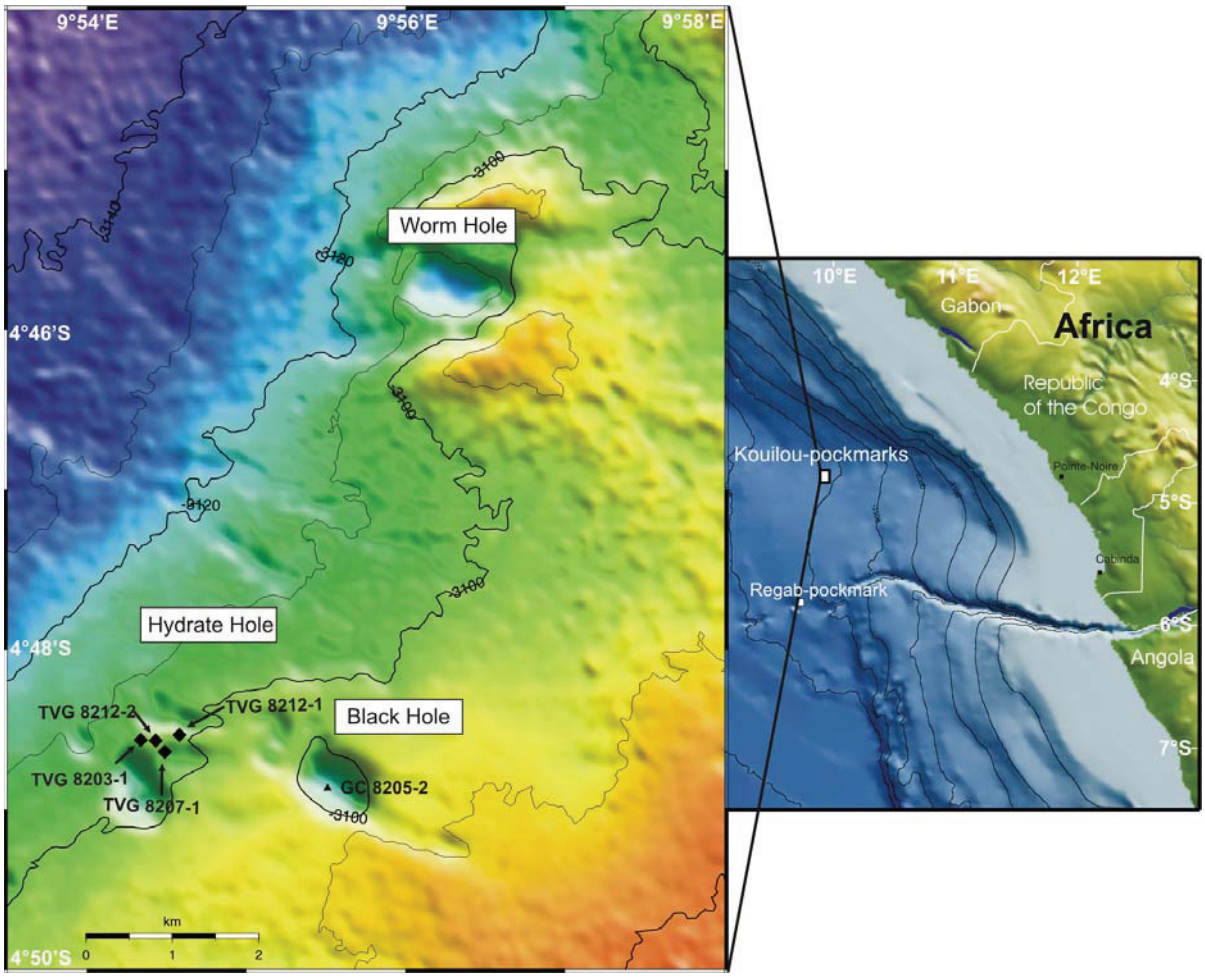

Figure 1. Right: Overview map of the south-west African continental margin and the Congo Canyon (modified after Sahling et al., 2008). Left: detailed map showing the Worm Hole, Black Hole and Hydrate Hole of the Kouilou pockmark field. The locations of samples collected during RV Meteor Cruise M56 are indicated by triangles (gravity cores) and diamonds (TV-guided grabs).

This field is located close to the REGAB pockmark (Charlou et al., 2004; Gay et al., 2006), which has well developed seep communities with vesicomyid and bathymodiolin bivalves and bush-like colonies of the vestimentiferan *Escarpia southwardae* (Andersen et al., 2004). Similar communities occur at the Kouilou pockmarks, although the faunas are dominated by vestimentiferan tube worms, which occur as aggregations of several tens to hundreds individuals. These vestimentiferans appear to be morphologically identical to *E. southwardae* (A. Andersen, pers. comm.), although until detailed taxonomic and molecular studies have been performed, we will refer to our specimens as the Kouilou vestimentiferan.

Anterior, as well as posterior parts of one exhumed vestimentiferan 'bush' from Hydrate Hole (sample 8203-1; Fig. 2) was studied in detail. At least some of the tubes forming this 'bush' were occupied by living animals prior to collection. Diameters of the most anterior and posterior parts of the tubes were measured using digital callipers, as were wall thicknesses, where possible. Pieces of wall from some of the tubes were cut from the anterior and posterior tube ends and at the position of the sediment/water interface. These pieces were carbon coated and imaged using a LEO 1530 Gemini field emission-scanning electron microscope (FE-SEM) and EDX at the University of Göttingen. The entire, root-ball-like posterior portion of the 'bush' was cast in synthetic resin and then cut into six slices for petrographic thin section preparation. Eighteen samples of carbonates containing tubular structures from Hydrate Hole and Black Hole (Table 1) were also sectioned in the same way for the preparation of 23 petrographic thin sections. Some of the thin sections were stained with Feigl's solution or a mixture of potassium ferricyanide and alizarin red dissolved in 0.1% HCl to determine the mineralogy of the carbonate phases. The stained and unstained thin sections were observed with a petrographic microscope using fluorescent, plane and crossed polarized light.

Terminology for crystal sizes follows Folk (1959): microcrystalline <4 μm, microsparitic 4 to 10 μm. The studied specimens are housed in the Geoscience Collection of the University of Bremen at the Faculty 5 (M56, GeoB 8203 to GeoB 8215).

Sample	Location	Description
GeoB 8203-1a GeoB 8203-1b GeoB 8203-1e	Hydrate Hole 04°48.57'S 009°54.50' E	Carbonate with non-mineralized tube Carbonate with non-mineralized tube Carbonate with non-mineralized tube
GeoB 8203-1-1/2/3/4/5/6	Hydrate Hole 04°48.57'S 009°54.50' E	Tube worm colony; 15 tube-wall subsamples for FE-SEM investigations
GeoB 8207-1a	Hydrate Hole 04°48.59'S 009°56.46' E	Carbonate with non-mineralized tube
GeoB 8207-1-3 / and 3a	Hydrate Hole 04°48.59'S 009°56.46' E	Carbonate with non-mineralized tube
GeoB 8212-1-4	Hydrate Hole 04°48.56'S 009°54.56' E	Carbonate with non-mineralized tube
GeoB 8212-2 GeoB 8212-2b GeoB 8212-2d	Hydrate Hole 04°48.56'S 009°54.50' E	Carbonate with mineralized tube Carbonate with mineralized tube Carbonate with mineralized tube
GeoB 8212-2-1 GeoB 8212-2-1a GeoB 8212-2-1b GeoB 8212-2-1c	Hydrate Hole 04°48.56'S 009°54.50' E	Carbonate with non-mineralized tube Carbonate with mineralized tube Carbonate with mineralized tube Carbonate with mineralized tube
GeoB 8212-2-2	Hydrate Hole 04°48.56'S 009°54.50' E	Carbonate with non-mineralized tube
GeoB 8212-2-5 / and 5a	Hydrate Hole 04°48.56'S 009°54.50' E	Carbonate with non-mineralized tubes
GeoB 8212-2-8 / 8a/ 8b/ 8c	Hydrate Hole 04°48.56'S 009°54.50' E	Carbonate with non-mineralized and mineralized tubes
GeoB 8212-2-35	Hydrate Hole 04°48.56'S 009°54.50' E	Root-ball like aggregation of non-mineralized tubes and carbonates; subsamples for FE-SEM investigations
GeoB 8205-2a	Black Hole 04°48.80'S 009°55.45' E	Carbonate with mineralized tube

Table 1. List of studied samples with vestimentiferan tubes. All samples were recovered with a TV- guided grab (TVG), with exception of GeoB 8205-2a, a gravity core (GC) from Black Hole.

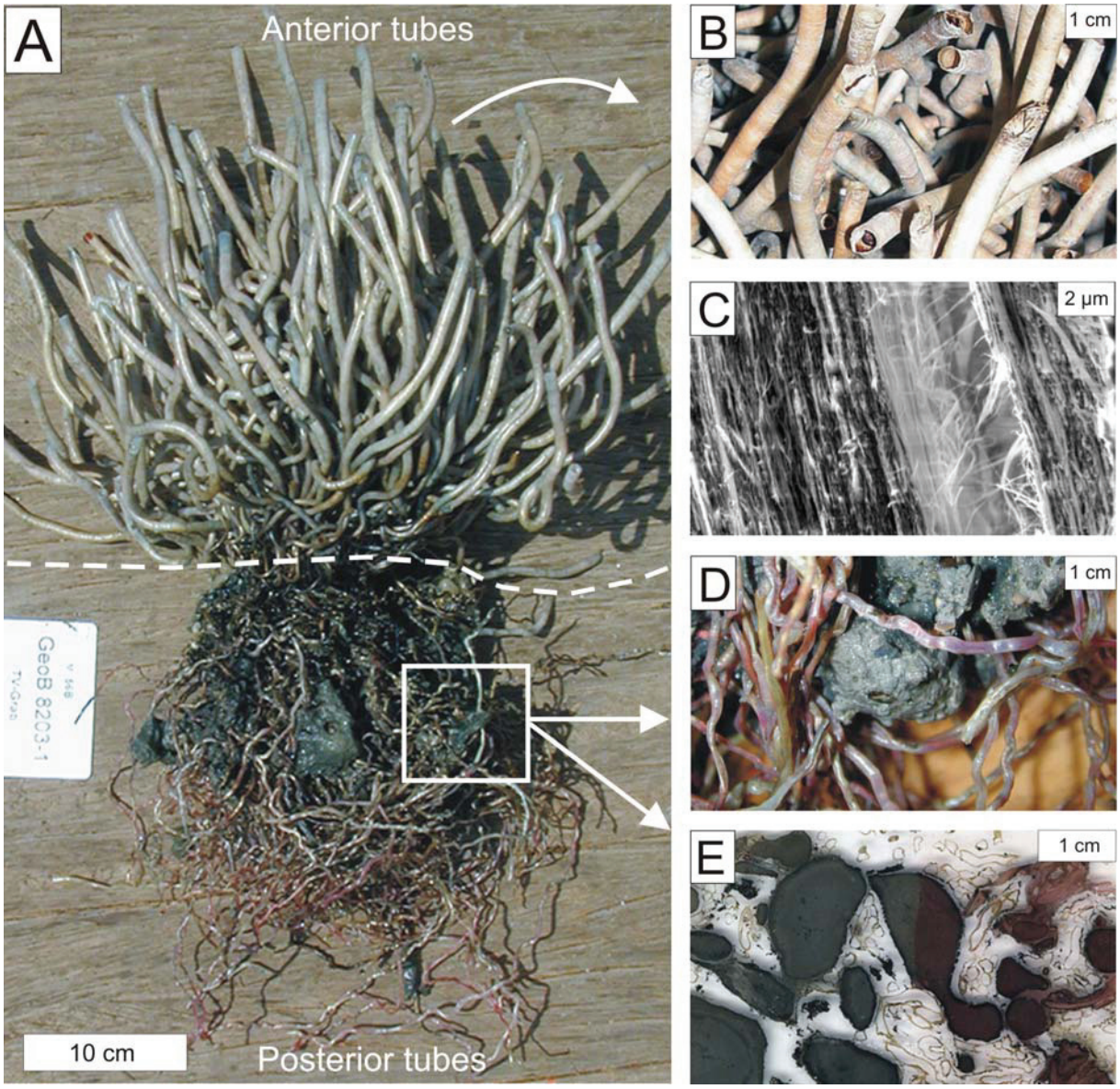

Figure 2. A: Exhumed vestimentiferan 'bush' from Hydrate Hole (sample GeoB 8203-1). The original sediment/water boundary is indicated by the dashed line. Inset box shows details D and E. B. Detail of anterior tubes. C. FE-SEM photomicrograph of longitudinal section of anterior tube wall showing densely packed lamellae. D. Carbonate nodules amongst the thin curled posterior 'root' tubes. E. Thin section of area D showing carbonate nodules (dark patches) surrounded by unmineralized posterior 'root' tubes in various orientations.

5.3 Results

The vestimentiferan 'bush' sample GeoB 8203-1 from Hydrate Hole consists of around 90 rigid anterior worm tubes and their respective posterior ends, which were previously anchored in the sediment (Figs. 2A, 3). The anterior tubes that projected from the sediment surface are slightly twisted and taper gently towards the posterior ends. They are up

to 270 mm in length and 3 to 7 mm in diameter at their open ends (Figs. 2B, 4). The walls of anterior tubes vary in thickness from 0.17 to 0.37 mm (n=8; mean 0.27±0.09), are formed of densely packed laminae (Fig. 2C) and do not have mineral precipitates on their external surfaces. The morphology of the posterior tube 'roots' differ from the anterior tubes in being variably coiled and between 1 and 2 mm in diameter (Figs. 2D, 3, 4). The walls are very thin, varying from 0.03 to 0.1 mm (n=8; mean 0.057±0.023). Irregularly shaped nodules 5 to 25 mm in size and formed of high-Mg-calcite cemented sediment are intimately associated with, but do not adhere to the posterior tubes (Figs. 2A,D,E).

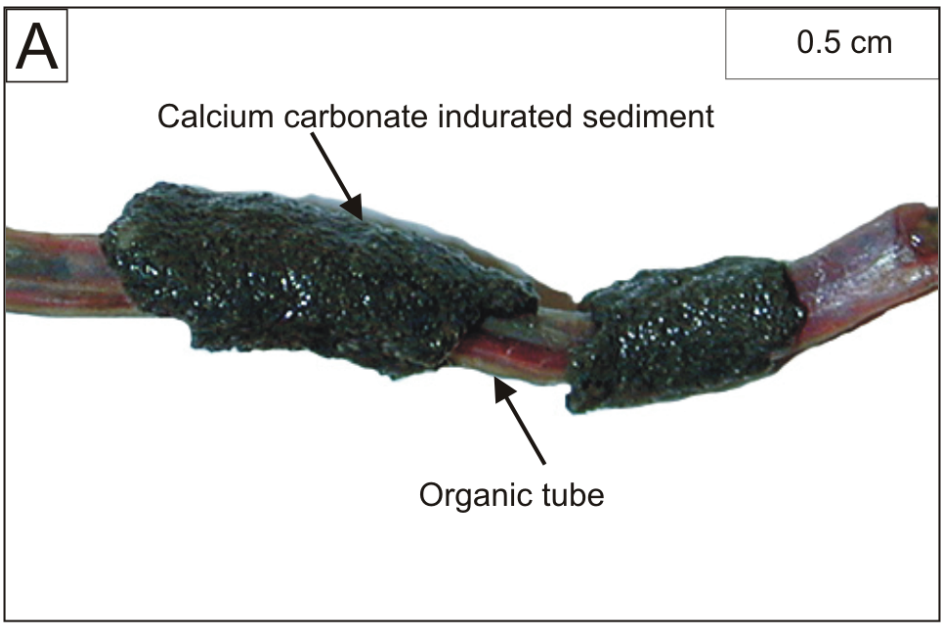

Figure 3. Part of posterior tube of living vestimentiferan surrounded by collar of calcium carbonate indurated sediment.

Portions of a few of the extracted posterior tubes of living Kouilou vestimentiferan specimens are surrounded by a collar of calcium carbonate indurated sediment (Fig.3), although FE-SEM investigations shows that there are no minerals growing directly on the surface of these tubes. Organic-walled and carbonate tubes are present in the eighteen carbonate samples from Hydrate Hole and Black Hole. Although these were not associated with living vestimentiferans, the diameter measurements of a number of these tubes indicates that they fit within the range observed for the posterior portions of living vestimentiferan tubes (Fig. 4).

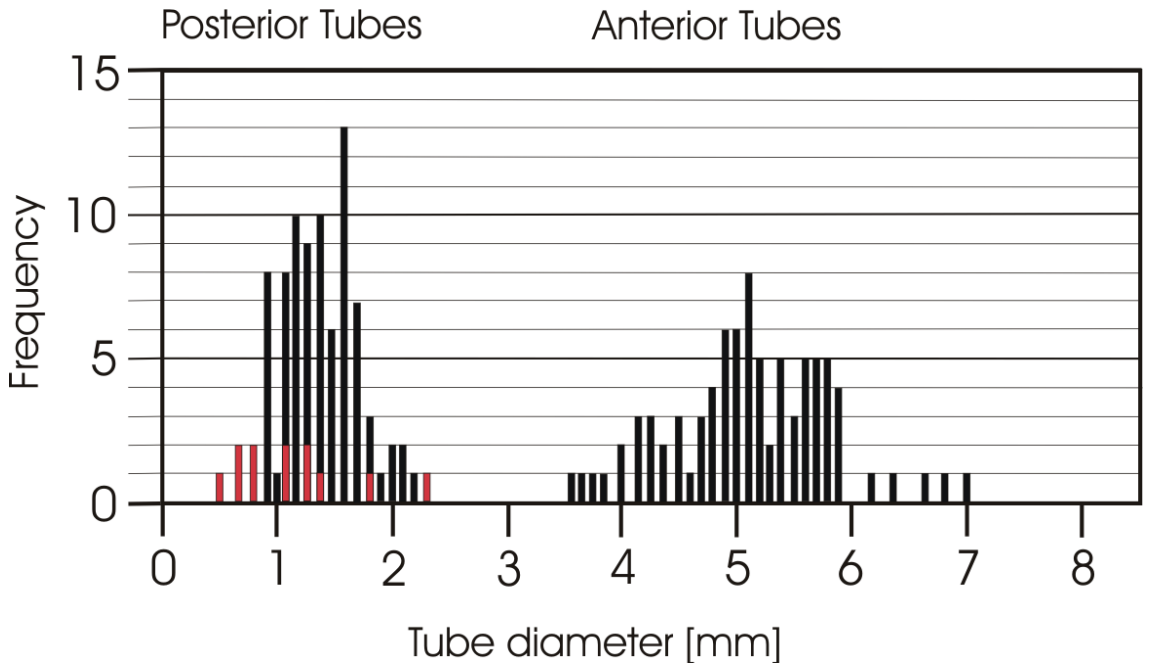

Figure 4. Measurement of unmineralized posterior and anterior worm tubes from vestimentiferan 'bush' sample GeoB 8203-1; black bars, n=85 posterior tubes, 80 anterior tubes (GeoB 8203-1-1vt to GeoB 8203-1-85vt). Tube diameters of mineralized tubes are indicated by red bars (see table 1).

Examination of the thin sections shows that some of the empty vestimentiferan tubes are surrounded by calcium carbonate indurated sediment, which adheres on the external tube wall surface (Fig. 5A). This calcium carbonate is in some cases disrupted close to the tube wall by layers tens to hundreds of microns thick of botryoidal aragonite crystals and/or isopachous aragonite (Fig. 5B). However, these aragonite layers never occur at the sediment-tube wall interface (Fig. 5B). Some of the sediment-enclosed tubes have been partially mineralized by microcrystalline to microsparitic aragonite crystals. This mineralization starts on the exterior wall layers and successively replaces the tube organic laminae inwards (Figs. 5C,D, 6A,B). This process is not always complete, however, with some organic laminae remaining unmineralized in the replaced portions of a few specimens (Fig. 6F). The mineralized parts of the tubes retain some of the fine-scale lamination of the original organic wall, picked out by very fine parallel layers of brown organic material, best seen in plane polarized light (Figs. 5C,D, 6A,B). Post-collection drying of the specimens prior to setting in resin has caused shrinkage of the non-mineralized organic parts of the tubes, causing these to pull away from the mineralized parts of the tubes and decrease in diameter (Figs. 5A, 6A).

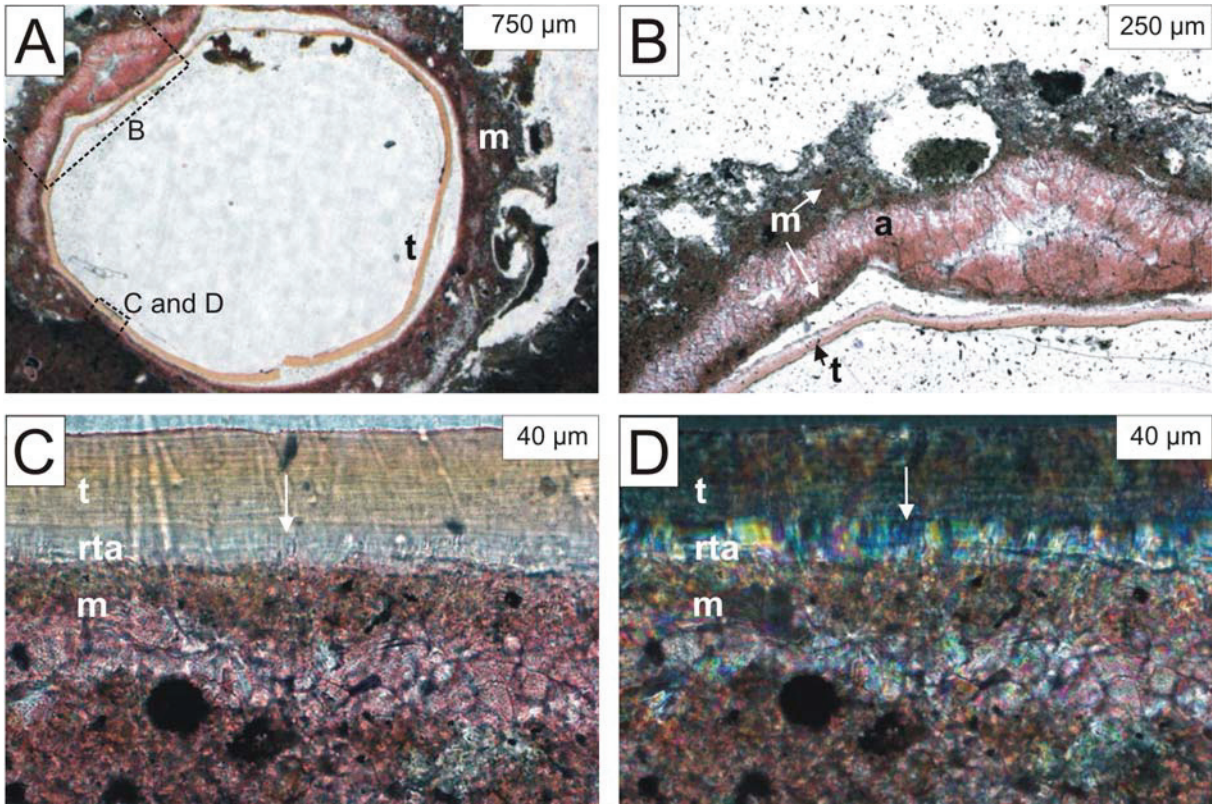

Figure 5. Thin section photomicrographs of stained mineralized tube in transverse section from sample GeoB 8212-2-5. A. The light-brown organic tube (t) is surrounded and enclosed by microcrystalline calcium carbonate (m). The dashed line box insets show the locations of photomicrographs B to D. B. Large-scale aragonite crystal layer (a) within the microcrystalline calcium carbonate. C. Microcrystalline aragonite crystals (rta) replace the exterior wall laminae (t) (white arrow). D. In crossed polarized light the aragonite replacement of the organic layers is highlighted.

A tube specimen from sample GeoB8212-2-8a shows a further stage of vestimentiferan tube wall mineralization where the aragonite-replaced tube wall laminae are separated from each other and enclosed by the growth of layers of larger splays of aragonite (Fig. 6C). Fluorescence microscopy shows that these layers contain less organic material than the replaced tube wall laminae (Fig. 6D). In some places the tube wall laminae that have been replaced by microcrystalline aragonite have been subsequently overgrown by fibrous radial aragonite crystals (Fig.6E).

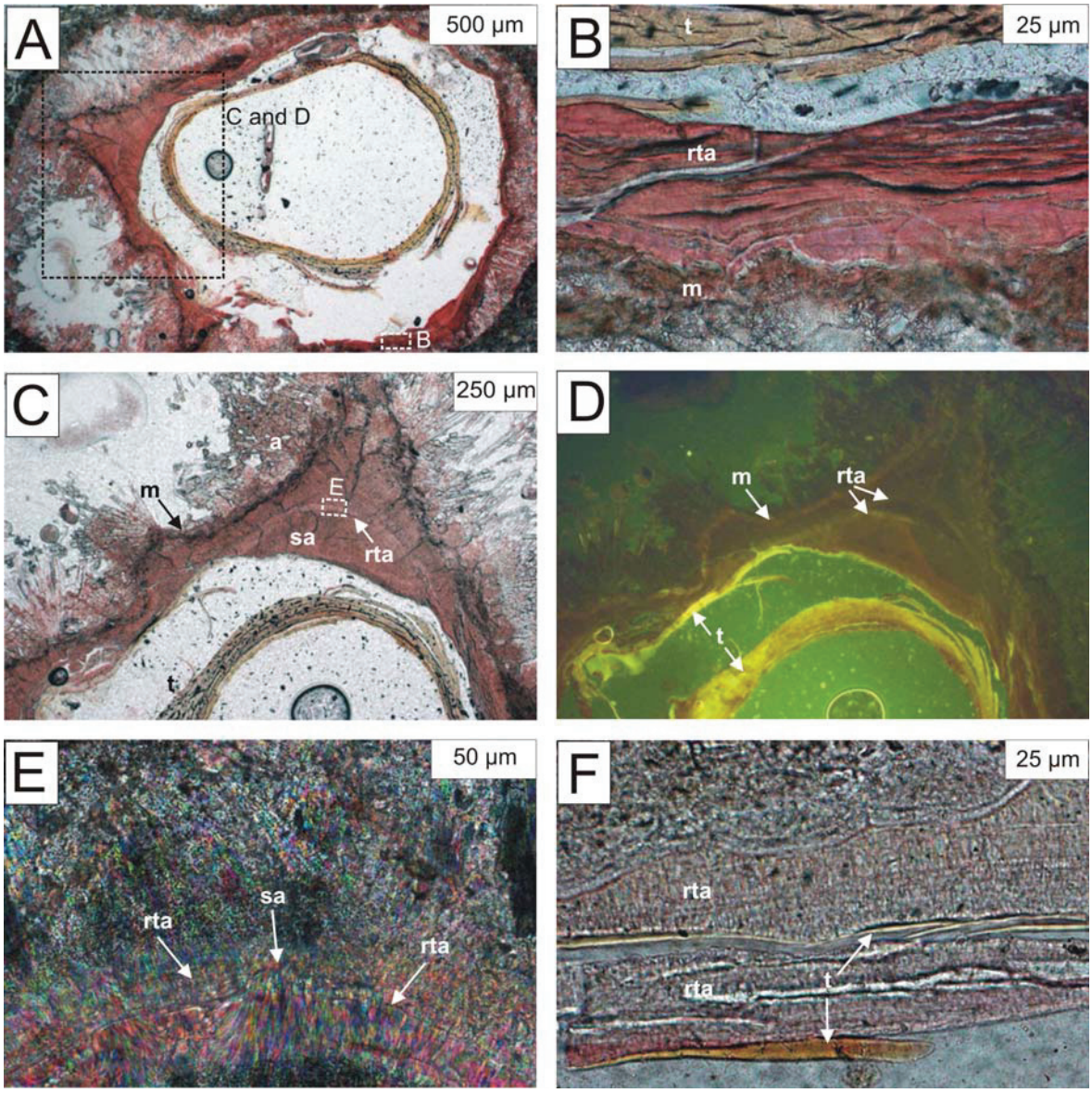

Figure 6. Thin section photomicrographs of stained mineralized tubes in transverse section from samples GeoB8212-2-8a (A-E) and GeoB 8212-2-1 (F). A. Overview image of partially mineralized tube with dashed line box insets showing the locations of photomicrographs B-D. B. Microcrystalline calcium carbonate (m) enclosing microcrystalline aragonite replaced tube wall (rta) showing fine-scale concentric lamination inherited from the organic tube wall (t), which has mostly pulled away from the replaced wall due to post-collection shrinkage. C. Layer of microcrystalline aragonite replaced tube wall (rta) enclosed in layers of larger, splays of aragonite (sa). Radiating splays of large aragonite crystals (sa) are also present within the enclosing microcrystalline calcium carbonate. The dashed line box inset shows the location of photomicrograph E. D. Fluorescence microscopy highlights the high organic content of the original tube wall, the replaced tube wall and the thin layer of micrite on the outside of the tube wall. E. Detail of replaced tube wall in cross polarized light showing the replaced tube wall (rta) being overgrown by radiating aragonite (sa) crystals, destroying the relict lamination from the original organic tube. F. A few organic laminae (t) are preserved within the replaced wall laminae (rta). The outer surface of the tube is towards the top of the photomicrograph.

Tube specimens shown in Fig. 7 have additional replacement textures of the organic tube walls by aragonite. In Fig. 7A a remnant of the organic tube wall is separated by a palisade of isopachous aragonite crystals from a thin layer of tube wall replaced by microcrystalline aragonite that still retains a relict texture of the original organic tube wall as thin parallel bands of brown organics. This texture is also seen in a specimen from sample GeoB 8212-2b (Figs. 7B,C) where bundles of aragonite splays separate relicts of the original tube wall laminae

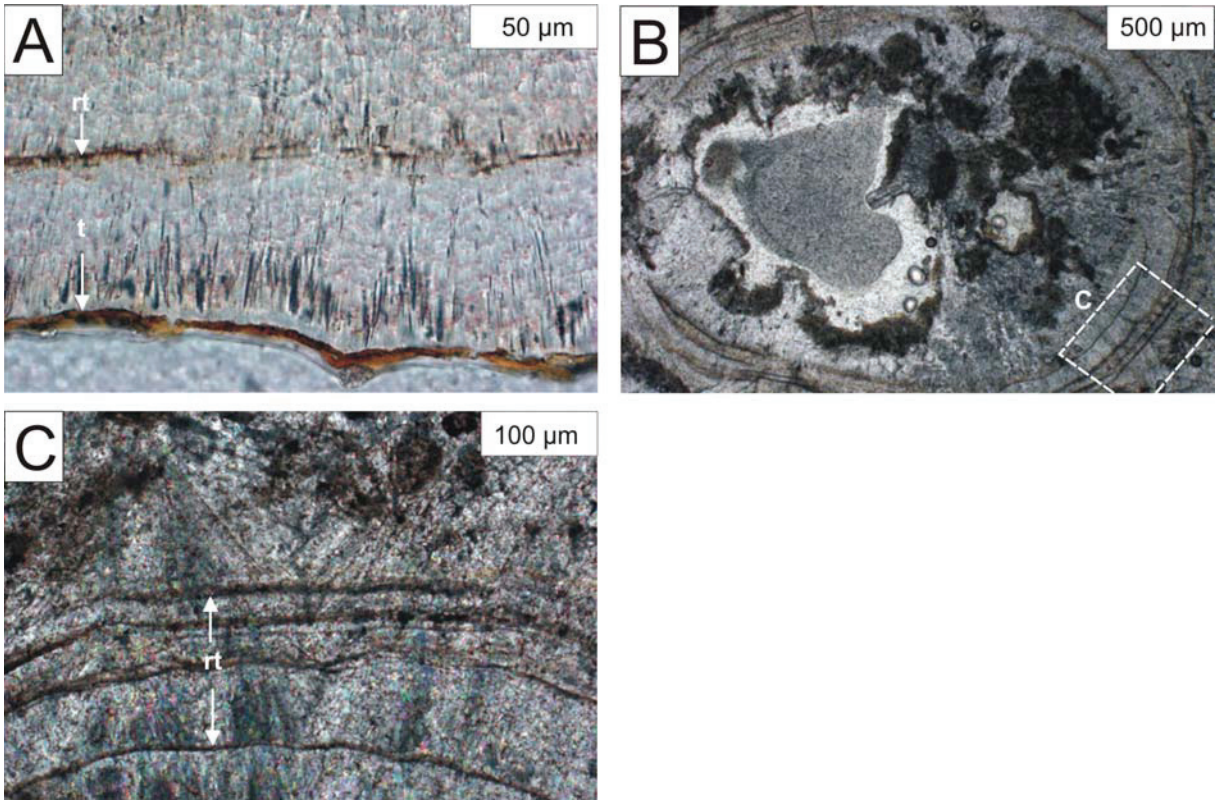

Figure 7. Thin section photomicrographs of stained mineralized tubes in transverse section from samples GeoB 8212-2-1c (A) and GeoB 8212-2b (B, C). A. Remnant of organic tube wall (t) separated from aragonite replaced tube wall laminae (rt) by isopachous aragonite palisade. B. Overview image of completely mineralized tube with aragonite replaced relicts of the original organic tube wall laminae (brownish colour) separated from each other by orientated splays of large aragonite crystals. The interior of the tube that would have originally contained the body of the animal is now partially infilled by large-scale aragonite crystals. Dashed line box inset shows the location of photomicrograph C, which has been rotated counter-clockwise such that the exterior of the tube is now at the top of the image. C Detail of completely replaced tube wall (rt) in crossed polarized light showing botryoidal aragonite growing through the replaced relicts of the original tube wall.

Based on our observations from Hydrate Hole and Black Hole we suggest that mineralization of the posterior 'root' portions of Kouilou vestimentiferan tubes is a post-mortem process that occurs along two pathways, starting from the exterior of the tube inwards and resulting in the partial to complete replacement of the original organic tube wall by microcrystalline and/or fibrous aragonite (Fig. 8). These pathways are almost certainly not mutually exclusive and we think the degree of replacement is a reflection of both decay of the organic tube and the local flux of bicarbonate ions resulting from AOM in the sediment (see below).

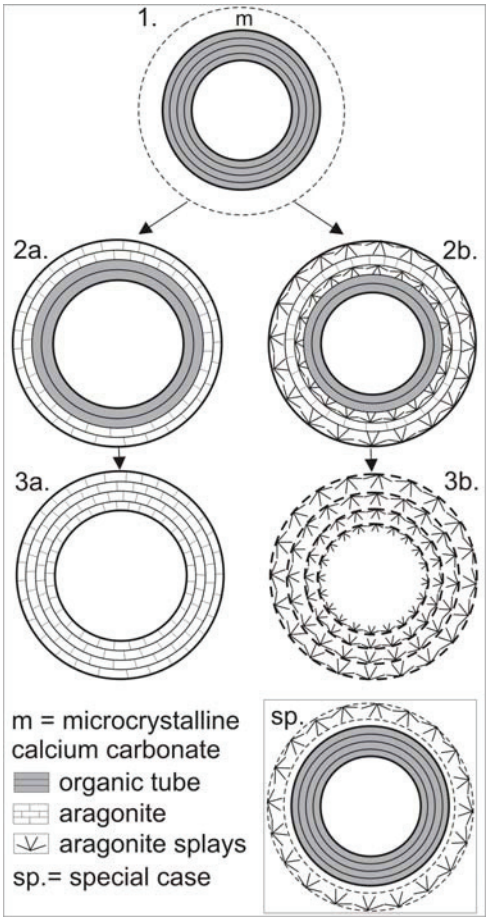

Figure 8. Suggested sequences of carbonate mineralization of Kouilou vestimentiferan tubes. All images are of posterior 'root' tubes in transverse section. 1. Organic tube wall enclosed in microcrystalline calcium carbonate (m). Sequence 2a-3a. Microcrystalline aragonite crystals replace the former organic tube wall laminae from the exterior of the tube wall inwards. Successive mineralization of individual laminae forms massive aragonitic tube walls preserving of the original texture as fine scale concentric laminations with brownish colour, representing relict organic material. In this sequence the diameter of the replaced tube is roughly the same as the original organic tube. Sequence 2b-3b. The process of microcrystalline aragonite replacement is the same as 2a, but large-scale aragonite crystals form between sequentially replaced laminae, or bundles of laminae, separating them from each other and substantially decreasing the internal diameter of the tube wall. Further mineralization leads to the replaced tube laminae becoming overgrown and embedded in splays of botryoidal aragonite. The special case (sp.) is where large scale aragonite crystals grow

within microcrystalline calcium carbonate enclosing the tube wall. This cannot be related in an obvious way to the other sequences and could occur before, during or after tube wall replacement.

5.4 Discussion

Because we do not have chemical measurements from the sediments of the Kouilou pockmarks nor information about the physiology of the Kouilou vestimentiferans we will use data from other well studied seep sites, in particular those from the Gulf of Mexico, to discuss the possible processes that lead to the diagenetic replacement of some of the posterior portions of the Kouilou vestimentiferan tubes. Pertinent here is the fact that there is no carbonate precipitation on the anterior (Figs. 2A,B) or posterior tubes (Figs. 2E,D) of the vestimentiferan 'bush' from Hydrate Hole, or directly on other living Kouilou specimen posterior tubes (Fig 3). This is what we would expect if the Kouilou vestimentiferans have a similar ecology to *Lamellibrachia luymesi*. In this species the anterior tubes project into an oxic environment where rapid carbonate mineralization is unlikely to occur, but the posterior 'root' tubes in the sediment experience a strongly reducing, alkaline environment where carbonates are forming due to the local flux of bicarbonate ions resulting from AOM. This should result in carbonates precipitating around or even on the 'roots', particularly as *L. luymesi* is locally accentuating AOM by pumping sulphate from the permeable 'roots' into adjacent sediment. However, according to Dattagupta et al. (2006, 2008), *L. luymesi* is able to prevent, or at least retard this happening by also pumping hydrogen ions from its 'roots' into the sediment. This system would of course cease on the death of individual vestimentiferans and their 'roots' would then become susceptible to having carbonate form on their exterior surfaces, particularly if already surrounded by a collar of carbonate indurated sediment (Fig. 3). Because of locally high flux of AOM derived carbonate ions the permeable 'root' may then get replaced from the exterior inwards. This process could be accentuated by post-mortem microbial decay of the 'root' proteins by microorganisms and the permeability of the 'roots' may make this process particularly rapid.

The discovery of carbonate indurated sediments forming around (but not directly on) the posterior tubes of some of the living Kouilou vestimentiferans (Fig. 3) contrasts somewhat with the theoretical models and experimental data of the ecology of *Lamellibrachia luymesi* (Cordes et al. 2005; Dattagupta, et al. 2006), because proton pumping from 'roots' to sediment should prevent local carbonate formation. We suggest that a simple answer to this potential discrepancy is that in the microenvironments local to some of the posterior tubes, the rate of AOM-related carbonate formation exceeds the rate of

proton pumping. This assumes that the Kouilou vestimentiferan species has a similar ecology to *L. luymesi* and that the enclosed posterior tubes are physiologically active.

Our observations of the mineralized Kouilou vestimentiferans show that the replacement of the 'root' tubes is initially on a very fine scale that preserves relicts of the original tube wall laminated structure. Subsequent aragonite formation causes partial recrystallisation of micron scale aragonite to larger fibrous, splays of aragonite. This may reflect some element of positive feedback in the diagenetic process and/or that some of the 'root' tubes are located in areas of particularly high methane flux, as this is known to promote significant aragonite formation (Luff and Wallmann 2003).

Our results show that the posterior 'roots' of vestimentiferan tubes at modern seeps can be replaced by aragonite to produce tubular structures with carbonate walls showing fine scale concentric laminations. Identical diagenetic features are seen in various fossil tubes from ancient seep carbonates. For example, tubes from the Devonian Hollard Mound, Morocco (Peckmann et al., 2005), and the Carboniferous Ganigobis limestones, Namibia (Fig. 9; Himmler et al., 2008) are of similar size and shape to the Kouilou tubes, are formed of carbonate and have concentric laminations in transverse section (Fig. 9A), often showing 'delamination' structures (Fig. 9B), which are analogous to the features shown here in Figs. 6 and 7.

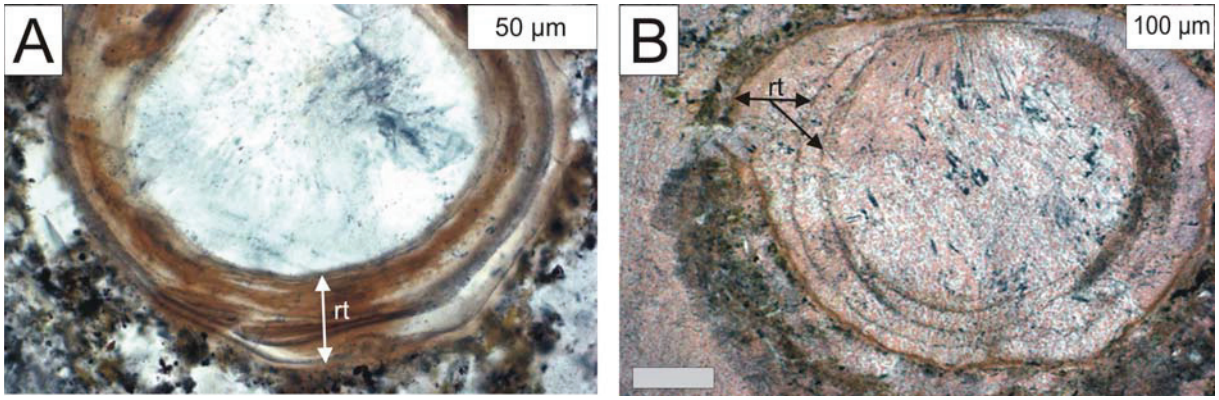

Figure 9.Fossil tubes in transverse section from the Carboniferous Ganigobis seep limestones, Namibia (Himmler et al., 2008). A. Tube with laminated tube wall (rt) formed of calcite. Compare to Congo tube walls in Fig. 6. B. Tube with outer coating of calcite cemented sediment and filling of splays of relict aragonite crystals (now recrystallized to calcite). The carbonate replaced tube wall (rt) shows de-lamination textures very like the Congo carbonate replaced tubes shown in Fig. 7.

The only major difference between the Hollard Mound and Ganigobis tubes and the Kouilou replaced vestimentiferan tubes are that the ancient tubes are formed of calcite, not aragonite.

However, aragonite is metastable under surface conditions and generally inverts to calcite over geological time, such that aragonite is exceptionally rare in rocks older than the Mesozoic (Tucker and Wright, 2004). Therefore, we think it is most likely that the carbonate forming the Hollard Mound and Ganigobis tubes was originally aragonite.

The Kouilou vestimentiferan tubes also resembles the tubes from the Oligocene Canyon River seep carbonates of the Lincoln Creek Formation, Washington State, USA, which Goedert et al. (2000) suggested are mineralized vestimentiferan tubes. Most of the Canyon River tubes are similar in size and shape to the anterior tube parts of the Congo vestimentiferans (Figs. 2A, 4), but there are some smaller tubes that are more like the posterior Kouilou tubes in size and having twisted and tangled morphologies. The walls of the Canyon River tubes are formed of microcrystalline aragonite or quartz replacing aragonite and Goedert et al. (2000) suggested that the tubes either originally had a high carbonate content, or were indurated very early by aragonite mineralization of an organic tube wall. Our data from the Kouilou vestimentiferan tubes shows that the latter hypothesis of Goedert et al. (2000) is entirely possible and strengthens their identification of the Canyon River tubes as those of vestimentiferans. The only discrepancy between that hypothesis and our data is that Goedert et al. (2000) suggested that the mineralization of the Canyon River tubes occurred on the anterior portions of vestimentiferan tubes while they were projecting into the water column. However, given that aragonite replacement of vestimentiferan tubes in the Kouilou pockmarks (and carbonate formation generally at seeps) occurs only in the sub-surface, we think that this is an unlikely scenario and that mineralization of the Canyon River tubes probably also occurred in this environment, perhaps after later sediment accumulation around the more anterior portions of the tubes.

Because of the morphological similarities between some tubes in ancient seep carbonates and modern seep vestimentiferan tubes and, through this study, the identification of a diagenetic replacement of organic vestimentiferan tubes by aragonite, we think that the designation by previous authors of the ancient seep tubes as vestimentiferans is considerably strengthened (Goedert et al., 2000; Peckmann et al., 2005; Himmler et al., 2008). Although the ancient seep tubular fossils may have been formed by a different group of organisms secreting a vestimentiferan-like laminated organic tube, we think this is less parsimonious than identifying the ancient tubes as being those of vestimentiferans. This has implications that the origin of the vestimentiferans, as the Palaeozoic seep tubes (e.g. Fig. 9) significantly

pre-date the molecular divergence date of 126 million years for the group (see Little and Vrijenhoek, 2003, for discussion).

5.5 Conclusions

Some of the empty posterior 'root' tubes of vestimentiferan worms from the Kouilou pockmark field on the Congo deep sea fan are partially or completely replaced by different sizes and morphologies of the carbonate mineral aragonite. This replacement occurs from the outside of the tube wall inwards and leaves fine-scale relict textures of the original organic tube wall as concentric laminations, sometimes showing brownish staining caused by organic material. Subsequent overgrowth by larger scale splays of aragonite can destroy this relict texture in places. The process of mineralization is unknown, but is likely a result of post-mortem microbial decay of the tube wall proteins by microorganisms and/or the precipitation from locally high flux of AOM derived carbonate ions. The aragonite replaced tubes from the Kouilou pockmarks show many similar features to carbonate tubes in ancient seep deposits and make it more likely that many of these fossil tubes are those of vestimentiferans, as has been suggested previously.

Acknowledgements

We thank Sebastian Flotow for the preparation of thin sections and three anonymous referees for their comments on an earlier draft of this paper. This study was supported by the Deutsche Forschungsgemeinschaft through the DFG-Excellence Cluster MARUM, Bremen (contribution no. MARUMXXXX) and a Marine and Climate Research Fellowship to CTSL from the Hanse-Wissenschaftskolleg, Delmenhorst, Germany.

6. General conclusions

The scientific issue of this thesis was the examination of three specific processes of carbonate formation such as i.) methane-derived carbonate formation ii.) carbonate authigenesis modified by vestimentiferan tube worms and iii.) the mineralization of vestimentiferan worm tubes by carbonate. The investigation of the methane-derived carbonates was accomplished to reconstruct the basically existing carbonate formation conditions at the lately discovered Kouilou-pockmarks. These pockmarks were object of investigations during R/V METEOR Cruise M56 off southwest Africa. During TV-sled surveys dense colonies of vestimentiferan tube worms were found widespread on the pockmarks seafloor. The extraction of such bush-like vestimentiferan colonies by a TV-guided grab revealed pronounced carbonate aggregates at those posterior tubes within the sediment. The surprising discovery results in many questions such as the role of tube worms on carbonate formation, whose solution was an emphasis of this work. In addition, the tube worm/carbonate aggregates contained mineralized worm tubes in different states of preservation and offered the opportunity to investigate those taphonomic processes.

The classification of the carbonate structures was accomplished based on the shapes of carbonate structures, the petrography, total carbonate contents, stable carbon and oxygen isotopic compositions and the analyses of biomarker. The dominant process of carbonate formation is based on the anaerobic oxidation of methane (AOM). Biomarker analyses revealed that ANME-1 and ANME-2 consortia are operating these processes at the Kouilou pockmarks. Simultaneously those highly negative carbon isotopic compositions as negative as –140 ‰ V-PDB show the usage of carbon from microbial methane formation. This is even supported by the carbon isotopic compositions of the carbonates as low as –58.9 ‰ V-PDB (mean: –49.7 ± 6.8). According to the results, carbonate formation was crucial depending on methane flux intensity, its migration pathways, just as well seawater infiltration and the accumulation of specific AOM consortia. Two well defined sediment milieus were extracted: carbonate formation in greater sediment depth and close to the seafloor. Nodular, tubular and irregular-complex structures composed of microcrystalline high-Mg-calcite are formed deeper in sediments during moderate methane flux intensities. This is indicated by the presence of ANME-1 biomarker and the in contrast less negative carbon isotopic compositions. Additionally, the positive oxygen isotope anomalies of up to 5.3‰ V-PDB

(mean: 4.4 ± 0.5‰) display a restricted infiltration of seawater and a contribution from hydrate water due to gas hydrate decomposition on carbonate formation.

In contrast, carbonate structures formed near to the seafloor reveal significantly differing attributes. The thin slabs composed of microcrystalline aragonite indicate higher methane flux intensities by the presence of ANME-2 consortia, and the more negative carbon isotopic compositions. Moreover, higher contribution of sea water in the precipitation fluids are displayed by the nearly seawater equivalent oxygen isotopic compositions and the higher total carbonate contents, resulting from higher pore volume in unconsolidated sediments. In addition, the occurrence of organic substances on some slabs, are probably relicts from microbial mats (*Beggiatoa?*), which usually occur at the sediment/ sea water interface. Furthermore, the formation of barite aggregate as present on some surfaces is indicative for barium-rich fluid up-flow and sulfate-rich pore waters.

Beside these characteristic carbonate formation milieus, few recovered structures were due to their shapes identified as casts of molds. The burrowing activities of benthic organisms like bivalves and holothurians are assumably responsible for rapid infiltration of seawater into deeper sediments. In respect to that, both environments described above could change within short intervals as displayed by fine-scale variations in carbonate mineralogy of some of these structures. The irregularly mix of pore and seawater creates microenvironmental niches of variable pore water chemistry. The punctual occurrence of protodolomite supposable reflects the specifically assemblages and activities of microorganisms in such niches.

A close relationship of vestimentiferan tube worms, their metabolic activity within the sediments, and the aggregation of carbonate at their posterior tubes could be demonstrated. The formation of very complex tube worm/carbonates most likely starts with the fixation of worm tubes on already existing carbonates within the sediments. These attached carbonates, mainly nodules composed of high-Mg-calcite, form in bush-like tube worm colonies considerable parts of the final carbonate structure. After tube worm colonization their metabolic activity modifies the AOM induced carbonate formation by the uptake of sulfide, and the elimination of sulfate and hydrogen ions. Their removal of sulfide off the sediment enables ongoing carbonate precipitation and prevents carbonate dissolution by balancing the pH, which is a critical parameter for carbonate formation. Additionally, the change in carbonate mineralogy towards a predominant aragonite formation after tube worm colonisation is most likely a result of sulfate release to the sediment by the tube worms itself, as aragonite is the favoured mineral precipitated during these conditions. Simultaneously,

high sulfate concentrations stimulate the turnover of AOM consortia, and, supply the needs of sulfide for the tube worms' themselves. Moreover, their release of hydrogen ions to prevent carbonate formation direct on the tube surface, is very likely responsible for the co-occurrence of still unaltered organic tubes of living worms, and partly (dead) or totally lithified (degraded) tubes on some structures. However, tube worm/carbonate aggregates are products of recurring carbonate formation and form finally structures which resemble lithified root-balls.

Diagenetic tube mineralization of Kouilou vestimentiferans finally leads to the formation of two characteristic mineralization patterns. Mineralization proceeds from the outside of the tube wall inwards, and the laminar organic tube wall get replaced by the carbonate mineral aragonite. The formation of the characteristic mineralization pattern depends on the size and fabric of the aragonite crystals. Microcrystalline aragonite successively replaces the individual wall laminae and preserves the former tube configuration. Accompanied with this process is the complete loss of organic material, which is likely a result of post-mortem microbial decay of the tube wall proteins.

The growth of large-scale aragonite splays on the organic wall laminae results in laminae separation, and the lateral spreading of the tube wall which finally initiates the reduction of the internal tube diameter. Few remains of the former wall laminae get preserved and are responsible for the configuration of brownish concentric lines between the circular bands of isopachous aragonite splays.

Rapidly occuring recrystallisation processes are observed even on only partly mineralized worm tubes. Microcrystalline aragonite crystals get overgrown by larger, radiating splays of aragonite. The growth of these crystals is responsible for the delamination of still unaltered organic laminae and the formation of bulges. Surprisingly, exactly these features were even observed on ancient tube worm fossils of Devonian and Carboniferous age, and make it more likely, that many of these fossil tubes are vestimentiferans.

7. Perspectives

One important aspect of geological structures is related to the time of their first appearance or development. Until now no time-estimates were accomplished on the Kouilou pockmarks. Due to the sediment out blow and the disturbance of the sedimentary record by fluid and gas migration, sediment analyses will not be very helpful. In this context, $^{230}Th/^{234}U$ measurements on carbonate structures is at least for the approximate time-determination of carbonate formation an established method. The accomplishment of these measurements in high resolution e.g. by the use of MIC-ICP-MS (multi ion counting-inductivity coupled-mass spectrometry) or LA-ICP-MS (laser ablation-inductivity coupled-mass spectrometry), would additionally allow to estimate the ratios of sea and pore water, participating on carbonate precipitation fluids. Supplementary analyses of rare-earth-elements e.g. Ce anomalies reflecting differences in pH and redox conditions permit information on spatially occurring heterogeneities. Moreover, the precision of temperature calculation via oxygen isotopic compositions is upgradeable by adding of $\delta^{88/86}Sr$ isotope measurements, as a potential proxy for temperature. Altogether, this would expand the detailed knowledge on variations in methane flux intensities, carbonate formation processes and environments, and peculiar features which had taken place at the Kouilou-pockmarks.

It would also be of high interest to accomplish in-situ measurements of e.g. pH, sulfide and sulfate concentrations directly on the posterior tube surface of agile vestimentiferan tube worms to calculate their approximate metabolic turn over. This would give insights in the effective impact of chemosymbiotic tube worms on pore water chemistry, the additional turn over of methane, and the subsequent consequences on carbonate formation. Moreover, detailed measurements of these processes are necessary to achieve high resolution results of methane migration and emission at methane seeps, and will improve the results of global methane-budged calculations.

The general processes involved in diagenetic mineralization of vestimentiferan worm tubes are still unknown. Although the reconstruction of mineralization sequences gave evidence that mineralization co-occurred with tube wall degradation on the Kouilou vestimentiferans, it is actually neither proven that established degradation processes cause tube mineralization nor to what fraction it is affected by the methane seep environment. Is the co-occurrence of both characteristic mineralization patterns of the Kouilou tubes a result of variations in microbial activity and/or seep chemistry? The investigations of these processes

are assumably related to insights into spatial variations in the assemblage of microorganisms responsible for the degradation of organic matter at cold seeps, as well as in small-scale variations in methane seepage.

8. References

Allison, P.A., 1988. The role of anoxia in the decay and mineralization of proteinaceous macro-fossils. Paleobiology 14, 139-154.

Aloisi, G., Pierre, C., Rouchy, J.-M., Foucher, J.-P., and Woodside, J., 2000. Methane-related authigenic carbonates of eastern Mediterranean Sea mud volcanoes and their possible relation to gas hydrate destabilization. Earth and Planetary Science Letters 184, 321-338.

Andersen, A.C., Hourdez, S., Marie, B., Jollivet, D., Lallier, F.H., Sibuet, M., 2004. Escarpia southwardae sp. nov., a new species of vestimentiferan tubeworm (Annelida, Siboglinidae) from West African cold seeps. Canadian Journal of Zoology 82, 980-999.

Baker, P.A., and Kastner, M., 1981. Constrains on the formation of sedimentary dolomite. Science 213, 214-216.

Berner, R.A., 1969. Migration of iron and sulfur within anaerobic sediments during early diagenesis. American Journal of Science 267, 19-42.

Berner, R.A., 1970. Sedimentary pyrite formation. American Journal of Science 268, 1-23.

Berndt, M.E., Allen, D.E. and Seyfried, W.E., 1996. Reduction of CO_2 during serpentinisation of olivine at 300 °C and 500 bar. Geology 24, 351-354.

Bergquist, D.C., Williams, F.M., and Fisher, C.R., 2000. Longevity record for deep-sea invertebrate. Nature 403, 499-500.

Bergquist, D.C., Andras, J.P., McNelis, T., Howlett, S., van Horn, M.J., Fisher, C.R., 2003. Succession in Gulf of Mexico cold seep vestimentiferan aggregations: The importance of spatial variability. Marine Ecology 24, 31-44.

Birgel, D., Himmler, T., Freiwald, A. and Peckmann, J., 2008. A new constraint on the antiquity of anaerobic oxidation of methane: Late Pennsylvaninan seep limestones from southern Namibia. Geology 36, 543-546.

Black, M.B., Halanych, K.M., Maas, P.A.Y., Hoeh, W.R., Hashimoto, J., Desbruyères, D., Lutz, R.A., and Vrijenhoek, R.C., 1997. Molecular systematics of vestimentiferan tubeworms from hydrothermal vents and cold-water seeps. Marine Biology 130, 141-149.

Blumenberg, M., Seifert, R., Reitner, J., Pape, T., and Michaelis, W., 2004. Membrane lipid patterns typify distinct anaerobic methanotrophic consortia. The Proceedings of the National Academy of Sciences USA 101, 11111-11116.

Boetius, A., Ravenschlag, K., Schubert, C.J., Rickert, D., Widdel, F., Gieseke, A., Amann, R., Jørgensen, B.B., Witte, U., and Pfannkuche, O., 2000. A marine microbial consortium apparently mediating anaerobic oxidation of methane. Nature 407, 623-626.

Bohrmann, G., Greinert, J., Suess, E., and Torres, M., 1998. Authigenic carbonates from the Cascadia subduction zone and their relation to gas hydrate stability. Geology 26, 647-650.

Bohrmann, G., Jung, C., Heeschen, K., Weinrebe, W., Baranov, B., Cailleau, B., Heath, R., Hühnerbach, V., Hort, M., Kath, T., Masson, D., and Trummer, I., 2002. Widespread fluid expulsion along the seafloor of the Costa Rica convergent margin. Terra Nova 14, 69-79.

Bohrmann, G., Ivanov, M.K., Foucher, J.P., Spiess, V., Bialas, J., Greinert, J., Weinrebe, W., Abegg, F., Aloisi, G., Artemov, Y., Blinova, V., Drews, M., Heidersdorf, F., Krabbenhöft, A., Klaucke, I., Krastel, S., Leder, T., Polikarpov, I., Saburova, M., Schmale, O., Seifert, R., Volkonskaya, A. and Zillmer, M., 2003. Mud volcanoes and gas hydrates in the Black Sea: new data from Dvurechenskii and Odessa mud volcanoes. Geo-Marine Letters 23, 239-249.

Bohrmann, G. and Torres, M., 2006. Gas hydrates in marine sediments. In: H. Schulz and M. Zabel (Editors), Marine Geochemistry. Springer, pp. 481- 512.

Borowski, W.S., Paull, C.K. and Ussler, W., III, 1999. Global and local variations of interstitial sulfate gradients in deep-water, continental margin sediments: Sensitivity to underlying methane and gas hydrates. Marine Geology 159, 131-154.

Buczynski, C., and Chafetz, H.S., 1991. Habit of bacterially induced precipitates of calcium carbonate and the influence of medium viscosity on mineralogy. Journal of Sedimentary Petrology 61, 226-223.

Burton, E.A., 1993. Controls on marine carbonate cement mineralogy: review and reassessment. Chemical Geology 105, 163-179.

Brown, K.M., 1990. The nature and hydrogeologic significance of mud diapirs and diatremes for accretionary system. Journal of Geophysical Research 95, 8969-8982.

Campbell, K.A., Carlson, C., Bottjer, D.J., 1993. Fossil cold seep limestones and associated chemosymbiotic macroinvertebrate faunas, Jurassic-Cretaceous Great Valley Group, California. In: S. Graham and W. Lowe (Editors), Advances in the Sedimentary Geology of the Great Valley Group Pacific Section. Society of Economic Paleontologists and Mineralogists, pp. 37-50.

Campbell, K.A., Farmer, J.D., and Des Marais, D., 2002. Ancient hydrocarbon seeps from Mesozoic convergent margin of California: carbonate geochemistry, fluids and palaeoenvironments. Geofluids 2, 63-94.

Campbell, K.A., 2006. Hydrocarbon seep and hydrothermal vent paleoenvironments and paleontology: Past developments and future research directions. Palaeogeography, Palaeoclimatology, Palaeoecology 232, 362-407.

Canfield, D.E. and Raiswell, R., 1991. Carbonate precipitation and dissolution: its relevance to fossil preservation. In: P.A. Allison and D.E.G. Briggs (Editors), Taphonomy: Releasing the Data Looked in the Fossil Record Plenum Press, New York, pp. 411-453.

Castanier, S., Le Métayer-Levrel, G., and Perthuisot, J.-P., 1999. Ca-carbonates precipitation and limestone genesis-the microbiogeologist point of view. Sedimentary Geology 126, 9-23.

Castellini, D.G., Dickens, G.R., Snyder, G.T., and Ruppel, C.D., 2006. Barium cycling in shallow sediment above active mud volcanoes in the Gulf of Mexico. Chemical Geology 226, 1-30.

Cavagna, S., Clari, P. and Martire, L., 1999. The role of bacteria in the formation of cold seep carbonates: geological evidence from Monferrato (Tertiary, NW Italy). Sedimentary Geology 126, 253-270.

Cavanaugh, C.M., Gardiner, S.L., Jones, M.L., Jannasch, H.W., and Waterbury, J.B., 1981. Procaryotic cells in the hydrothermal vent tube worm Riftia pachyptila Jones: possible chemoautotrophic symbionts. Science 213, 340-342.

Charlou, J.L., Donval, J.P., Fouquet, Y., Ondreas, H., Cochonat, P., Levaché, D., Poirier, Y., Jean-Baptiste, P., Fourré, E., and Chazallon, B., 2004. Physical and chemical characterization of gas hydrates and associated methane plumes on the Congo-Angola Basin. Chemical Geology 205, 405-425.

Chevaldonné, P., Jollivet, D., Desbruyères, D., Lutz, R.A., and Vrijenhoek, R.C., 2002. Sister-species of eastern Pacific hydrothermal vent worms (Ampharetidae, Alvinellidae, Vestimentifera) provide new mitochondrial COI clock calibration in Desbruyères, D., and Juniper, S.K., eds., Proceedings of the 2nd international symposium on deep-sea hydrothermal vent biology. Brest, Cahiers de Biologie Marine 43, 367-370.

Childress, J.J., Arp, A.J., and C. R. Fisher, J., 1984. Metabolic and blood characteristics of hydrothermal vent tube-worm Riftia pachyptila. Marine Biology 83, 109-124.

Childress, J.J., Fisher, C.R., Brooks, J.M., II, M.C.K., Bidigare, R. and Anderson, A.E., 1986. A methanotrophic marine molluscan (Bivalvia, Mytilidae) symbiosis: mussels fueled by gas. Science 233, 1306-1308.

Claypool, G.E. and Kaplan, I.R., 1974. The origin and distribution of methane in marine sediments. In: I.R. Kaplan (Editor), Natural Gases in Marine Sediments. Plenum, New York, 99-139.

Clennell, M.B., Hovland, M., Booth, J.S., Henry, P. and Winters, W.J., 1999. Formation of natural gas hydrates in marine sediments, 1, Conceptual model of gas hydrate growth conditioned by host sediment properties. Journal of Geophysical Research 104, 22985-23003.

Coleman, D.F. and Ballard, R.D., 2001. A highly concentrated region of cold hydrocarbon seeps in the southeastern Mediterranean Sea. Geo-Marine Letters 21, 162-167.

Cordes, E.E., Bergquist, D.C., Shea, K., and Fisher, C.R., 2003. Hydrogen sulphide demand of long-lived vestimentiferan tube worm aggregations modifies the chemical environment at deep-sea hydrocarbon seeps. Ecology Letters 6, 212-219.

Cordes, E.E., Arthur, M.A., Shea, K., Arvidson, R.S., and Fisher, C.R., 2005. Modeling the mutualistic interactions between tubeworms and microbial consortia: PLOS Biology 3, 1-10.

Dählmann, A., and De Lange, G., 2003. Fluid-sediment interactions at Eastern Mediterranean mud volcanoes: a stable isotope study from ODP Leg 160. Earth and Planetary Science Letters 212, 377-391.

Dattagupta, S., Miles, L.L., Barnabei, S., Fisher, C.R., 2006. The hydrocarbon seep tubeworm Lamellibrachia luymesi primarily eliminates sulfate and hydrogen ions across its roots to conserve energy and ensure sulfide supply. The Journal of Experimental Biology 209, 3795-3805.

Dattagupta, S., Arthur, M.A., and Fisher, C.R., 2008. Modification of sediment geochemistry by hydrocarbon seep tubeworm Lamellibrachia luymesi: A combined empirical an modeling approach. Geochimica et Cosmochimica Acta 72, 2298-2315.

Davidson, D.W., Leaist, D.J., and Hesse, R., 1983. Oxygen-18 enrichment in water of clathrate hydrate. Geochimica et Cosmochimica Acta 47, 2293-2295.

Elvert, M., Suess, E., and Whiticar, M.J., 1999. Anaerobic methane oxidation associated with marine gas hydrates: superlight C-isotopes from saturated and unsaturated C_{20} and C_{25} irregular isoprenoids. Naturwissenschaften 86, 295-300.

Elvert, M., Hopmans, E.C., Treude, T., Boetius, A., and Suess, E., 2005. Spatial variations of methanotrophic consortia at cold methane seeps: implications from a high-resolution molecular and isotopic approach. Geobiology 3, 195-209.

Emery, K.O., Uchupi, E., Phillips, J., Bowin, C., and Mascle, J., 1975. Continental margin off Western Africa: Angola to Sierra Leone. The American Association of Petroleum Geologists Bulletin 59, 2209-2265.

Folk, R.L., 1959. Practical classification of limestones. American Association of Petroleum Geologists Bulletin 43. 1-38.

Foustoukos, D.I. and Seyfried, W.E., 2004. Hydrocarbons in hydrothermal vent fluids: the role of Chromium-bearing catalysts. Science 304, 1002-1004.

Freytag, J.K., Girguis, P.R., Bergquist, D.C., Andreas, J.P., Childress, J.J., Fisher, C.R., 2001. A paradox resolved: Sulfide acquisition by roots of seep tubeworms sustains net chemoautotrophy. Proceedings of the National Academy of Sciences of the USA 98, 13408-13413.

Gaill, F., Persson, J., Sugiyama, J., Vuong, R., Chanzy, H., 1992a. The chitin system in the tubes of deep-sea hydrothermal vent worms. Journal of Biology 109, 116-128.

Gay, A., Lopez, M., Cochonat, P., and Sermondadaz, 2004. Polygonal faults-furrows system related to early stages of compaction - upper Miocene to recent sediments of the Lower Congo Basin. Basin Research 16, 101-116.

Gay, A., Lopez, M., Ondreas, H., Charlou, J.L., Sermondadaz, G., and Chochonat, P., 2006. Seafloor facies related to upward methane flux within a Giant Pockmark of the Lower Congo Basin. Marine Geology 226, 81-95.

Gay, A., Lopez, M., Berndt, C. and Séranne, M., 2007. Geological controls on focused fluid flow associated with seafloor seeps in the Lower Congo Basin. Marine Geology 244, 68-92.

Given, K.R., and Wilkinson, B.H., 1984, Kinetic control of morphology, composition, and mineralogy of abiotic sedimentary carbonates. Journal of Sedimentary Petrology 55, 109-119.

Goedert, J.L., Campbell, K.A., 1995. An Early Oligocene chemosynthetic community from the Makah Formation, northwestern Olympic peninsula. The Veliger 38, 22-29.

Goedert, J.L., Peckmann, J., Reitner, J., 2000. Worm tubes in an allochthonous cold-seep carbonate from Lower Oligocene rocks of Western Washington. Journal of Paleontology 74, 992-999.

Greinert, J., Bohrmann, G. and Elvert, M., 2002. Stromatolithic fabric of authigenic carbonate crusts: result of anaerobic methane oxidation at cold seeps in 4,850 m water depth. International Journal of Earth Sciences 91, 698-711.

Han, X., Suess, E., Sahling, H., and Wallmann, K., 2004. Fluid venting activity on the Costa Rica Margin: new results from authigenic carbonates. International Journal of Earth Sciences 93, 596-611.

Haas, A., Little, C.T.S., Sahling, H., Bohrmann, G., Peckmann, J. (sub). Mineralization of vestimentiferan tubes at methane seeps on the Congo deep sea fan.

Halanych, K.M., Lutz, R.A., and Vrijenhoek, R.C., 1998. Evolutionary origins and age of vestimentiferan tube-worms. Cahiers de Biologie Marine 39, 355-358.

Haq, B.U. 2003. Climate Impact of Natural Gas Hydrate. In: Max, M.D.(Ed), Natural Gas Hydrate in Oceanic and Permafrost environments. Kluwer Academic Publishers, Dordrecht, The Netherlands, 137-148.

Hedberg, H.D., 1980. Methane generation and petroleum migration. Problems of Petroleum Migration, 10. American Association of Petroleum Geologists Stud. Geol., 179-206 pp.

Himmler, T., Freiwald, A., Stollhofen, H., Peckmann, J., 2008. Late Carboniferous hydrocarbon-seep carbonates from the glaciomarine Dwyka Group, southern Namibia. Palaeogeography, Palaeoclimatology, Palaeoecology 257, 185-197.

Hinrichs, K.-U., Hayes, J.M., Sylva, S.P., Brewer, P.G., and DeLong, E.F., 1999. Methane-consuming archaebacteria in marine sediments. Nature 398, 802-805.

Hinrichs, K.-U., Summons, R.E., Orphan, V., Sylva, S.P. and Hayes, J.M., 2000. Molecular and isotopic analysis of anaerobic methane-oxidizing communities in marine sediments. Organic Geochemistry 31, 1685-1701.

Hoehler, T.M. and Alperin, M.J., 1996. Anaerobic methane oxidation by methanogen-sulfate reducer consortium: geochemical evidence and biochemical considerations. In: M.E. Lidstrom and F.R. Tabita (Editors), Microbial Growth on C_1 Compounds. Kluwer Academic Publishers, Dordrecht.

Hovland, H. and Judd, A.G., 1988. Seabed pockmarks and seepages. Graham & Trotman, London, 293 pp.

Hovland, M., and Cruzi, P., 1989, Gas seepage and assumed mud diapirism in the Italian central Adriatic Sea. Marine and Petroleum Geology 6, 161-169.

Hovland, M., Svensen, H., Forsberg, C.F., Johansen, H., Fichler, C., Fosså, J.H., Jonsson, R. and Rueslåtten, H., 2005. Complex pockmarks with carbonate-ridges off mid-Norway: Products of sediment degassing. Marine Geology 218, 191-206.

Hudson, J.C., and Anderson, T.F., 1989. Ocean temperature and isotopic composition through time, in Clarkson, E.N.K., Curry, G.B., and Rolfe, W.D.I., eds.. Transactions of the Royal Society of Edinburgh, 80: 183-192.

Iversen, N. and Jørgensen, B.B., 1985. Anaerobic methane oxidation rates at the sulfate-methane transition in marine sediments from Kattegatt and Skagerrak (Denmark). Limnology and Oceanography 30, 944-955.

Joye, S.B., Boetius, A., Orcutt, B.N., Montoya, J.P., Schulz, H.N., Erickson, M.J., and Lugo, S.K., 2004, The anaerobic oxidation of methane and sulfate reduction in sediments from Gulf of Mexico cold seeps. Chemical Geology 205, 219-238.

Jørgensen, B.B., 1982. Mineralization of organic matter in the sea bed - the role of sulphate reduction. Nature 296, 643-645.

Judd, A.G., Long, D., and Sankey, M., 1994. Pockmark formation and activity, UK block 15/25, North Sea. Bulletin of the Geological Society of Denmark 41, 34-49.

Judd, A.G., 2003. The global importance and context of methane escape from the seabed. Geo-Marine Letters 23, 147-154.

Judd, A. and Hovland, M., 2007. Seabed Fluid Flow-The Impact on Geology, Biology, and the Marine Environment. Cambridge University Press, New York, 475 pp.

Julian, D., Gaill, F., Wood, E., Arp, A.J., Fisher, C.R., 1999. Roots as a site of hydrogen sulfide uptake in the hydrocarbon seep vestimentiferan Lamellibrachia sp.. Journal of Experimental Biology 202, 2245-2257.

Kelts, K., and McKenzie, J., 1982. Diagenetic dolomite formation in Quaternary anoxic diatomaceous muds of Deep Sea Drilling Project Leg 64, Gulf of California. Initial Report DSDP 64, 553-570.

Kennicutt II, M.C., Brooks, J.M., Bidigare, R.R., Fay, R.R., Wade, T.L., and McDonald, T.J., 1985. Vent-type taxa in a hydrocarbon seep region on the Louisiana slope. Nature 17, 351-353.

Kennicutt, M.C., Brooks, J.M., Bidigare, R.R. and Denoux, G.J., 1988. Gulf of Mexico hydrocarbon seep communities - I. Regional distribution of hydrocarbon seepage and associated fauna. Deep-Sea Research I 35A, 1639-1651.

Kim, S.T., and O'Neil, J.R., 1997. Equilibrium and nonequilibrium oxygen isotope effects in synthetic carbonates. Geochimica et Cosmochimica Acta 61, 3461-3475.

King, L.H., and MacLean, B., 1970. Pockmarks on the Scotian shelf. Geological Society of America Bulletin 81, 3141-3148.

Knittel, K., Boetius, A., Lemke, A., Eilers, H., Lochte, K., Pfannkuche, O. and Linke, P., 2003. Activity, distribution, and diversity of sulfate reducers and other bacteria in sediments above gas hydrate (Cascadia Margin, OR). Geomicrobiology Journal 20, 269-294.

Knittel, K., Lösekann, T., Boetius, A., Kort, R. and Amman, R., 2005. Diversity and distribution of methanotrophic archaea at cold seeps. Applied Environmental Microbiology 71, 467-479.

Kochevar, R.E., Childress, J.J., Fisher, C.R. and Minnich, E., 1992. The methane mussel: roles of symbiont and host in the metabolic utilization of methane. Marine Biology 112, 389-401.

Kulm, L.D., Suess, E., Moore, J.C., Carson, B., Lewis, B.T., Ritger, S.D., Kadko, D.C., Thornburg, T.M., Embley, R.W., Rugh, W.D., Massoth, G.J., Langseth, M.G., Cochrane, G.R. and Scamann, R.L., 1986. Oregon subduction zone: venting, fauna, and carbonates. Science 231, 561-566.

Kvenvolden, K.A., Soloviev, V.A., and Ginsburg, G.D., 1993. Worldwide distribution of subaquatic gas hydrates. Geo-Marine Letters 13, 32-40.

Kvenvolden, K.A., 1998. A primer on the geological occurence of gas hydrate. In: J.P. Henriet and J. Mienert (Editors), Gas Hydrates: Relevance to World Margin Stability and Climate Change. Special Publications. Geological Society, London, pp. 9-30.

Kvenvolden, K.A. 2003. Natural Gas Hydrate: Introduction and History of Discovery. In: Max, M.D.(Ed), Natural Gas Hydrate in Oceanic and Permafrost environments. Kluwer Academic Publishers, Dordrecht, The Netherlands, pp 9-16.

Leefmann, T., Bauermeister, J., Kronz, A., Liebetrau, V., Reitner, J. and Thiel, V., 2008. Miniaturized biosignature analysis reveals implications for the formation of cold seep carbonates at Hydrate Ridge. Biogeosciences 5, 731-738.

Levin, L.A., Ziebis, W., Mendoza, G.F., Growney, V.A., Tryon, M.D., Brown, K.M., Mahn, C., Gieskes, J.M. and Rathburn, A.E., 2003. Spatial heterogeneity of macrofauna at northern

California methane seeps: influence of sulfide concentration and fluid flow. Marine Ecology Progress Series 265, 123-139.

Levin, L.A., 2005. Ecology of cold seep sediments: Interactions of infauna with flow, chemistry, and microbes. Oceanography and Marine Biology: An Annual Review 43, 1-46.

Little, C.T.S., Vrijenhoek, R.C., 2003. Are hydrothermal vent animals living fossils? Trends in Ecology and Evolution 18, 582-588.

Lösekann, T., Knittel, K., Nadalig, T., Fuchs, B., Niemann, H., Boetius, A., and Amann, R., 2007. Diversity and abundance of aerobic and anaerobic methane oxidizers at the Haakon Mosby Mud Volcano, Barents Sea. Applied and Environmental Microbiology 73, 3348-3362.

Luff, R., and Wallmann, K., 2003. Fluid flow, methane fluxes, carbonate precipitation and biogeochemical turnover in gas hydrate-bearing sediments at Hydrate Ridge, Cascadia Margin: Numerical modeling and mass balances. Geochimica et Cosmochimica Acta 67, 3403-3421.

Luff, R., Wallmann, K., and Aloisi, G., 2004. Numerical modeling of carbonate crust formation at cold vent sites: significance for fluid and methane budgets and chemosynthetic biological communities. Earth and Planetary Science Letters 221, 337-353.

Luff, R., Greinert, J., Wallmann, K., Klaucke, I. and Suess, E., 2005. Simulation of long-term feedbacks from authigenic carbonate crust formation at cold vent sites. Chemical Geology 216, 157-174.

Lumsden, D.S., 1979. Discrepancy between thin-section and x-ray estimates of dolomite in limestone. Journal of Sedimentary Petrology 49, 429-436.

MacDonald, I.R., Boland, G.S., Baker, J.S., Brooks, J.M., Kennicutt II, M.C. and Bidigare, R.R., 1989. Gulf of Mexico hydrocarbon seep communities. Marine Biology 101, 235-247.

MacDonald, I.R., Buthman, D.B., Sager, W.W., Peccini, N.B. and Jr., N.L.G., 2000. Pulsed oil discharge from a mud volcano. Geology 28, 907-912.

Martens, C.S. and Berner, R.A., 1974. Methane Production in Interstitial Waters of Sulfate-Depleted Marine Sediments. Science 185, 1167-1169.

Martin, R.E., 1999. Taphonomy: a process approach. Cambridge paleobiology series, 4. Cambridge University press, 508 pp.

Mayer, L.A., Shor, A.N., Clarke, J.H. and Piper, D.J.W., 1988. Dense biological communities at 3850 m on the Laurentian Fan and their relationship to the deposits of the 1929 Grand Banks earthquake. Deep-Sea Research I 35A: 1235-1246.

Megonigal, J.P., Hines, M.E. and Visscher, P.T., 2005. Anaerobic Metabolism: Linkages to Trace Gases and Aerobic Processes. Treatise on Geochemistry. Pergamon, Oxford. Biogeochemistry 8, 317-424.

Mozley, P.S., and Burns, S.J., 1993. Oxygen and carbon isotopic composition of marine carbonate concretions: An overview. Journal of Sedimentary Research 63, 73-83.

Mozley, P.S., 1996. The internal structure of carbonate concretions in mudrocks: a critical evaluation of the conventional concentric model of concretion growth. Sedimentary Geology 103, 85-91.

Naganuma, T., Okayama, M., Hattori, M., Kanie, Y., 1995. Fossil worm tubes from the presumed cold-seep carbonates of the Miocene Hayama Group, central Miura Peninsula, Japan. The Island Arc 4, 199-208.

Nauhaus, K., Treude, T., Boetius, A., and Krüger, M., 2005. Environmental regulation of the anaerobic oxidation of methane: comparison of ANME-I and AMNE-II-communities. Environmental Microbiology 7, 98-106.

Niemann, H., Elvert, M., Hovland, M., Orcutt, B., Judd, A., Suck, I., Gutt, J., Joye, S., Damm, E., Finster, K. and Boetius, A., 2005. Methane emission and consumption at a North Sea gas seep (Tommeliten Area). Biogeosciences 2, 335-351.

Niemann, H., Lösekann, T., De Beer, D., Elvert, M., Nadalig, T., Knittel, K., Amann, R., Sauter, E., Schlüter, M., Klages, M., Foucher, J.P., and Boetius, A., 2006. Novel microbial communities of the Haakon Mosby mud volcano and their role as a methane sink. Nature 443, 854-858.

Niemann, H. and Elvert, M., in press. Diagnostic lipid biomarker and stable carbon isotope signatures of microbial communities mediating the anaerobic oxidation of methane with sulphate. Organic Geochemistry.

Olu, K., Lance, S., Sibuet, M., Henry, P., Fiala-Médioni, A., and Dinet, A., 1997. Cold seep communities as indicators of fluid expulsion patterns through mud volcanoes seaward of the Barbados accretionary prism. Deep-Sea Research I, 44, 811-841.

Olu-Le Roy, K., Caprais, J.-C., Fifis, A., Fabri, M.-C., Galéron, J., Budzinsky, H., Le Ménach, K., Khripounoff, A., Ondréas, H., and Sibuet, M., 2007, Cold-seep assemblages on a giant pockmark off West Africa: spatial patterns and environmental control. Marine Ecology 28, 1-16.

Orphan, V.J., House, C.H., Hinrichs, K.U., McKeegan, K.D. and DeLong, E.F., 2002. Multiple archaeal groups mediate methane oxidation in anoxic cold seep sediments. Proceedings of the National Academy of Sciences USA 99, 7663-7668.

Pancost, R.D., Sinninghe Damsté, J.S., de Lint, S., van der Maarel, M. J. E. C., Gottschal, J.C., and the Medinaut Shipboard Scientific Party, 2000. Biomarker evidence for widespread anaerobic methane oxidation in Mediterranean sediments by a consortium of methanogenic archaea and bacteria. Applied and Environmental Microbiology 66, 1126-1132.

Pancost, R.D., Bouloubassi, I., Aloisi, G., Sinninghe Damsté, J.S., the Medinaut Shipboard Scientific Party, 2001. Three series of non-isoprenoidal dialkyl glycerol diethers in cold-seep carbonate crusts. Organic Geochemistry 32, 695-707.

Pape, T., Blumenberg, M., Seifert, R., Egorov, V., Gulin, S.B., and Michaelis, W., 2005. Lipid geochemistry of methane-seep-related Black Sea carbonates. Palaeogeography, Palaeoclimatology, Palaeoecology 227, 31-47.

Paull, C.K., Hecker, B., Commeau, R., Freeman-Lynde, R.P., Neumann, C., Corso, W.P., Golubic, S., Hook, J.E., Sikes, E., and Curray, J., 1984, Biological communities at the Florida Escarpment resemble hydrothermal vent taxa. Science 226, 965-967.

Paull, C.K., Chanton, J., P., Neumann, A.C., Coston, J.A., Martens, C.S. and Showers, W., 1992. Indicators of methane-derived carbonates and chemosynthetic organic carbon deposits: examples from the Florida escarpment. Palaios 7, 361-375.

Paull, C.K., Schlining, B., Ussler III, W., Paduan, J.B., Caress, D., Greene, H.G., 2005. Distribution of chemosynthetic biological communities in Monterey Bay, California. Geology 33, 85-88.

Park, A., Dewers, T. and Ortoleva, P., 1990. Cellular and oscillatory self-induced methane migration. Earth Science Reviews 29, 249-265.

Peckmann, J., Thiel, V., Michaelis, W., Clari, P., Gaillard, C., Martire, L., and Reitner, J., 1999. Cold seep deposits of Beauvoisin (Oxfordian, southeastern France) and Marmorito (Miocene, northern Italy): microbially induced authigenic carbonates. International Journal of Earth Sciences 88, 60-75.

Peckmann, J., Reimer, A., Luth, U., Luth, C., Hansen, B.T., Heinicke, C., Hoefs, J., and Reitner, J., 2001, Methane-derived carbonates and authigenic pyrite from the northwestern Black Sea. Marine Geology 177, 129-150.

Peckmann, J., Goedert, J.L., Thiel, V., Michaelis, W., and Reitner, J., 2002. A comprehensive approach to the study of methane-seep deposits from the Lincoln Creek Formation, western Washington State, USA. Sedimentology 49, 855-873.

Peckmann, J., and Thiel, V., 2004. Carbon cycling at ancient methane-seeps. Chemical Geology 205, 443-467.

Peckmann, J., Little, C.T.S., Gill, F., Reitner, J., 2005. Worm tube fossils from the Hollard Mound hydrocarbon-seep deposit, Middle Devonian, Morocco: Palaeozoic seep-related vestimentiferans? Palaeogeography, Palaeoclimatology, Palaeoecology 227, 242-257.

Pierre, C., and Fouquet, Y., 2007. Authigenic carbonates from methane seeps of the Congo deep-sea fan. Geo-Marine Letters 27, 249-257.

Plotnick, R.E., 1986a. Taphonomy of a modern shrimp: implications for the arthropod fossil record. Palaios 1, 286-293.

Raiswell, R., and Fisher, Q.J., 2000. Mudrock-hosted carbonate concretions: a review of growth mechanisms and their influence on chemical and isotopic composition. Journal of the Geological Society 157, 239-251.

Reeburgh, W.S., 1976. Methane consumption in Cariaco Trench waters and sediments. Earth and Planetary Science Letters 28, 337-344.

Reeburgh, W.S., 1996. "Soft spots" in the global methane budget. In: M.E. Lidstrom and F.R. Tabita (Editors), Microbial Growth on C1 Compounds. Kluwer Academic Publishers, Dordrecht, pp. 334-342.

Reitner, J., Peckmann, J., Reimer, A., Schumann, G., and Thiel, V., 2005a. Methane-derived carbonate build-ups and associated microbial communities at cold seeps on the lower Crimean shelf (Black Sea). Facies 51, 66-79.

Reitner, J., Peckmann, J., Blumenberg, M., Michaelis, W., Reimer, A., and Thiel, V., 2005b. Concretionary methane-seep carbonates and associated microbial communities in Black Sea sediments. Palaeogeography, Palaeoclimatology, Palaeoecology 227, 18-30.

Riding, R., 2000. Microbial carbonates: the geological record of calcified bacterial-algal mats and biofilms. Sedimentology 47, 179-214.

Ritger, S., Carson, B., and Suess, E., 1987. Methane-derived authigenic carbonates formed by subduction-induced pore-water expulsion along the Oregon/Washington margin. Geological Society of America Bulletin 98, 147-156.

Sahling, H., Rickert, D., Lee, R.W., Linke, P. and Suess, E., 2002. Macrofaunal community structure and sulfide flux at gas hydrate deposits from the Cascadia convergent margin, NE Pacific. Marine Ecology Progress Series 231, 121-138.

Sahling, H., Bohrmann, G., Spiess, V., Bialas, J., Breitzke, M., Ivanov, M., Kasten, S., Krastel, S., and Schneider, R., 2008, Pockmarks in the Northern Congo Fan area, SW Africa: Complex seafloor features shaped by fluid flow. Marine Geology 249, 206-225.

Schneider, R.R., Price, B., Müller, P.J., Kroon, D., and Alexander, I., 1997. Monsoon related variations in Zaire (Congo) sediment load and influence of fluvial silicate supply on marine productivity in the east equatorial Atlantic during the last 200.000 years. Paleoceanography 12, 463-481.

Seilacher, A., Reif, W.-E. and Westphal, F., 1985. Sedimentological, ecological and temporal patterns of fossil Lagerstätten. Extraordinary fossil biotas: their ecological and evolutionary significance, 311. Philosophical Transactions of the Royal Society of London, 5-23 pp.

Séranne, M., 1999. Early Oligocene stratigraphic turnover on the west African continental margin: a signature of the Tertiary greenhouse-to-icehouse transition. Terra Nova 11, 135-140.

Shillito, B., Lechaire, J.P., Goffinet, G., Gaill, F., 1995. Composition and morphogenesis of the tube of vestimentiferan worms. In: L.M. Parson, C.L. Walker and D.R. Dixon (Editors), Hydrothermal Vents and Processes. Geological Society of America pp. 295-302.

Sibuet, M. and Olu, K., 1998. Biogeography, biodiversity and fluid dependence of deep-sea cold-seep communities at active and passive margins. Deep-Sea Research II 45, 517-567.

Sibuet, M., Olu-Le Roy, K., 2002. Cold seep communities on continental margins: Structure and quantitative distribution relative to geological and fluid venting patterns. In: G. Wefer et al. (Editors), Ocean Margin Systems. Springer-Verlag, Berlin, pp. 235-251.

Sibuet, M., Galéron, J., Khripounoff, A., Menot, L., Olu-LeRoy, K., Durrieu, J., Miné, J., and TotalFinaElf, 2002, Deep Sea Ecosystems on the Equatorial African Margin: First results of a Pluridisciplinary Environmental Programme and Discovery of Chemosynthesis Based Ecosystem, SPE International conference on health, safety and environment in oil and gas exploration and production: Kuala Lumpur, Malaysia, Society of Petroleum Engineers, p. SPE 73875.

Sloan, E.D.j., 1998. Physical/chemical properties of gas hydrates and application to world margin stability and climatic change. In: J.P. Henriet and J. Mienert (Editors), Gas Hydrates: Relevance to World Margin Stability and Climate Change. Special Publications. Geological Society, London, pp. 31-50.

Spiess, V., Zühlsdorff, L., Villinger, H., Flueh, E., Bialas, J., Kasten, S., Schneider, R., Bohrmann, G., and Sahling, H., 2006, Gas hydrate in hemipelagic sediments-Congo, in Stroink, L., ed., Gas hydrates in the Geosystem, Volume Results from the First Funding Period (2001-2004): Potsdam, The German National Research Programm on Gas hydrates. Koordinierungsbüro Geotechnologien, 170-185.

Stadnitskaia, A., Muyzer, G., Cololen, M.J.L., Hopmans, E.C., Baas, M., van Weering, T.C.E., Ivanov, M.K., Poludetkina, E. and Sinninghe Damsté, J.S., 2005. Biomarker and 16S rDNA evidence for anaerobic oxidation of methane and related carbonate precipitation in deep-sea mud volcanoes of the Sorokin Trough, Black Sea. Marine Geology 217, 67-96.

Stadnitskaia, A., Nadezhkin, D., Abbas, B., Blinova, V., Ivanov, M.K. and Sinninghe Damsté, J.S., 2008. Carbonate formation by anaerobic oxidation of methane: Evidence from lipid biomarker and fossil 16S rDNA. Geochimica et Cosmochimica Acta 72, 1824-1836.

Suess, E., Carson, B., Ritger, S.D., Moore, J.C., Jones, M.L., Kulm, L.D., and Cochrane, G.R., 1985. Biological communities at vent sites along the subduction zone off Oregon. Bulletin of the Biological Society of Washington 6, 475-484.

Suess, E. and Whiticar, M.J., 1989. Methane-derived CO_2 in pore fluids expelled from the Oregon subduction zone. Palaeogeography, Palaeoclimatology, Palaeoecology 71, 119-136.

Suess, E., Bohrmann, G., Huene, R.v., Linke, P., Wallmann, K., Lammers, S., Sahling, H., Winckler, G., Lutz, R.A. and Orange, D., 1998. Fluid venting in the eastern Aleutian subduction zone. Journal of Geophysical Research, 103, 2597-2614.

Suess, E., Torres, M.E., Bohrmann, G., Collier, R.W., Greinert, J., Linke, P., Rehder, G., Trehu, A., Wallmann, K., Winckler, G. and Zuleger, E., 1999. Gas hydrate destabilization: enhanced dewatering, benthic material turnover and large methane plumes at the Cascadia convergent margin. Earth and Planetary Science Letters 170, 1-15.

Taniguchi, M., Burnett, W.C., Cable, J.E., and Turner, J.V., 2002. Investigation of submarine groundwater discharge. Hydrological Processes 16, 2115-2129.

Tarutani, T., Clayton, R.N., and Mayeda, T.K., 1969. The effect of polymorphism and magnesium substitution on oxygen isotopic fractionation between calcium and water. Geochimica et Cosmochimica Acta 33, 987-996.

Thiel, V., Peckmann, J., Seifert, R., Wehrung, P., Reitner, J., and Michaelis, W., 1999. Highly isotopically depleted isoprenoids: Molecular markers for ancient methane venting. Geochimica et Cosmochimica Acta 63, 3959-3966.

Torres, M.E., Brumsack, H.J., Bohrmann, G., and Emeis, K.C., 1996. Barite fronts in continental margin sediments: a new look at barium remobilization in the zone of sulfate reduction and formation of heavy barites in diagenetic fronts. Chemical Geology 127, 125-139.

Tréhu, A.M., Bohrmann, G., Rack, F.R., Torres, M.E., et al., 2003. Proc. ODP, Initial Reports 204: College Station, TX (Ocean Drilling Program).

Tucker, M.E., and Wright, V.P., 1990. Carbonate Sedimentology: Oxford, Blackwell Scientific, pp 482 .

Tucker, M.E. and Wright, P.V., 2004. Carbonate Sedimentology. Blackwell Science Ltd, reprint.

Tunnicliffe, V., Juniper, S.K., and Sibuet, M., 2003. Reducing environments of the deep-sea floor, in Tyler, P.A., ed., Ecosystems of the Deep Oceans. Amsterdam, Elsevier, pp. 81-110.

Uenzelmann-Neben, G., 1998. Neogene sedimentation history of the Congo Fan. Marine and Petroleum Geology 15, 635-650.

Valentine, D.L., 2002. Biogeochemistry and microbial ecology of methane oxidation in anoxic environments: a review. Antonie van Leeuwenhoek 81, 271-282.

van Lith, Y., Warthmann, R., Vasconcelos, C., and McKenzie, J.A., 2003. Sulphate-reducing bacteria induce low-temperature Ca-dolomite and high Mg-calcite formation. Geobiology 1, 71-79.

Vasconcelos, C. and McKenzie, J.A., 1997. Microbial mediation of modern dolomite precipitation and diagenesis under anoxic conditions (Lagoa Vermelha, Rio de Janeiro, Brazil). Journal of sedimentary research 67, 379-390.

von Rad, U., Rösch, H., Berner, U., Geyh, M., Marchig, V., and Schulz, H., 1996. Authigenic carbonates derived from oxidized methane vented from the Makran accretionary prism off Pakistan. Marine Geology 136, 55-77.

Wallmann, K., Linke, P., Suess, E., Bohrmann, G., Sahling, H., Schlüter, M., Dählmann, A., Lammers, S., Greinert, J. and Mirbach, N.v., 1997. Quantifying fluid flow, solute mixing, and biogeochemical turnover at cold vents of the eastern Aleutian subduction zone. Geochimica et Cosmochimica Acta 61, 5209-5219.

Walter, L.M., 1986. Relative efficiency of carbonate dissolution and precipitation during diagenesis: a progress report on the role of solution chemistry, in Gautier, D.L., ed., Roles of Organic Matter in Mineral Diagenesis. Society of Economic Paleontologists and Mineralogists 38 (Spec. Publ.), 1-12.

Wartmann, R., Van Lith, Y., Vasconcelos, C., McKenzie, J.A., and Karpoff, A.-M., 2000. Bacterially induced dolomite precipitation in anoxic culture experiments. Geology 28, 1091-1094.

Whiticar, M.J., and Werner, F., 1981, Pockmarks: Submarine vents of natural gas or freshwater seeps? Geo-Marine Letters 1, 193-199.

Whiticar, M.J., Faber, E. and Schoell, M., 1986. Biogenic methane formation in marine and freshwater environments: CO_2 reduction vs. Acetate fermentation - Isotope evidence. Geochimica et Cosmochimica Acta 50, 693-709.

Whiticar, M.J., 1999. Carbon and hydrogen isotope systematics of bacterial formation and oxidation of methane. Chemical Geology 161, 291-314.

Wright, D.T., 2000. From Global to Microbial. Society for Sedimentary Geology 66, 7-20.

Zeebe, R.E., 1999. An explanation of the effect of seawater carbonate concentration on foraminiferal oxygen isotopes. Geochimica et Cosmochimica Acta 63, 2001-2007.

Zühlsdorff, L., and Spiess, V., 2004. Three-dimensional seismic characterization of a venting site reveals compelling indications of natural hydraulic fracturing. Geology 32, 101-104.

Für die Vergabe und Betreuung der vorliegenden Arbeit möchte ich Prof. Gerhard Bohrmann und Prof. Jörn Peckmann herzlich danken. Die umfassende und wohlwollende Unterstützung hat wesentlich zum Gelingen der Arbeit beigetragen.

Dr. Heiko Sahling war als weiterer Betreuer ein zentraler Diskussionspartner, für dessen Hilfestellungen und Anregungen hier herzlichst gedankt sei.
Dr. Crispin Little (Leeds) möchte ich für die engagierte Zusammenarbeit, die hilfreichen Ideen und die Durchführung der Englischkorrektur danken.

Meinen Kolleginnen und Kollegen aus den Arbeitsgruppen Marine Geologie und Geobiologie sei für ihre unkomplizierte Unterstützung und den freundschaftlichen Umgang herzlichst gedankt. Unser gemeinsames wissenschaftliches Arbeiten hat den Fortgang der Arbeit maßgeblich beeinflusst. Die meist schweißtreibenden aber ungemein entspannten gemeinsamen Ausflüge, ob Paddeln, Radeln oder Boßeln sind mir eine schöne Erinnerung an unsere gemeinsame Zeit.

Besonders Danken möchte ich meinen „Bürogenossen“ Markus und Stephan für die vielen lebhaften Diskussionen und Gespräche und ihre stoische Unempfindlichkeit gegen mein winterliches Lüften.
Auch die monatlichen Doktorandenfrühstücke mit Esther, Simone (+ Elena), Benny, Lars und Florian halfen sehr, die kleinen Widrigkeiten des „Doktorandendaseins“ zu kompensieren.

Meinem Sohn Jannick und meinem Partner Stefan danke ich für ihre liebevolle Unterstützung während dieser aufregenden Zeit.